UNIVERSITY OF CALIFORNIA,
IRVINE

Frameworks for Improving Multi-Index Drought Monitoring Using Remote Sensing Observations

DISSERTATION

submitted in partial satisfaction of the requirements
for the degree of

DOCTOR OF PHILOSOPHY

in Civil and Environmental Engineering

by

Alireza Farahmand

Dissertation Committee:
Professor Amir AghaKouchak, Chair
Professor Soroosh Sorooshian
Professor Kou-lin Hsu
Professor Steven J. Davis

2016

DEDICATION

To
my mother,
father,
and sister.

TABLE OF CONTENTS

LIST OF FIGURES

LIST OF ABBRVATIONS

λ_{AET} AET rate

λ_{PET} PET rate

R_{VIS} Visible reflectance

R_{mIR} Middle IR reflectance

AIRS Atmospheric Infrared Sounder

ALEXI Atmosphere-Land Exchange Inverse

AET Actual ET

AMSR Advanced Microwave Scanning Radiometer for EOS

AVHRR Advanced Very High Resolution Radiometer

CCI Climate Change Initiative

CLSM Catchment Land Surface Model

CMORPH CPC Morphing Technique

CWSI Crop Water Stress Index

CTVI Corrected Transformed Vegetation Index

DDI Distance Drought Index

DSI Drought Severity Index

EDI Evaporative Drought Index

ESI Evaporative Stress Index

ET Evapotranspiration(mm/day)

ETM Enhanced Thematic Mapper

EVI Enhanced Vegetation Index

GEO Geostationary

GIDMaPS Global Integrated Drought Monitoring and Prediction System

GOES-R Geostationary Operational Environmental Satellites R series

GOSAT Greenhouse Gases Observing Satellite

GPCP Global Precipitation Climatology Project

GPM Global Precipitation Mission

GPP Gross Primary Production

GRACE Gravity Recovery and Climate Experiment

GRACE-DAS GRACE Data Assimilation System

IPAD International Production Assessment Division

IR Infrared

LEO Low Earth Orbit

LST Land Surface Temperature

MIDI Microwave Integrated Drought Index

MSDI Multivariate Standardized Drought Index

MODIS Moderate Resolution Imaging Spectroradiometer

MPDI Modified Perpendicular Drought Index

MW Microwave

NDDI Normalized Difference Drought Index

NDVI Normalized Difference Vegetation Index

NDWI Normalized Difference Water Index

NEP Net Ecosystem Production

NIR near infrared

NMDI Normalized Multi-band Drought Index

NPP net primary production

NRVI Normalized Ratio Vegetation Index

NSDI Normalized Difference Snow Index

P Precipitation

PCI Precipitation Condition Index

PDI Perpendicular Drought Index

PERSIANN Precipitation Estimation from Remotely Sensed Information using Artificial Neural Networks

PET Potential ET

PVI Perpendicular Vegetation Index

SM soil moisture

PDSI Palmer Drought Severity Index

PNP Percent of Normal Precipitation

R Red

RDI Reconnaissance Drought Index

SA Snow Albedo

SAVI Soil-Adjusted Vegetation Index

SCA Snow Covered Area

SCIAMACHY Absorption Spectrometer for Atmospheric Cartography

SCLP Snow and Cold Land Processes

SD Snow Depth

SMCI Soil Moisture Condition Index

SDCI Scaled Drought Condition Index

SPI Standardized Precipitation Index

SSI Standardized Soil Moisture Index

SRHI Standardized Relative Humidity Index

SVI Standardized Vegetation Index

SWE snow water equivalent

SWIR Short Wave Infrared

TCA Temperature Condition Index

TCI Temperature Condition Index

TES Tropospheric Emission Spectrometer

TIR Thermal Infrared

TIROS-1 Television and Infrared Observation Satellite

TM Landsat Thematic Mapper

TMPA Multi-satellite Precipitation Analysis

TRMM Tropical Rainfall Measuring Mission

TTVI Thiam's Transformed Vegetation Index

TVI Transformed Vegetation Index

TWS terrestrial water storage

USDA United States Department of Agriculture

USDM United States Drought Monitor

VCI Vegetation Condition Index

VegDRI Vegetation Drought Response Index

VIIRS Visible Infrared Imager Radiometer Suite

VIS Visible

VTCI Vegetation Temperature Condition Index

WACMOS Water Cycle Multi-Mission Observation Strategy

WDI Water Deficit Index

WMO World Meteorological Organization

ACKNOWLEDGMENTS

I would like to express my deepest appreciation for my committee chair, Professor Amir AghaKouchak who has helped me in the preparation of this thesis. Without his guidance, this dissertation would not have been possible.

I would like to thank my committee members Professor Soroosh Sorooshian and Professor Kou-lin Hsu and Professor Steven J. Davis for their efforts on reviewing this dissertation.

I would like to thank all my family and friends for supporting me.

CURRICULUM VITAE

Alireza Farahmand

EDUCATION

Doctor of Philosophy in Civil and Environmental Engineering **2016**
University of California, Irvine *Irvine, California*

Master of Science in Civil and Environmental Engineering **2013**
University of California, Irvine *Irvine, Iran*

Bachelor of Science in Civil and Environmental Engineering **2010**
University of Wuppertal *Wuppertal, Germany*

RESEARCH EXPERIENCE

Research Scientist **2016**
Jet Propultion Labratory *Pasadena, California*

Graduate Research Assistant **2011–2016**
University of California, Irvine *Irvine, California*

TEACHING EXPERIENCE

Teaching Assistant: Engineering Practicum **Winter 2014-2016**
Teaching Assistant: Hydrology **Fall 2012**
Teaching Assistant: Water Resources Management **Winter 2013**
University of California, Irvine *Irvine, California*

HONORS AND AWARDS **UC Irvine Water Sustainability Fellowship for solving Anza Borrego desert drought related problems**, University of California, Irvine, 2014.
National Science Foundation Lead Entrepreneur for assessing potential market for software GIDMaPS, University of California, Irvine, 2014.
National Science FOundation schoalriship for attending Philander Fest Symposium at Princeton University , Princeton, 2012.
German Academic Exchange (DAAD) fellowship for attending summerschool on Earthquake-Safe buildings , Wuppertal, Germany, 2006-2008.

Publications

A. AghaKouchak, A. Farahmand, J. Teixeira , B.D. Wardlow, F.S. Melton, M.C. Anderson, C.R. Hain, Remote Sensing of Drought: Progress, Challenges and Opportunities **2015**
Reviews of Geophysics, 53, 2, 452-480, doi: 10.1002/2014RG000456.

A. AghaKouchak, H. Norouzi , K. Madani , A. Mirchi , M. Azarderakhsh , A. Nazemi , N. Nasrollahi , A. Mehran ,A. Farahmand , E. Hasanzadeh, Aral Sea Syndrome Desiccates Lake Urmia: Call for Action, **2015**
Journal of Great Lakes Research, 41, 1, 307-311, doi: 10.1016/j.jglr.2014.12.007.

A. Farahmand, A. AghaKouchak , J. Teixeira , A Vantage from Space Can Detect Earlier Drought Onset: An Approach Using Relative Humidity, **2015**
Scientific Reports, 5, 8553, doi: 10.1038/srep08553.

A. Farahmand, and A. AghaKouchak, A Generalized Framework for Deriving Nonparametric Standardized Drought Indicators **2015**
Advances in Water Resources, 76, 140-145, doi: 10.1016/j.advwatres.2014.11.012

A. AghaKouchak, L. Cheng , O. Mazdiyasni, A. Farahmand , Global Warming and Changes in Risk of Concurrent Climate Extremes: Insights from the 2014 California Drought, **2014**
Geophysical Research Letters, 41, 8847-8852, doi: 10.1002/2014GL062308.

Z. Hao , A. AghaKouchak , N. Nakhjiri, A. Farahmand ,lobal Integrated Drought Monitoring and Prediction System, **2014**
Scientific Data, 1:140001, 1-10, doi: 10.1038/sdata.2014.1.

A. Farahmand, and A. AghaKouchak, A Satellite-Based Global Landslide Model, **2013**
Natural Hazards and Earth System Sciences, 13, 1259-1267, doi:10.5194/nhess-13-1259-2013.

SOFTWARE

Standardized Drought Analysis Toolbox (SDAT)

ABSTRACT OF THE DISSERTATION

Frameworks for Improving Multi-Index Drought Monitoring Using Remote Sensing Observations

By

Alireza Farahmand

Doctor of Philosophy in Civil and Environmental Engineering

University of California, Irvine, 2016

Professor Amir AghaKouchak, Chair

Droughts are among the most common and devastating natural disasters. Reducing damages associated with droughts relies on monitoring and prediction information as well as plans to cope with droughts. The overarching goal of this dissertation is to improve current capabilities in drought monitoring using space-based observations, with a focus on integrating remotely sensed data products that are not commonly being used for drought monitoring. The first chapter of this dissertation, surveys current and emerging drought monitoring approaches using remotely-sensed observations from climatological and ecosystem perspectives. Current and future satellite missions offer opportunities to develop composite and multi-sensor (or multi-index) drought assessment models. While there are immense opportunities, there are major challenges including data continuity, unquantified uncertainty, sensor changes, and community acceptability. One of the major limitations of many of the currently available satellite observations is their short length of record. A number of relevant satellite missions and sensors (e.g., Atmospheric Infrared Sounder (AIRS), Gravity Recovery and Climate Experiment) provide only slightly over a decade of data, which may not be sufficient to study droughts from a climatological perspective. However, they still provide valuable information about relevant hydrologic and ecological processes linked to this natural hazard. Therefore, there is a need for models and algorithms that combine mul-

tiple data sets and/or assimilate satellite observations into model simulations to generate long-term climate data records. To address this gap, Chapter 2 introduces Standardized Drought Analysis Toolbox (SDAT), which includes a generalized framework for deriving nonparametric univariate and multivariate standardized drought indices. Current indicators suffer from deficiencies including some prior distributional assumption, temporal inconsistency, and statistical incomparability. Different indicators have varying scales and ranges and their values cannot be compared with each other directly. Most drought indicators rely on a representative parametric probability distribution function that fits the data. However, a parametric distribution function may not fit the data, especially in continental/global scale studies. Particularly, when the sample size is relatively small as in the case of many satellite precipitation products. SDAT is based on a nonparametric framework that can be applied to different climatic variables including precipitation, soil moisture and relative humidity, without having to assume representative parametric distributions. The most attractive feature of the framework is that it leads to statistically consistent drought indicators based on different variables. We show that using SDAT with satellite observation leads to more reliable drought information, compared to the commonly used parametric methods.

We argue that satellite observations not currently used for operational drought monitoring, such as near-surface air relative humidity data from the Atmospheric Infrared Sounder (AIRS) mission, provide opportunities to improve early drought warning. In the third chapter of this dissertation, we outline a new drought monitoring framework for early drought onset detection using AIRS relative humidity data. The early warning and onset detection of drought is of particular importance for effective agriculture and water resource management. Previous studies show that the Standard Precipitation Index (SPI), a measure of precipitation deficit, detects drought onset earlier than other indicators. Here satellite-based near surface air relative humidity data can further improve drought onset detection and early warning. This chapter introduces the Standardized Relative Humidity Index (SRHI) based on the NASA's AIRS observations. SRHI relies on SDAT's nonparametric framework, intro-

duced in Chapter 2. The results indicate that the SRHI typically detects the drought onset earlier than SPI. While the AIRS mission was not originally designed for drought monitoring, its relative humidity data offers a new and unique avenue for drought monitoring and early warning. Early warning aspects of SRHI may have merit for integration into current drought monitoring systems.

One of the research opportunities identified in Chapter 1 is using current (and future) satellite missions to develop composite and multi-indicator drought models. In Chapter 4, we outline a framework for assessing impacts of droughts on forest health using a multi-sensor approach. This framework relies on the relationship between climate conditions (e.g., temperature, precipitation, relative humidity, Vapor Pressure Deficit) and forest health based on greenness of vegetation. Wildfires, tree mortality and forest productivity increase during drought periods. Using the proposed multi-index approach, Chapter 4 aims to investigate the effects of recent summer, dry-season and winter droughts on the forest health in western United States. We use Vapor Pressure Deficit (VPD) as an indicator that combines temperature and relative humidity for forest stress assessment. Normalized Difference Vegetation Index (NDVI) is commonly used for assessing vegetation health. During summer and growing season, VPD values are generally high. The results show that the VPD and NDVI provide consistent information on forest health. In addition to VPD, we use conditional probability of NDVI in high temperature and low relative humidity percentiles over the summer and the growing season. We show that combining temperature and relative humidity using a conditional probability approach offers multi-sensor information on forest condition. During winter, on the other hand, VPD and temperature is relatively lower. NDVI distributions in winter were found to be more associated with precipitation as opposed to relative humidity and temperature. We believe the a joint indicator based on temperature and relative humidity can be considered as a link between climate condition and actual impact on the ecosystem.

Chapter 1

Remote Sensing of Drought: Progress, Challenges and Opportunities

This Chapter has been published in Reviews of Geophysics. Citation: AghaKouchak A., Farahmand A., Teixeira J., Wardlow B.D., Melton F.S., Anderson M.C., Hain C.R. (2015), Remote Sensing of Drought: Progress, Challenges and Opportunities, *Reviews of Geophysics* , *49* (2), 452-480, doi: 10.1002/2014RG000456.

1.1 Introduction

Drought and water scarcity pose significant water and food security concerns, and may lead to economic risks and financial challenges, especially for developing economies [329, 95]. The phenomenon of meteorological drought is a consequence of regional variability in the global water cycle, a process tightly associated with climatic circulation patterns [233, 119, 243, 152, 98]. For this reason, a global perspective of drought conditions is often necessary to study the cause of specific regional droughts. For example, a recent study links global droughts during the late 1990s and early 2000s to warm and cold sea surface temperatures in the western and eastern tropical Pacific, respectively [122]. Conversely, a regional or continental drought could also lead to global impacts. For example, the 2010 Russian drought and heat wave led to an increase in global food prices [321], resulting in indirect impacts far beyond the drought-affected region. These issues highlight the importance of global, rather than regional, drought monitoring to understanding the biophysical processes involved, as well as improving drought prediction and early warning [100].

Historically, droughts have been monitored and investigated using ground-based observations [116, 272, 259], primarily from meteorological [223] and agricultural perspectives [87]. Globally, however, many areas used for agricultural production are not well instrumented to provide ground-based observations of precipitation, near-surface air temperature, water vapor, and atmospheric evaporative demand that are consistent over the long-term. In many other regions the available observations are not sufficient to capture the spatio-temporal variability of drought-related variables such as precipitation [69]. Furthermore, observations from different meteorological stations often have different record lengths and variable data quality [69], which makes consistent global drought analysis using ground-based observations challenging [13].

Satellite remote sensing of the Earth's weather began in earnest with the Television and

Infrared Observation Satellite (TIROS-1) mission in 1960 [211]. The success of this mission led to a series of additional weather- and climate-oriented satellite remote sensing missions. Remote sensing satellites can be broadly categorized into two types: Geostationary (GEO) and Low Earth Orbit (LEO) satellites [154]. GEOs orbit at around 36,000 km above the surface of the Earth and their orbits are synchronized with Earth's rotation, allowing them to provide information for a fixed field of view over a portion the Earth's surface. LEOs orbit at 200-1200 km altitudes [212], and are typically placed in sun-synchronous orbits to obtain more than one observation per day over a given location. Current GEOs carry multispectral radiometers that typically collect information in the visible and infrared (VIS/IR) portion of the electromagnetic spectrum, while LEOs carry a diverse range of sensors, including multispectral and hyperspectral sensors, laser altimeters, microwave (MW) sensors and others. Both GEO and LEO satellite observations have been used extensively for drought monitoring and impact assessment [23, 149, 81, 317, 190].

Remote sensing observations have been used to monitor drought-related variables from a climatological viewpoint and also to assess and quantify drought impacts from an ecosystem perspective. In the former, satellite multispectral, thermal infrared or microwave data are used to retrieve a drought-related variable including precipitation [280], soil moisture [73, 48] or evapotranspiration [258, 17, 27, 236]. The drought variable is then converted into a drought indicator by calculating the extent of an anomaly or departure from the longer-term environmental baseline. Those data are used to quantitatively assess and categorize drought severity.

Satellite observations have also been used to assess drought ecosystem impacts – including vegetation health and growth – by assessing the photosynthetic capacity of plants [297]. Precipitation deficits can lead to reduced photosynthetic capacity and changes in absorption of solar radiation in photosynthetically active wavelengths by plants [34]. Combinations of satellite visible (VIS) and infrared (IR) images have been widely used to monitor plant

changes and water stress [35, 114, 297, 320].

In the past decade, the science community has been able to access unprecedented new remote sensing data sets of precipitation, snow, soil moisture, land-surface temperature, evaporation, total water storage, vegetation and land cover [213, 320]. These satellite observations have opened new avenues in global drought monitoring from different perspectives (e.g., meteorological, agricultural, hydrological, and ecological). The advantages of satellite-based sensors relative to traditional ground-based observations include global, near real-time observations, consistent data records, and improved spatial resolution [118, 38, 39, 204]. The increasing volume of satellite observations and data products has led the science community into the era of *big data* [263], and provided unique opportunities to develop advanced drought monitoring capabilities based on multiple sources of data. However, the abundance of data also presents major scientific challenges, including uncertainty assessment, managing data volumes, merging or fusion of multiple data sources, and ensuring consistency between different observations and data sets.

This chapter first reviews the progress in remote sensing of drought from climatological and ecosystem perspectives, including satellite-based drought indicators. Then, major research gaps and challenges in advancing remote sensing of drought are discussed. Finally, a path for future research that could lead to a major advance in drought monitoring and impact assessment using space-based observations is outlined. This chapter focuses only on satellite remote sensing, and not aircraft and airborne remote sensing platforms, since the latter typically have limited geographical or temporal coverage.

1.2 Progress in Remote Sensing of Drought from a Climatological Perspective

Droughts are broadly classified into four groups including meteorological (deficit in precipitation), agricultural (deficit in soil moisture), hydrological (deficit in runoff, groundwater, or total water storage), and socio-economic (considering water supply, demand and social response) droughts [329]. All types of droughts can be associated with sustained precipitation deficit. However, different elements of the hydrologic cycle respond to droughts differently. In this section, progress in remote sensing of drought-related variables and development of satellite-based drought severity indicators are reviewed.

1.2.1 Precipitation

A commonly used precipitation-based drought index is the Standardized Precipitation Index (SPI) [187], which was recommended by the World Meteorological Organization (WMO) as a global measure of meteorological drought [333, 115]. Deriving SPI involves describing the frequency distribution of precipitation using either a parametric distribution function [187] or a non-parametric approach [111] for different precipitation accumulation periods (e.g., 1-, 3-, or 6-month periods). The SPI is computed by transforming the cumulative probability of precipitation into the standard normal distribution. A sequence of negative SPI indicates a dry period, while a sequence of positive values represent a wet spell. In addition to SPI, precipitation percentiles and the Percent of Normal Precipitation (PNP) [323] are also used as measures of departure from the climatology and thus, wet/dry conditions.

Several techniques have been developed for routine retrieval of rainfall using satellite data collected in multiple wavebands. Satellite IR and VIS images of cloud-top temperature can be converted into a precipitation rate using empirical statistical relationships [33, 143, 299].

Passive microwave (MW) sensors offer a more physically-based approach to instantaneous precipitation estimation [166, 165]. While MW sensors provide more accurate precipitation information, they are limited by their infrequent overpasses (≈ 2 observations per day for any location). GEO IR/VIS data, on the other hand, provide more frequent precipitation information ($\approx$ 15-30 min) although with higher uncertainty [280]. Studies suggest that combining both satellite MW and IR information leads to better precipitation estimates, especially of diurnal patterns, by combining the strengths of both types of sensors [144]. Currently, several satellite precipitation data sets are available to the public including the CPC Morphing Technique (CMORPH) [144], Tropical Rainfall Measuring Mission (TRMM) Multi-satellite Precipitation Analysis (TMPA) [132], Precipitation Estimation from Remotely Sensed Information using Artificial Neural Networks (PERSIANN) [128, 281, 125], and the Global Precipitation Climatology Project (GPCP) [4] – for a comprehensive review of precipitation algorithms see, [170, 153]. These data sets have been extensively intercompared and validated against ground-based observations [12, 293, 70, 49].

Satellite precipitation data sets have been widely used for both model-based and data-driven drought monitoring [21, 226, 58]. The experimental African Drought Monitor integrates satellite observations of precipitation for assessing hydrologic conditions [268]. One limitation of current near real-time satellite precipitation products is their short length of record. There are a number of products that provide low resolution long-term records (e.g., GPCP); however, they do not provide real-time observations necessary for operational drought monitoring systems. In a recent study, a near real-time satellite-based precipitation data set was proposed for operational drought monitoring that combines the near real-time satellite data with the long-term GPCP observations using a Bayesian data merging model [13]. The data set includes SPI based on PERSIANN and TMPA with climatology obtained from GPCP observations. The Bayesian data merging component makes the data from different sensors/algorithms climatologically consistent for drought monitoring. A sample merged product of GPCP (1979-2009) and PERSIANN (2010-present) is presented for July 2010 in

Figure 1.1. The figure shows that the merged product captures the 2010 Russian drought [321], as well as the 2010 Amazon drought [171, 185]. Furthermore, the figure highlights the precipitation deficit in East Africa, which led to a major drought during 2010-2011 [84]. The main advantage of this data set is that near real-time satellite data are available to the public within hours to days from the original observations, allowing for near real-time drought monitoring.

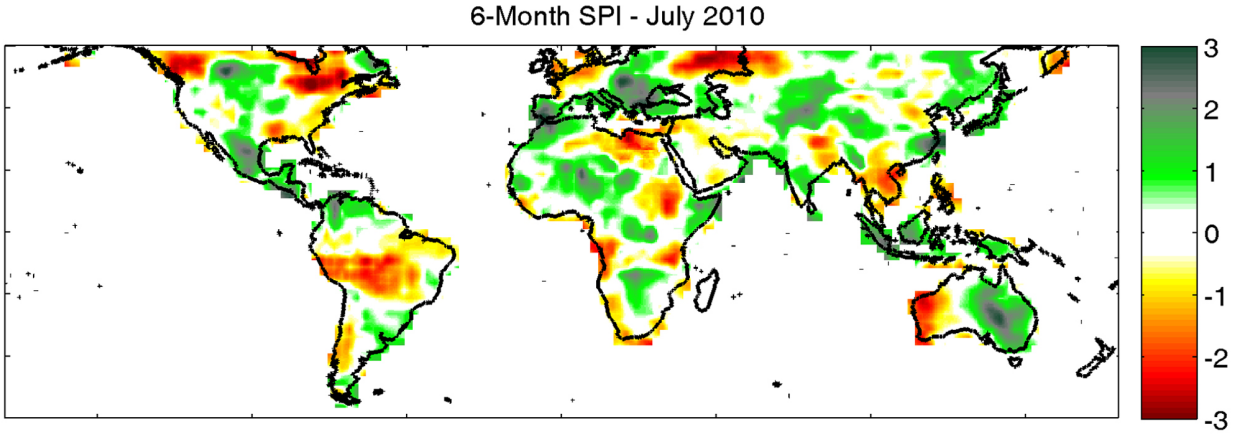

Figure 1.1: Combining different remote sensing data sets (here, GPCP and PERSIANN) for global near real-time drought monitoring using Standardized Precipitation Index (SPI) - July 2010.

1.2.2 Soil Moisture

Soil moisture is a fundamental component of the water cycle and plays a key role in drought monitoring and prediction, especially in water-limited ecosystems [62]. Soil moisture is often used as a measure of agricultural drought since it affects plant growth and productivity [42, 329]. A number of soil moisture-based indices have been developed and used for drought monitoring, including the Standardized Soil Moisture Index (SSI) [110] and the soil moisture percentile [267, 313]. Soil moisture is a particularly important variable for monitoring drought persistence and development [5]. The input soil moisture to these drought indicators can be obtained from land surface model simulations or from satellite estimates.

Most satellite soil moisture algorithms are based on passive MW [218, 138, 217], active MW [311, 289], or a blend of data from both types of sensors [331, 103, 74, 175]. The principal of MW-based soil moisture retrieval relies on the relationship between soil permittivity and liquid water content. There are empirical relationships that link passive MW brightness temperature and active MW backscattering to volumetric water content of soil. MW soil moisture observations typically represent the top 2-5 cm of soil depth [74, 218, 318]. For root-zone soil surface moisture estimates, MW soil moisture observations can be coupled to an appropriate land-surface model. For a comprehensive review of optical, thermal, passive MW, and active MW soil moisture monitoring approaches, see [318].

The long-term satellite-based soil moisture time series obtained from the Water Cycle Multi-Mission Observation Strategy (WACMOS) have been used for drought detection and monitoring in the Horn of Africa region [19]. The United States Department of Agriculture (USDA) International Production Assessment Division (IPAD) estimates surface and root-zone soil moisture with a two-layer modified Palmer soil moisture model forced by global precipitation and near-surface air temperature measurements [225]. In this approach, the near-surface air temperature is used to approximate potential evapotranspiration, although this approach has limitations in energy-limited evapotranspiration estimation [193, 65]. Soil moisture data retrieved from the Advanced Microwave Scanning Radiometer on Earth Observing System (AMSR-E) [137] have been integrated into the real-time USDA IPAD soil model to improve drought monitoring and prediction [43].

Recently, the Climate Change Initiative (CCI) for Soil Moisture offers global satellite-based soil moisture data derived from multiple sensors [310, 175]. As the CCI Soil Moisture dataset provides over 30 years of data, it can be used for monitoring agricultural drought, and monthly or seasonal changes in soil moisture patterns within a much longer historical context than most remote sensing-based data products derived from a single sensor or satellite mission (see Figure 1.2). The CCI soil moisture data have gaps, mainly over densely vege-

tated land areas, even at monthly scales (see the Amazon and central Africa in Figure 1.2). However, there are opportunities to assimilate data sets like CCI into land surface models, or to apply satellite-derived datasets for calibration of land surface model parameters to generate long-term, consistent soil moisture fields [246]. It is also noted that the spatial patterns in the CCI soil moisture and satellite precipitation data are generally consistent, even though they are sampling different components of the hydrologic budget (e.g., compare Australia and Russia in Figures 1.1 and 1.2). The CCI soil moisture data have not been fully explored for global drought monitoring and assessment yet, and it is anticipated that future studies on global trends and patterns of droughts will use this data set.

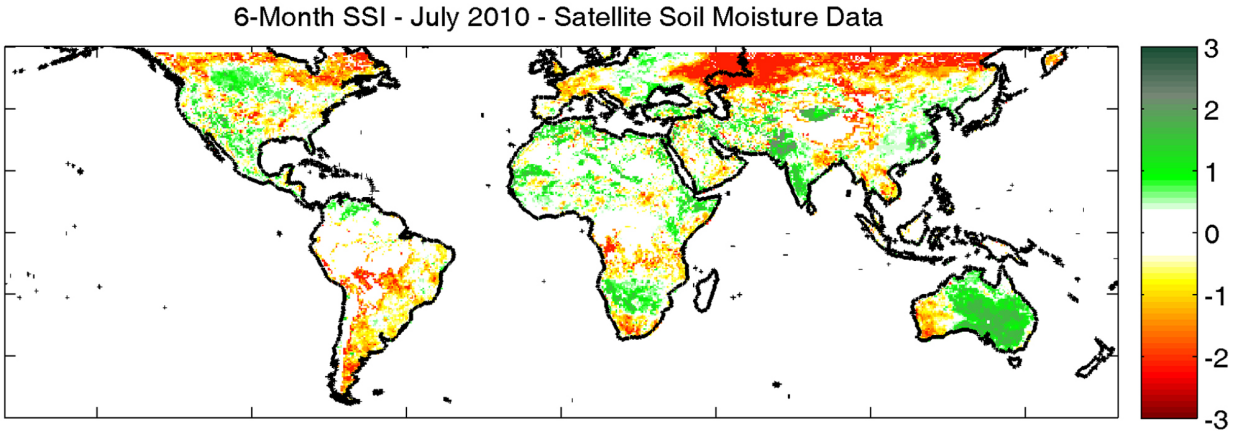

Figure 1.2: Standardized Soil Moisture (SSI) based on CCI satellite soil moisture observations - July 2010.

1.2.3 Groundwater and Terrestrial Water Storage

Estimates of drought impacts on terrestrial water storage and groundwater conditions at regional to global scales can be obtained using the Gravity Recovery and Climate Experiment (GRACE) mission. GRACE responds to all factors that change the gravity-field of an area, including the terrestrial water storage (TWS). Launched in 2002, the GRACE mission tracks global variations in gravity fields that can be converted into estimates of TWS [252]. The principle of gravimetry and TWS estimation relies on the fact that bulk surface and sub-

surface water mass has a gravitational potential that can alter the Earth's gravity field, allowing changes in the Earth's gravitational field to be used as an indicator of changes in the total amount of water stored in the vertical hydrologic continuum. GRACE consists of two identical satellites that orbit the Earth at an altitude of approximately 500 kilometers, and separated from one another by a distance of about 220 kilometers. Changes in the Earth's gravity fields alter the distance between the two spacecraft. Having accurate measures of the distance between the two spacecraft, one can quantify temporal TWS anomalies, which include the sum of surface water, groundwater, soil moisture, snow/ice, and moisture stored in vegetation [250].

Having TWS, changes to groundwater ΔG can be approximated as $\Delta G = \Delta TWS - \Delta SM - \Delta SWE$, where SM and SWE represent soil moisture and snow water equivalent, respectively [251]. GRACE-based TWS data have been widely used for drought monitoring and water storage assessment over different areas including the Canadian Prairie [339], Australia [169, 303, 304], the Amazon River basin [51], and western and central Europe [172]. During the 2011 Texas drought, the TWS data set was found to be a valuable tool for monitoring statewide water storage depletion, and for linking meteorological and hydrological drought conditions [181].

Currently, GRACE provides twelve years of data, which may not be sufficient for climatological drought assessment. An additional limitation of GRACE data for regional drought assessments has been the spatial resolution of ¿150,000 km^2 per pixel for GRACE TWS data [127]. Recently, GRACE data have been downscaled to higher resolutions via assimilation into land surface models [341]. This approach offers potential for improved drought monitoring and assessment of associated reductions in groundwater supplies at finer spatial scales. Using the GRACE Data Assimilation System (GRACE-DAS) [341] and the Catchment Land Surface Model (CLSM) [164], a GRACE-based drought indicator has been developed and integrated into the United States and North America Drought Monitor [127]. In addition

to drought monitoring, GRACE data can potentially be used for assessing drought recovery and termination. Given that GRACE offers information on the total water storage deficit [291], it can be used to estimate the amount of water (precipitation) needed to recover from drought events.

1.2.4 Evapotranspiration

Evapotranspiration (ET) is an important component of the water and energy cycle, reflecting mass and energy exchange between the atmosphere and ecosystem [265, 316]. Several recent studies highlight the importance of temperature and atmospheric evaporative demand in drought assessment and characterization [65, 121, 193, 270, 7]. While ground-based measurement of ET at large spatial extents is challenging, remote sensing data sets offer a unique opportunity to provide large-scale estimates of ET. A unique feature of ET for drought monitoring is that it describes both water/moisture availability and the rate at which it is consumed [22]. Broadly, remote sensing based ET estimation methods can be categorized into the following groups based on (a) principles of water balance [16, 264], (b) principles of surface energy balance [17, 23, 266, 283], (c) vegetation indices [94, 338], and (d) hybrid approaches based on vegetation indices and surface temperature information [47]. Water balance models track changes in moisture in the soil for ET estimation, whereas energy balance models use Land Surface Temperature (LST) as proxy information for surface heat (i.e., sensible heat flux) and moisture/water fluxes [147, 219, 205, 93].

Several drought indicators have been developed that integrate ET as an input variable such as the Crop Water Stress Index (CWSI) [134, 136], Water Deficit Index (WDI) [203], Evaporative Stress Index (ESI) [27, 24], Evaporative Drought Index (EDI) [336], Drought Severity Index (DSI) [208], and Reconnaissance Drought Index (RDI) [295, 294].

The CWSI is based on the ratio of the actual ET (AET) to potential ET (PET), and is

expressed as: $CWSI = 1 - AET/PET$. The WDI, follows the same concept, but is based on the AET rate (λ_{AET}) and PET rate (λ_{PET}): $WDI = 1 - \lambda_{AET}/\lambda_{PET}$. The ESI is defined as the standardized anomalies in the ratio of AET to PET [27]. In this approach, the ET estimation is based on thermal infrared remote sensing data and the Atmosphere-Land Exchange Inverse (ALEXI) model [25, 194, 28]. Figure 1.3 shows the ALEXI-based Evaporative Stress Index (ESI) for July 2010, derived using MODIS day-night land surface temperature differences. ESI clearly shows deficits in actual evapotranspiration associated with drought conditions particularly over Russia and central Asia, Brazil, South Africa and southwestern Australia. Evaluation studies indicate that ESI is a promising drought indicator for characterizing streamflow and soil moisture anomalies [53], and provides valuable information for early warning of rapidly developing drought conditions, often referred to as "flash" droughts [26, 220]. Similar to ESI, EDI is based on AET and PET ($EDI = 1 - AET/PET$), and has been used to monitor drought at continental and global scales [337].

The DSI is defined as the summation of the normalized ratio of AET/PET and the Normalized Difference Vegetation Index (NDVI) [208]. In this approach, the ratio of AET/PET is derived using shortwave satellite observations from the Moderate-resolution Imaging Spectroradiometer (MODIS) within a Penman-Monteith ET formulation [206, 207, 209]. Results indicate that the DSI is consistent with not only precipitation-based drought indices, but also with satellite-based vegetation net primary production (NPP) [257] records. Unlike most drought indices, DSI is not a standardized measure of drought severity, but rather a dimensional index ranging from $[-\infty, \infty]$, where a lower index value indicates a more severe drought condition.

The RDI is defined as the ratio of the aggregated precipitation (P) and PET, and has been widely used in the literature for drought monitoring (e.g., [295, 294]). The P/PET ratio is also termed as the Aridity Index [301], and can be standardized for cross-comparison with other drought indicators. The RDI is different from the other indices in the sense that it does

not use AET. The RDI has been used with PET estimates derived from satellite-retrieved air temperature data [57]. However, this is a simplistic assumption and many other key meteorological variables affect PET [193, 65].

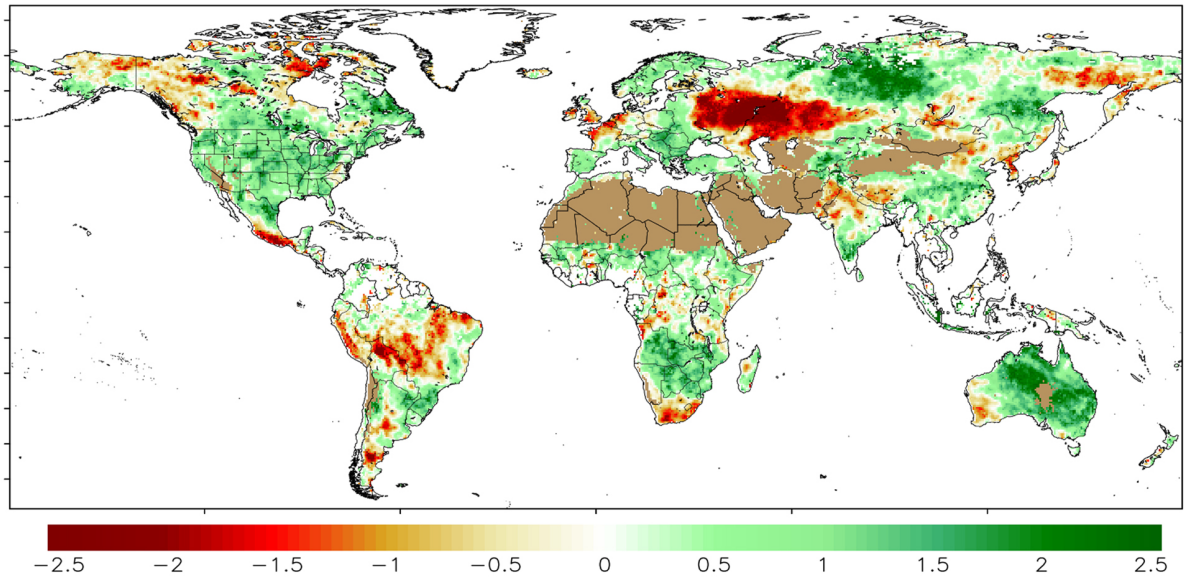

Figure 1.3: Evaporative Stress Index (ESI) for July 2010, expressed as standardized anomalies. Red indicates lower than normal AET/PET, or depressed rates of relative water use. Regions where ET is persistently low and standardized anomalies cannot be reliably determined are shown in brown.

1.2.5 Snow

Snow is considered a natural reservoir of water resources, and in some regions snow melt constitutes a substantial fraction of the annual runoff [163]. A winter snow deficit could potentially lead to a summer hydrological drought (e.g., reduced stream flows or groundwater levels) or agricultural drought (e.g., depleted soil moisture reserves to support plant functions) and hence, monitoring snow is fundamental to drought assessment in many regions. From a hydrological viewpoint, the drought-relevant snow parameters include: Snow Water Equivalent (SWE), Snow Covered Area (SCA), Snow Depth (SD), and Snow Albedo (SA) [163, 222]. Remotely sensed snow estimation methods can be broadly categorized into three groups: (a) optical; (b) MW; and (c) composite optical and MW. Optical-based prod-

ucts provide estimates of only SCA, whereas MW-based and composite products provide information on SCA, SD and SWE.

The basis of optical snow monitoring relies on the fact that snow exhibits a strong spectral gradient in reflectance, from high albedo in visible wavelengths to low reflectance in middle IR wavelengths [67, 163, 332]. Thus, snow can be monitored using the ratio of the visible reflectance (R_{VIS}) and the middle IR reflectance (R_{mIR}) [254]. Alternatively, snow can be detected using the Normalized Difference Snow Index (NDSI) defined as $(R_{VIS} - R_{mIR})/(R_{VIS} + R_{mIR})$ [109]. A suite of optical-based snow products are available from MODIS with a wide range of temporal and spatial resolutions [109]. A number of snow algorithms have also been developed based on the Advanced Very High Resolution Radiometer (AVHRR) satellite data record [277]. However, the accuracy of optical-based snow estimates can be compromised by clouds that exhibit similar spectral features [163, 44]. Furthermore, persistent cloud cover can hinder temporally continuous snow monitoring.

Microwave radiation, on the other hand, penetrates through clouds and provides a unique opportunity for temporally continuous snow monitoring [163, 260]. More importantly, microwaves can penetrate into snow, allowing estimation of SWE and SD that cannot be obtained from optical-based methods. A number of algorithms have been developed for estimation of SCA using microwave data sets [102]. Microwave-based estimates of SWE and SD are mainly based on an empirical regression between variations in observed SWE and SD and the difference in brightness temperature in two low frequency channels [162]. There are static empirical algorithms in which one set of regression parameters are used [167, 99], as well as dynamic empirical algorithms in which different regression coefficients are used in various regions and for different seasons [83, 150].

Currently, microwave sensors are only available onboard polar orbiting satellites that have longer revisit times relative to optical sensors onboard geostationary satellites. For this reason, the temporal frequency of microwave-based snow estimates is typically lower than

those of the optical-based products. Recently, snow retrieval algorithms have been developed based on merged optical and microwave data sets to address limitations of individual sensors [82, 173].

Remotely sensed and in situ snow information has been used in a number of drought studies [326, 163, 222, 106, 201]. Most studies focus on assimilating satellite snow information into land surface or hydrological models to improve streamflow simulation and hence, hydrological drought prediction [63, 31]. Unlike other drought-related variables, snow-based indicators of drought are still in their infancy, primarily because there is a lag between snow occurrence and change in surface water and soil moisture availability that varies in space and time. Snowmelt runoff could affect water availability in a few weeks (e.g., low elevation snow and in lower latitudes) or a few months (e.g., high elevation snow and in higher latitudes). This lag time is a significant strength and could lead to early drought warning. However, even over one particular location, depending on seasonal temperatures and the timing of snow accumulation, the lag time from snowfall, snowmelt, and runoff varies substantially. This highly-variable lag is the main challenge in deriving snow-based indicators for drought monitoring.

1.3 Progress in Remote Sensing of Drought from an Ecological Perspective

Drought can be assessed based on observed changes in vegetation health and land cover from remotely sensed data [297, 276, 214]. The launch of the first AVHRR instrument in 1979 transformed remote sensing of drought by providing high temporal resolution information for systematic monitoring of vegetation patterns and conditions. Quantitative assessment of vegetation condition is generally based on the spectral signature of vegetation greenness

expressed in the red (R) and near-infrared (NIR) portions of the electromagnetic spectrum [42].

The Normalized Difference Vegetation Index (NDVI) [256] is the most frequently used vegetation index [296, 149, 85] and the first remote sensing-based measure used to monitor agricultural drought. The NDVI is the difference between reflected R and NIR radiation divided by the their sum [256]: $(NDVI = (\rho_{NIR} - \rho_R)/(\rho_{NIR} + \rho_R))$. Since the soil spectrum and non-vegetated surfaces do not exhibit distinct differences in spectral absorption between the R and NIR bands, the NDVI can be used to separate vegetation from the soil background [149] and provide a measure of general vegetation health. Time series decomposition [64, 182] provides the means to assess rare or recurrent vegetable conditions, which may be related to deep-root or shallow-rooted vegetable types in carbon ecosystems.

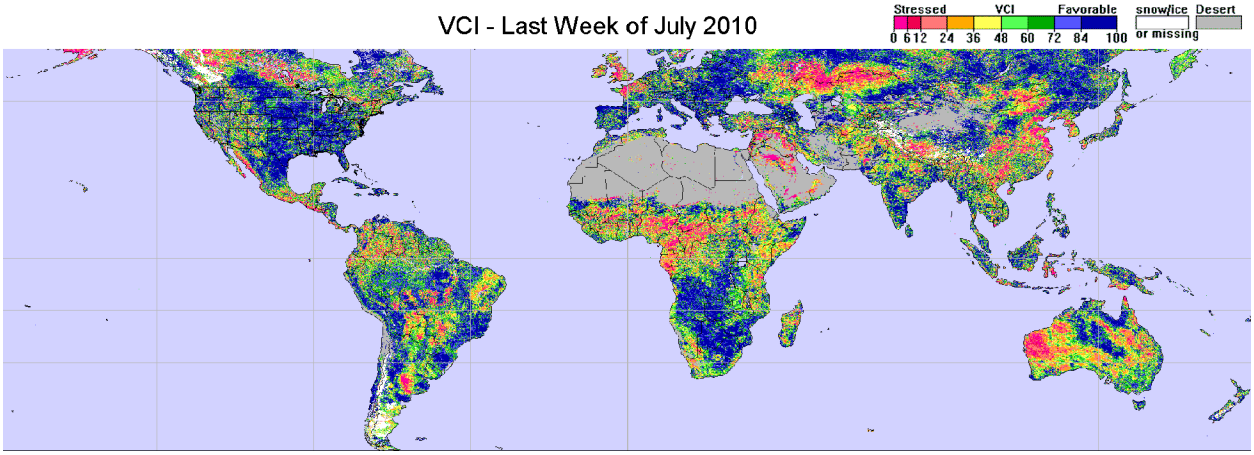

Figure 1.4: Vegetation Condition Index (VCI) for the last week of July 2010 (Source: NOAA/NIDIS Global Vegetation Health data).

A significant relationship has been reported between NDVI and precipitation and soil moisture [61, 80, 3, 120, 248, 315], and thus the NDVI (or its derivatives) has been widely used for drought assessment and vegetation health monitoring [297, 237, 215, 141, 190]. The general vegetation health can be temporally decomposed to monitor changes in recurrent (shallow-rooted) and persistent (deeper-rooted) vegetation for many landscapes across the globe [64, 182, 253]. This is particularly important when monitoring drought in savannahs

or areas with mixed trees and ecosystems across semi-arid regions [64].

Building on the original definition of NDVI, a number of other indicators have been developed such as the Transformed Vegetation Index (TVI) [60, 296], Perpendicular Vegetation Index (PVI) [325], Corrected Transformed Vegetation Index (CTVI) [231], and Thiam's Transformed Vegetation Index (TTVI) [290] - see [276, 230] for a comprehensive list. These indices describe the vegetation condition by combining spectral information from different parts of the electromagnetic spectrum that are sensitive to biophysical characteristics of vegetation, such as chlorophyll content, water content, and internal leaf structure.

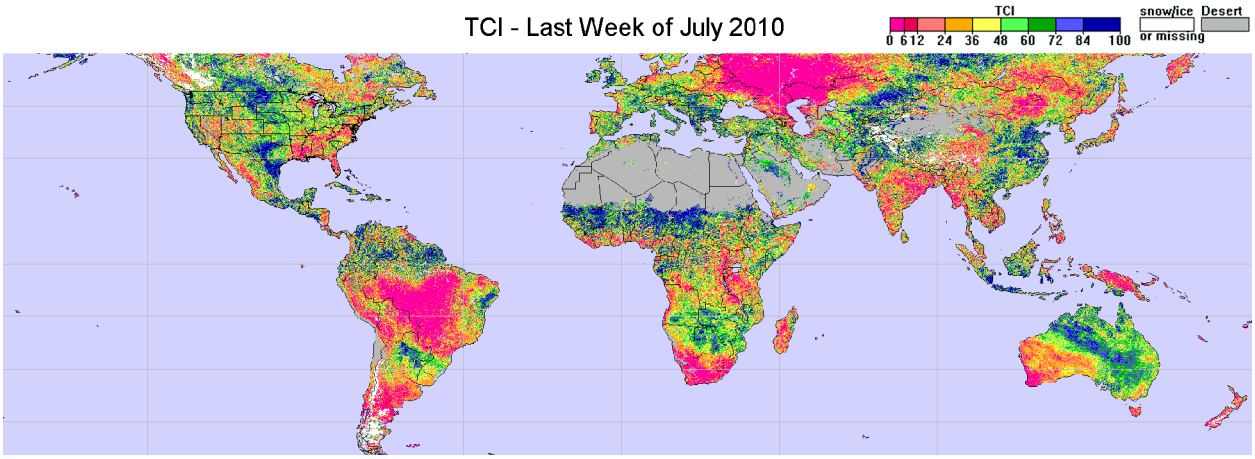

Figure 1.5: Temperature Condition Index (TCI) for the last week of July 2010 (Source: NOAA/NIDIS Global Vegetation Health data).

The Vegetation Condition Index ($VCI = (NDVI - NDVI_{min})/(NDVI_{max} + NDVI_{min})$), for example, scales NDVI values between its minimum and maximum values to separate the short-term weather signal from the long-term ecological signal for drought monitoring [158], and it has been used for monitoring drought and phonological change in several studies [160, 174, 241, 278, 190] - Figure 1.4. Use of the monthly VCI is more appropriate in areas with a large land management signal (e.g., cropping), and hence is suitable for monitoring agricultural drought [190]. A standardized form of NDVI, known as the Standardized Vegetation Index (SVI), is based on the z-score of NDVI values [232, 227]: $SVI = (NDVI_{ijk} - \overline{NDVI}_{ij})/\sigma_{ij}$. The SVI is computed for each pixel (i), week (j) and

year (k). The terms $\overline{NDVI}_{ij}$ and σ_{ij} denote the mean and standard deviation of the pixel (i) over $k = 1, \ldots, n$ years.

There are other indices based on R and NIR bands such as the Normalized Ratio Vegetation Index (NRVI) [37], Soil-Adjusted Vegetation Index (SAVI) [131], Perpendicular Drought Index (PDI) [92], Modified Perpendicular Drought Index (MPDI) [91], Distance Drought Index (DDI) [238], and Enhanced Vegetation Index (EVI) [129]. The latter, for example, improves sensitivity over high biomass regions, and reduces the soil background effects and atmospheric influence [145, 276, 130]. A recent study shows that the vegetation water indices outperform the vegetation greenness indices, including the EVI, in high biomass ecosystems [46]. More specifically, the Normalized Difference Infrared Index using MODIS band 6 (NDIIb6), and band 7 (NDIIb7) [133], and the D1640 [306] (Depth of MODIS band 6 (1640 nm) relative to the response between MODIS band 7 (2130 nm) and band 5 (1240 nm)) provide better agreement with precipitation, indicating that in high biomass environments variations in vegetation water content are more dynamic than changes in vegetation greenness properties [306, 46].

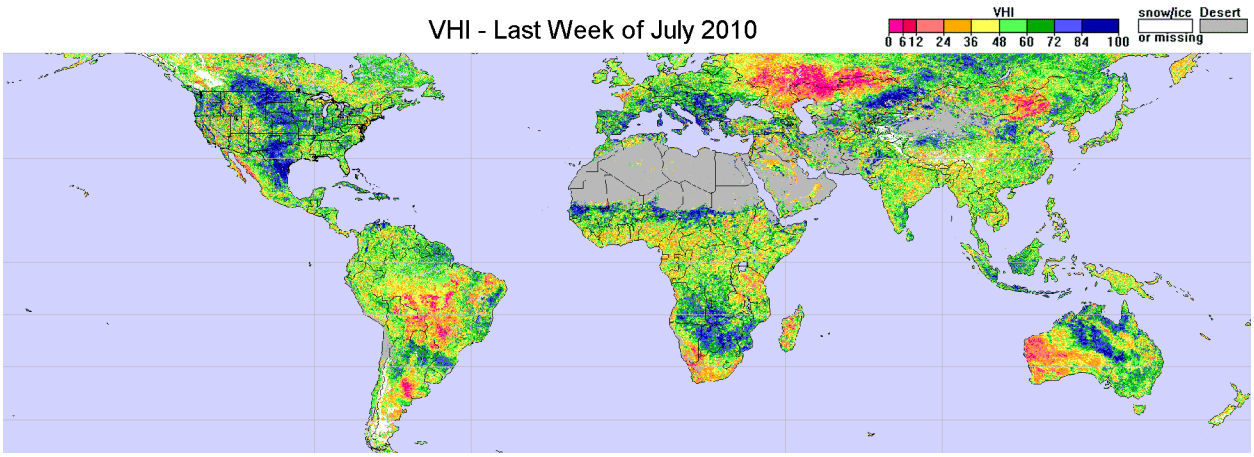

Figure 1.6: Vegetation Health Index (VHI) for the last week of July 2010 (Source: NOAA/NIDIS Global Vegetation Health data).

Drought stress can also be quantified using remotely sensed surface brightness temperature derived from thermal channels from multiple satellite instruments (e.g., AVHRR, MODIS,

VIIRS, TM, ETM+, TIRS). The land surface temperature (LST) computed from thermal infrared (TIR) bands has been found to provide valuable information on surface moisture conditions [107]. The Temperature Condition Index (TCI) is based on TIR observations to determine temperature-related vegetation stress. The TCI is defined as $TCI = 100(B_{max} - B)/(B_{max} - B_{min})$, where B, B_{max} and B_{min} denote the smoothed weekly temperature, and its multi-year maximum and minimum, respectively [156]. Using data from instruments such as AVHRR and MODIS, TCI may be computed at weekly time scales. An example of TCI for the last week of July 2010 is presented in Figure 1.5, which is consistent with drought information based on precipitation and soil moisture (Figures 1.1 and 1.2). One limitation of TCI is that it does not account for day-of-year or time-of-day, since it only relies on smoothed weekly temperatures and their multi-year maxima and minima. This issue has been addressed in the development of the Normalized Difference Temperature Index (NDTI) [191, 192] that can be considered as a time-of-day version of the CWSI [192].

Studies show that TCI coupled with VCI provides a powerful tool for monitoring vegetation stress and drought condition [278], and the two indices have been widely used over different regions [302, 140]. The reflective-based and thermal-based information have been combined for effective and integrated (vegetation-temperature) drought information using a combination of the reflective and thermal channels (e.g., combination of NDVI and LST - [190, 149, 40]). The Vegetation Temperature Condition Index (VTCI) [312] integrates NDVI, LST and thermal properties, and provides one index that reflects drought information based on both temperature and vegetation [229]. The Vegetation Health Index (VHI) is among the commonly used reflective-thermal indicators that integrates the VCI and TCI [156]: $VHI = \alpha VCI + (1-\alpha)TCI$, where α refers to the relative contribution of the VCI and TCI. Similar to the VCI and TCI, the VHI is typically computed on a weekly time scale, and has been used for both drought detection and early warning in different regions [262, 161]. An example of VHI is provided in Figure 1.6, which essentially combines information from Figures 1.4 and 1.5.

In recent years, various ways of combining NDVI and LST information have been explored for drought monitoring and impact assessment [287, 279]. Such methods rely on the relationship (typically, negative correlation) between LST and NDVI [168, 189, 190, 149]. The relationship between the LST and NDVI depends on the season-of-year and time-of-day [284, 191, 192]. Furthermore, the LST-NDVI relationship is associated with moisture condition and climatic/radiation regimes [149]. A comprehensive study of LST-NDVI relationship over the North American continent and during the summer growing season (April-September) showed that the LST-NDVI correlation is negative when water is the limiting factor for vegetation growth, while the correlation is positive when solar radiation is the limiting factor for vegetation growth [149]. It is recommended to restrict the use of empirical LST-NDVI relationships for drought monitoring to regions and periods with negative correlation between LST and NDVI (i.e., where water is the primary limiting factor [149]).

A number of vegetation stress and drought indicators have been developed using Short Wave Infrared (SWIR) data such as the Normalized Difference Water Index (NDWI) [88, 105, 104]. The NDWI is defined as the difference between two SWIR bands (typically, 0.86 nm and 1.24 nm) divided by their sum ($NDWI = (\rho_{0.86\mu m} - \rho_{1.24\mu m})/(\rho_{0.86\mu m} + \rho_{1.24\mu m})$). These two channels sense similar depth through the vegetation canopy and are less sensitive to atmospheric scattering effects than NDVI. Other SWIR bands (e.g., 1.55 μm, 1750 μm, 0.64 μm, 2.13 μm) have been also employed for deriving NDWI using data from the Landsat Thematic Mapper (TM) onboard Landsat 5, and the Enhanced Thematic Mapper (ETM) onboard Landsat 7 [139, 50, 318].

Sensitivity of NDWI and NDVI to drought conditions has been explored and different results have been reported [104, 105]. To combine information from NDVI and NDWI, the Normalized Difference Drought Index (NDDI) has been proposed as: $NDDI = (NDVI - NDWI)/(NDVI + NDWI)$ [104]. It is should be noted that SWIR bands respond to soil moisture and leaf water content differently and, thus, combining multiple SWIR bands

(rather than one SWIR band) with a NIR band may improve sensitivity for drought monitoring [319]. To address this issue, the Normalized Multi-band Drought Index (NMDI) has been proposed for monitoring soil and vegetation moisture condition using Moderate Resolution Imaging Spectroradiometer (MODIS) data [317]: $NMDI = (\rho_{0.86\mu m} - (\rho_{1.64\mu m} - \rho_{2.13\mu m}))/(\rho_{0.86\mu m} + (\rho_{1.64\mu m} - \rho_{2.13\mu m}))$. In NMDI, the 0.86 μm band is NIR whereas the 1.64 μm and 2.13 μm are SWIR bands. By combining information from different channels, the NMDI enhances the sensitivity to drought severity [317]. Similar efforts have focused on combining Visible data with SWIR information which led to the development of the Visible and Shortwave infrared Drought Index (VSDI) [343]. This indicator combines MODIS Blue (band 3), Red (band 1), and SWIR (band 6) information.

1.4 Composite and Multi-Index Drought Models

Several studies argue that drought monitoring efforts should be based on multiple variables/indicators [110, 152, 148] to provide a more robust and integrated measure of drought that captures the diverse range of vegetation response to drought across different ecosystems. The Vegetation Drought Response Index (VegDRI) [288, 45] integrates climate-based drought indices, satellite-based observations of vegetation conditions, and other biophysical information (e.g., land cover type, soil characteristics, elevation) to describe the levels of vegetation drought stress. The model concept of VegDRI builds upon the NDVI [256]. While NDVI is proven to provide valuable information on vegetation health, one may not be able to identify the root causes of vegetation stress solely from NDVI [117]. The main reason is that many factors such as fire, land cover change, plant disease, pest infestation, biomass harvesting, and flooding can cause anomalies in the NDVI similar to those caused by drought. To address this limitation, VegDRI incorporates climate-based data from SPI and the Palmer Drought Severity Index (PDSI) [224] as additional indicators of dryness, and

analyzes them in combination with satellite-based NDVI information [45].

In a recent study, a triple collocation analysis (TCA) of different soil moisture products (i.e., microwave AMSR-E, thermal remote sensing using ALEXI, and physically-based model simulations) has been suggested for composite drought monitoring [29]. The final composite soil moisture product takes advantage of the strength of each approach. The approach was validated for the 2010-2011 Horn of Africa drought, and has shown promising results for drought monitoring [29].

An alternative composite model is the Microwave Integrated Drought Index (MIDI) [342], designed for monitoring short-term drought, especially meteorological drought over semi-arid regions. The MIDI integrates satellite-based precipitation data from the Tropical Rainfall Measuring Mission (TRMM), and soil moisture and land surface temperature data from the Advanced Microwave Scanning Radiometer for EOS (AMSR-E): $MIDI = \alpha PCI + \beta SMCI + (1 - \alpha - \beta)TCI$ where PCI is the precipitation condition index, SMCI is the soil moisture condition index, and TCI is the temperature condition index. Based on the same concept, additional indices can be obtained based on two variables (e.g., $\alpha PCI + (1 - \alpha)SMCI$). A similar concept is used in the Scaled Drought Condition Index (SDCI) [247] which is a multi-sensor indicator designed for agricultural drought monitoring in both arid/semi-arid and humid regions. The SDCI combines TRMM-based precipitation data, with LST and NDVI information (all three scaled from 0 to 1) for composite drought assessment: $SDCI = \alpha LST + \beta TRMM + \gamma NDVI$, where $\alpha + \beta + \gamma = 1$. Evaluation of SDCI has shown that the SDCI outperformed the VHI and NDVI over both arid (Arizona and New Mexico) and humid/sub-humid (North Carolina and South Carolina) regions [247].

There are also composite approaches that combine physically-based model simulations and satellite observations for drought monitoring. For example, the United States Drought Monitor (USDM) [286] provides weekly drought monitoring information based on a composite of indicators from satellite observations (e.g., VegDRI, VHI, ESI, and GRACE TWS), in situ

measurements, and guidance from experts on the ground. The final product collectively analyzes all of this information, which is fused into a single USDM map of drought conditions relying on expertise from climatologists from across the United States.

Finally, the Global Integrated Drought Monitoring and Prediction System (GIDMaPS) [112] provides composite drought information based on the Multivariate Standardized Drought Index (MSDI) [111]. The MSDI has been developed for multi-index drought assessment using precipitation and soil moisture, and has been used in a number of drought studies [6, 110]. A unique feature of MSDI is that it combines meteorological and agricultural drought information into a composite assessment. Different data sets, including satellite observations and model simulations, can be used as inputs to obtain a composite drought map (see an example in Figure 1.7 based on global precipitation and soil moisture data). This model is standardized, and thus provides drought information comparable with other standardized indices such as SPI and SSI. Results indicate that MSDI provides objective drought information consistent with the USDM observations over the United States [111].

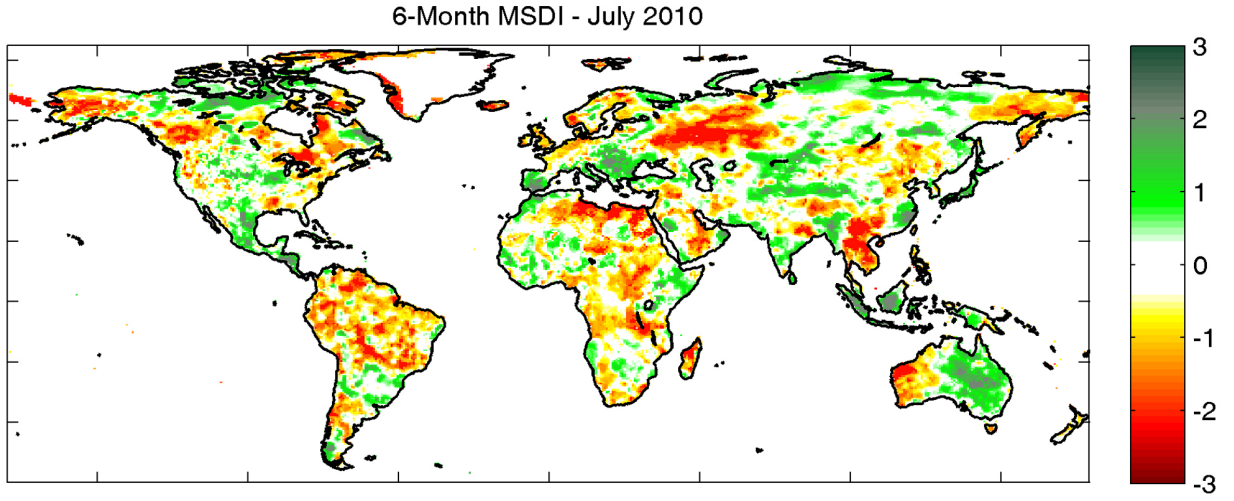

Figure 1.7: Multivariate Standardized Drought Index (MSDI) for July 2010, derived from the NASA's Modern-Era Retrospective Analysis for Research and Applications (MERRA-Land) precipitation and soil moisture data.

1.5 Research Gaps, Challenges and Opportunities

1.5.1 Microwave-Based Vegetation Indices

Vegetation indicators, such as NDVI obtained from optical satellite sensors, have been widely used to evaluate the impacts of droughts on ecosystems [296]. Optical-based vegetation indicators provide valuable information on vegetation response to climate variability. However, they are sensitive to cloud cover, atmospheric effects, aerosols, water vapor, and land cover condition [20, 273, 176]. One limitation of the optical-based indicators is that they primarily provide information on conditions at the top of the canopy, especially in densely vegetated regions [273]. A rapidly growing and influential area in remote sensing of drought is microwave-based vegetation monitoring [54, 20, 177, 142] that provides information on live aboveground biomass and canopy density. Unlike optical sensors, microwave sensors are less affected by atmospheric conditions, and can penetrate into dense canopy. Furthermore, microwave sensors can collect information on vegetation conditions during both day and night [273].

High spatial resolution, microwave-based vegetation monitoring is one key to improving our understanding of drought impacts on ecosystem conditions, especially for monitoring vegetation response and carbon cycling specifically during drought events. The vegetation optical depth (VOD; [195, 221, 142, 179]), for example, offers a unique approach for monitoring global phenology since it is sensitive to vegetation water content and canopy biomass. VOD has been extensively used to assess vegetation dynamics in drylands [20], overgrazing [178], and start-of-season analysis [142]. VOD and optical-based methods such as NDVI provide complementary information on the above-ground biomass and canopy top greenness, respectively [20]. Combining the two approaches provide insights on the ecosystem response that cannot be achieved from each individual model [20]. Collectively, microwave sensors offer a relatively long-term record for investigating the impact and relative importance of

droughts on global vegetation and biomass change. Future research in this direction can significantly improve our understanding of ecosystem responses to drought. The upcoming Global Ecosystem Dynamics Investigation (GEDI) lidar, which is a laser-based instrument designed for 3-D analysis of Earth's forests, will also offer a unique avenue to monitor forest degradation, carbon cycles and biomass.

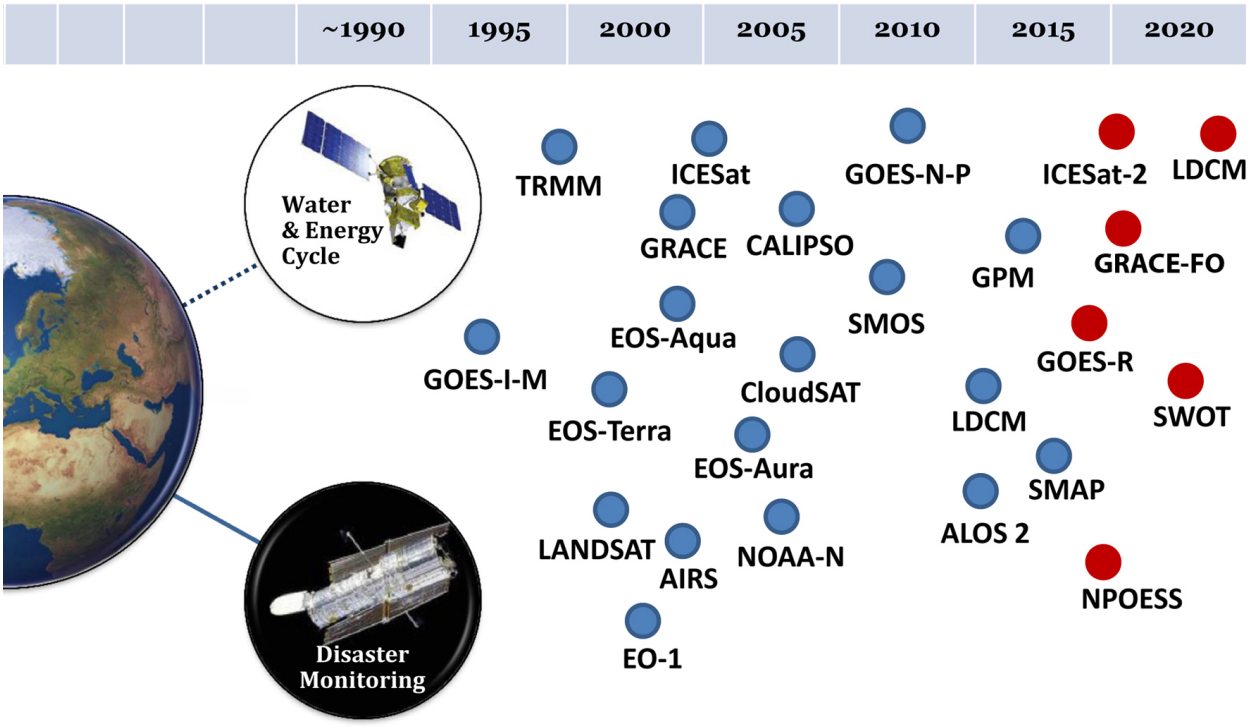

Figure 1.8: Current and future satellite missions relevant to drought monitoring and assessment (TRMM: Tropical Rainfall Measuring Mission; GRACE: Gravity Recovery and Climate Experiment; FO: FOllow-On; ICEsat: Ice, Clouds, and Land Elevation Satellite; CALIPSO: Cloud-Aerosol Lidar and Infrared Pathfinder Satellite Observations; EOS-Aqua: Earth Observing System Aqua; EOS-Terra: Earth Observing System Terra; EOS-Aura: Earth Observing System Aura; AIRS: Atmospheric Infrared Sounder; EO-1: Earth Observing-1; GOES: Geostationary Operational Environmental Satellite; NOAA-N: NOAA Polar Operational Environmental Satellites N Series; SMOS: Soil Moisture and Ocean Salinity satellite; ICESat-2: Ice, Clouds, and Land Elevation Satellite; GPM: Global Precipitation Measurement; LDCM: Landsat Data Continuity Mission; SWOT: Surface Water and Ocean Topography; SMAP: Soil Moisture Active-Passive; ALOS 2: Advanced Land Observing Satellite; NPOESS: National Polar-orbiting Operational Environmental Satellite System) – the list in not comprehensive.

1.5.2 Data continuity, consistency and management

Since the early 2000s, the number of satellite sensors and types of remote sensing observations have increased substantially, and many more are in the design and planning stages (see Figure 1.8 for a non-comprehensive list of missions). Some of the most important recent or upcoming missions relevant to drought monitoring include the Global Precipitation Mission (GPM), Geostationary Operational Environmental Satellites R series (GOES-R), GRACE Follow-On, SMAP, and SWOT missions (Figure 1.8). While these satellite missions provide opportunities to study droughts from different viewpoints, there are major challenges ahead such as data continuity, unquantified uncertainty, sensor changes, community acceptability, and data maintenance.

Data continuity is fundamental to reliable satellite data record development for drought applications. Most satellites are designed for less than a decade of operation, though many operate beyond their design life. Ideally, data sets should extend by planning for follow-up missions. However, planning, approval, and design processes of satellite missions can take decades and require substantial investments. The GPM, GOES-R, and GRACE Follow-On are examples of missions planned to avoid gaps in the current satellite-based precipitation and total water storage records. Another example is the Visible Infrared Imager Radiometer Suite (VIIRS; [146, 322, 307]), which is designed as the operational successor to MODIS and AVHRR. Long-term continuation of these and other satellite missions will remain an issue in the future as these systems age. The capability of extending multi-decadal observations to develop robust drought climatologies remains uncertain.

Another major challenge is to ensure that the data volumes are well managed and that the data records are easily available to the science community and the public. This requires major hardware infrastructure to serve the data, and data professionals to process, curate and disseminate the data. Securing funding for the required hardware and attracting long-

term support for maintaining staff for data management are very challenging.

1.5.3 Multi-Index Composite Drought Monitoring

Recent studies show that combining multiple data sets improves drought detection [112] and monitoring [208]. Several multi-index (multi-sensor) drought monitoring indicators/frameworks have been developed to improve description of drought onset, development and termination [152, 148, 288, 110, 286, 242]. Availability of multiple satellite data sets offers a unique avenue to explore multi-index or multivariate drought indicators.

Integration of snow into drought monitoring models is one of the least investigated areas and merits further exploration. The Snow and Cold Land Processes (SCLP) mission will provide microwave-based snow and snow water equivalent information [255]. Integration of snow information into seasonal precipitation or runoff forecasts could lead to a quantum improvement in drought monitoring and seasonal prediction in areas that rely on snowmelt such as the western U.S. Multiple data sets describing different but inter-linked environmental parameters provides the opportunity to develop more composite and multivariate (or multi-indicator) drought models similar to the ones discussed in Section 1.4.

Ground-based observations of many drought related variables (e.g., snow, soil moisture, water vapor, total water storage) are very limited or unevenly distributed across the world. This may limit development of multi-index indicators in data sparse regions. Given the variety of satellite observations (Figure 1.8), remote sensing allows moving toward an integrated multi-index composite drought assessment framework conceptually illustrated in Figure 1.9. However, multi-index and composite drought models are in their infancy. More research is needed to develop robust statistical and mathematical frameworks for generating multi-index drought information.

1.5.4 Improving early drought detection using satellite observations

Early drought detection is fundamental to pro-active decision-making and disaster preparedness. Previous studies indicate that precipitation-based indicators (e.g., SPI) are better for drought detection compared to other indicators (e.g., SSI) - [200, 110]. Different satellite data sets provide an opportunity to monitor droughts from multiple viewpoints and potentially improve drought detection. For example, a number of satellite missions and sensors (e.g., AIRS) provide near-surface air relative humidity information that is not currently being used for drought monitoring. Since near-surface air relative humidity directly influences evaporation, and as such is connected to precipitation (integrated a period of time), it is reasonable to expect that it could provide valuable drought information.

Figure 1.10 displays the SPI and Standardized Relative Humidity Index (SRHI [79]) derived by standardizing AIRS near-surface air relative humidity data using an empirical approach. Here, a generalized empirical standardization approach is used that can be applied to different variables for deriving consistent drought indicators [78]. The left and right panels in Figure 1.10 show drought conditions based on SPI and SRHI in May and July 2010, respectively. The 2010 Russian drought signal can be observed in relative humidity data as well. Furthermore, in May 2010 and two months prior to the peak of the event, SRHI shows a stronger and more severe drought signal. All these indicators suggest that satellite-based relative humidity can provide an opportunity for early drought detection. This, however, requires more in-depth research on consistency and reliability of relative humidity data for drought monitoring. In addition to relative humidity, there are many other satellite data sets that have not been fully explored for drought assessment, including water vapor, cloud cover, microwave emissivity, microwave-based vegetation optical depth, and solar radiation. More research on such data sets could improve early drought detection or contribute to better monitoring of drought development.

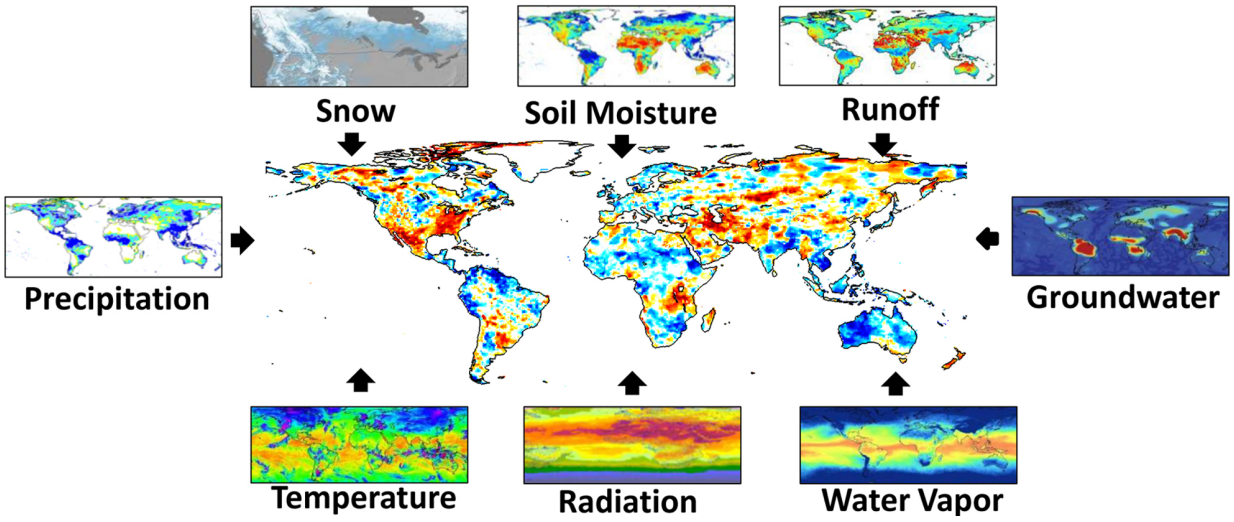

Figure 1.9: Multi-sensor (multi-index) composite drought monitoring using remote sensing observations: a schematic overview.

1.5.5 Developing climate data records

One of the major limitations of many of the currently available satellite datasets is their short length of record relative to meteorological stations, with Landsat and AVHRR-MODIS-VIIRS as notable exceptions. Some of the relevant satellite missions and sensors (e.g., GRACE) provide only slightly over a decade of data, which may not be sufficient to study droughts from a climatological perspective, though they provide valuable anomalies for drought impact assessment (e.g., [77]). Also, a number of satellite sensors are research instruments and there is no guarantee that the same (or sufficiently similar) instruments will be launched again to replace aging or failed instruments. Data continuity in the future largely relies on support for long-term investments in satellite Earth observations.

Lack of guaranteed support and commitment to invest in this field is a major roadblock for establishing consistent, long-term remote sensing data records necessary for accurate anomaly detection against a historical baseline. However, sensors that provide short-term records still provide valuable drought monitoring information, especially for drought impact assessment [250, 77]. There has been some work to create longer inter-sensor data records

for key remote sensing variables, such as the NDVI, by merging data from multiple satellite sensors such as AVHRR and MODIS [298]. Effective models and algorithms need to combine multiple data sets [13] from different sources and/or assimilate satellite observations into model simulations [127, 31, 341] to generate long-term environmental and climate data records.

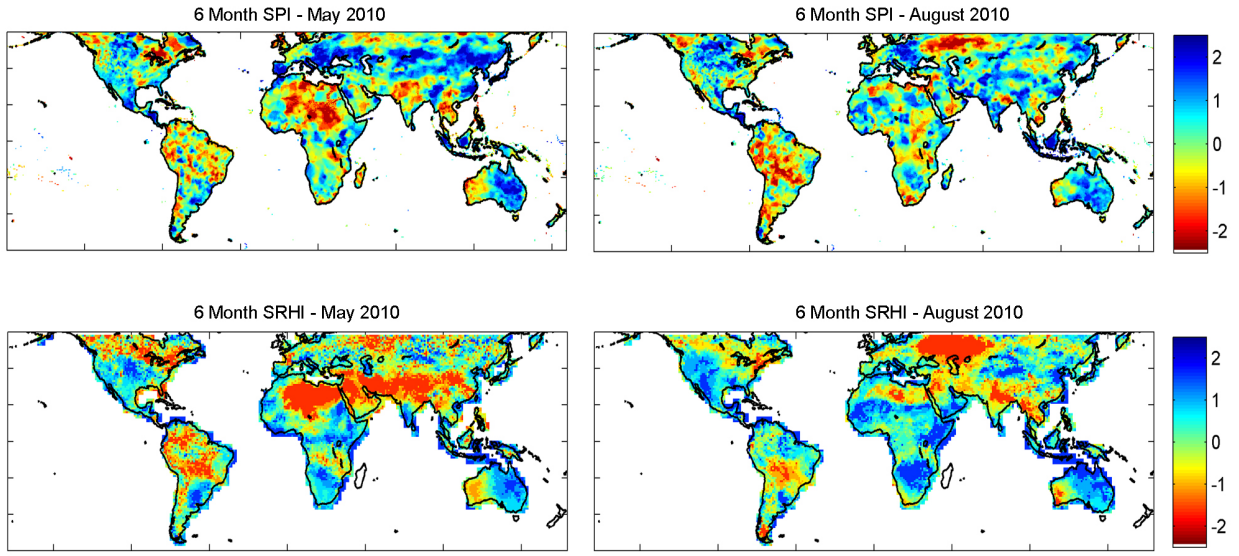

Figure 1.10: (top row) Standardized Precipitation Index (SPI) and (bottom row) Standardized Relative Humidity Index (SRHI) for May 2010 (left panels) and August 2010 (right panels).

1.5.6 Uncertainty

Satellite data sets are subject to retrieval and sensor uncertainties that are often unquantified [66, 196, 234]. For this reason, several models and indicators have been developed for uncertainty assessment of satellite observations [89, 75, 11, 126]. However, most satellite-based data products still do not provide uncertainty estimates or bounds. Land-surface and hydrologic models that use remote sensing data (as input or for data assimilation) are subject to other sources of error, including model structural and parameters uncertainties. Understanding input data uncertainty is fundamental to evaluating uncertainty of model-based simulations that use remote sensing information as input. Lack of uncertainty information

may prevent integration of satellite data into decision-making and operational applications.

More emphasis should be given to adequately characterizing the strengths and limitations of specific remote sensing tools and products, the results of which should be communicated to the general decision-making population in a non-technical manner. Further research in uncertainty assessment is required to develop uncertainty products (bounds) for current and future satellite data sets. This will significantly improve usability and acceptability of satellite observations within the drought community because these established bounds can provide guidance on the most appropriate times and locations to use data for a targeted decision making process.

1.5.7 Community acceptability

Product development as well as translating remote sensing observations and scientific data outputs in forms tailored for drought applications are critical for effective and sustained use of monitoring systems. This part of applied remote sensing is often overlooked, but is essential in communicating valuable new information from new and emerging satellite-based systems and tools. Clearly defining basic elements, such as cartographic color schemes, summarization of retrieved information (e.g., estimated soil moisture versus soil moisture anomaly), and data formats, is one of the most important parts of the data-to-information process of remote sensing tools developed for the drought community. Engaging drought experts and key decision makers in this process is key to developing useful and applicable information from remote sensing that will be more widely accepted and integrated into operational drought monitoring and early warning systems. Finally, providing quantitative measures of uncertainty of remote sensing information will improve community acceptability of the data.

1.5.8 Research gaps and objectives

In this dissertation, we propose three methodologies for improving the remote sensing of drought:

1. Drought indicators such as SPI are generally derived using parametric approaches in which climate data (i.e. precipitation) are fitted using a parametric distribution function. A single parametric distribution function, however, may not fit the entire data properly. On the other hand, using multiple parametric distribution functions lead to inconsistencies is the distribution of climate extremes. In chapter 2, we propose Standardize Drought Analysis Toolbox (SDAT) which offers non-parametric univariate and multivariate techniques for deriving drought indicators. SDAT techniques do not require parameter estimation and are statistically consistent.

2. Drought early detection has significant advantage for water resource and agriculture sectors. Precipitation and hence SPI are commonly used for drought early detection. Relative humidity which is defined as the ratio of actual water vapor to saturated water vapor is related to propitiation in the sense that precipitation is not expected in low humidity values. Chapter 3 introduces a new drought monitoring tool, Standardized Relative Humidity Index (SRHI). SRHI used AIRS relative humidity data to monitor droughts. We show that relative humidity which is not a common drought indicator, could detect drought onset earlier than precipitation.

3. Droughts and high temperatures typically result in high atmospheric evaporative demand and therefore high evapotranspiration rates. These lead to an increase in tree mortality and wildfire rates. In chapter 4, a multi-sensor multi index drought indicator is proposed to assess the impacts of recent western United States droughts on forest health. Combining multiple climate variables improve drought monitoring. We show that relative humidity, which has the potential for detecting drought onset earlier

than precipitation, along with temperature, can be used for assessing drought impacts during the summer and growing season. Precipitation, on the other hand, is a better variable for investigating the drought effects during winter period.

Chapter 2

A Generalized Framework for Deriving Nonparametric Standardized Drought Indicators

This Chapter has been published in Advances in Water Resources, Citation: Farahmand A., AghaKouchak A., (2015),A Generalized Framework for Deriving Nonparametric Standardized Drought Indicators, *Advances in Water Resources,* , *76* (140-145).

2.1 Introduction

Drought is an inevitable and recurring feature of the global water cycle that often leads to significant societal, economic, and ecologic impacts [329, 185, 10, 320, 124]. An essential step in analyzing a drought event is to define it based on relevant climatic variables/conditions [68]. Drought affects all elements of the hydrologic cycle, and hence can be defined with respect to different components of the water cycle. Numerous drought and dryness indices have been developed to describe the different types of droughts, including meteorological, agricultural, hydrological and socioeconomic [328].

One of the most common indices is the Standardized Precipitation Index (SPI; [187]), which describes precipitation condition relative to long-term climatology, and is known as an index of meteorological drought [116]. Many other drought indices have been developed based on one or more climate variables, including the Palmer drought severity index (PDSI, [223, 56]); Standardized Precipitation Evapotranspiration Index (SPEI; [309]); Standardized Soil Moisture Index (SSI, [110, 5]); Vegetation Drought Response Index (VegDRI, [288, 45]); Standardized Runoff Index (SRI, [275]); soil moisture percentile [267, 313]; Percent of Normal Precipitation (PNP, [323]), Multivariate Standardized Drought Index (MSDI, [111]), Crop Moisture Index (CMI, [224]); Remotely Sensed Drought Severity Index ([208]); and Evaporative Stress Index (ESI, [28]). Comprehensive reviews of drought indices are provided in **(author?)** [198] and **(author?)** [208].

Among the drought indices, SPI is one of the most commonly used indices that has been applied to local, regional and global scale studies (e.g., [199, 13, 314, 274, 30, 58]). The SPI is widely used, primarily for its simplicity, standardized nature, and flexibility of use across different time scales (e.g, 1-, 6-, 12-month) [116]. On the other hand, SPI has a potential limitation as it assumes that there exists a suitable parametric probability distribution function representative for modeling precipitation data [32].

SPI is typically derived by fitting a gamma probability distribution function to precipitation data. The accumulated Gamma probability is then transformed to the Cumulative Distribution Function (CDF) of the standard normal distribution. Though frequently used, the two-parameter gamma distribution may not be the best choice of distribution [240, 108]. Analyzing Texas droughts, **(author?)** [240] concluded that the SPI values are quite sensitive to the choice of parametric distribution function, especially in the tail of the distribution - see also **(author?)** [210]. Many parametric distribution functions-such as the three-parameter Pearson type III, normal, lognormal, Wakeby, Gamma, and kappa distributions-and different recommendations on the best choice of parametric distribution for modeling precipitation are reported (e.g., [108, 240, 32]).

On the other hand, **(author?)** [282] argued that the currently available indicators suffer from deficiencies including temporal inconsistency and statistical incomparability. Different indicators have varying scales and ranges and their values cannot be compared with each other directly. For example, SPI and PDSI cannot be directly compared as they have different scales [282]. A holistic approach to drought monitoring requires an investigation of multiple indicators (precipitation, soil moisture, runoff, evapotranspiration, etc.). The attractive feature of standardized indices is that they offer the opportunity to create statistically consistent indices based on precipitation (SPI), soil moisture (SSI), runoff (SRI), relative humidity (SRHI), etc. However, a generalized framework for generating spatially and temporally consistent drought indicators is essential in order to assess droughts based on multiple climate variables that often have different distribution functions.

This chapter introduces the Standardized Drought Analysis Toolbox (SDAT) that offers a generalized framework for deriving nonparametric univariate and multivariate standardized indices. The methodology can be applied to different climate and land-surface variables (precipitation, soil moisture, relative humidity, evapotranspiration, etc.) without having to assume the existence of representative parametric distributions. This is particularly useful

for drought information systems that offer data based on multiple drought indicators (e.g., [112, 202, 216, 271]). The same nonparametric framework can be used for deriving nonparametric standardized multivariate (joint) drought indices that can describe droughts based on the states of multiple variables. A multivariate drought model links individual indicators into a composite model as an overall assessment of drought. This chapter explains the mathematical concept behind SDAT, and provides example applications to different data sets. The paper is organized as follows. After this introduction, the nonparametric methodology and its differences with the original parametric model are described in Section 2. Example applications and results are presented in Section 3. The last section summarizes the findings and makes concluding remarks.

2.2 Methodology

In the original SPI, the frequency distribution of precipitation is described using a two-parameter gamma probability density function:

$$g(x) = \frac{1}{\beta^{\alpha}\Gamma(\alpha)} x^{\alpha-1} e^{\frac{-x}{\beta}} \tag{2.1}$$

where $\Gamma(\alpha)$ is the Gamma function, and x denotes precipitation accumulation. α and β are the shape and scale parameters of the gamma distribution that can be estimated using the maximum likelihood approach [71]. The cumulative probability $G(x)$ can be simplified to

the so-called incomplete cumulative gamma distribution function assuming $t = \frac{x}{\beta}$ [71]:

$$G(x) = \frac{1}{\Gamma(\alpha)} \int_0^x t^{\alpha-1} e^{-t} dt \tag{2.2}$$

Since Equation 2.2 is not valid for zero precipitation ($x = 0$), the complete cumulative probability distribution, including zeros, can be expressed as: $H(x) = q + (1-q)G(x)$, where q, and $1 - q$ are the probabilities of zero ($x = 0$), and non-zero ($x \neq 0$) precipitations. The SPI is then computed by transforming $H(x)$ to the standard normal distribution with a mean of zero and variance of one [187]. A sequence of positive SPI indicates a wet period, and a sequence of negative values represents a dry period.

Instead of the Gamma (or any other parametric) distribution function, the empirical probability can be used to derive a nonparametric standardized index. We propose to derive the marginal probability of precipitation (and other variables) using the empirical Gringorten plotting position [101]:

$$p(x_i) = \frac{i - 0.44}{n + 0.12} \tag{2.3}$$

where, n is the sample size, i denotes the rank of non-zero precipitation data from the smallest, and $p(x_i)$ is the corresponding empirical probability. Using this empirical approach, one does not need Equations 2.1 to 2.2 to derive the parametric probabilities. The outputs

of Equation 2.3 can be transformed into an Standardized Index (SI) as:

$$SI = \phi^{-1}(p) \tag{2.4}$$

where ϕ is the standard normal distribution function, and p is probability derived from Equation 2.3. One can also standardize the percentiles using the following commonly-used approximation of Equation 2.4 [1, 210, 72]:

$$SI = \begin{cases} -\left(t - \frac{C_0 + C_1 t + C_2 t^2}{1 + d_1 t + d_2 t^2 + d_3 t^3}\right) & \text{if } 0 < p \leq 0.5 \\ \\ +\left(t - \frac{C_0 + C_1 t + C_2 t^2}{1 + d_1 t + d_2 t^2 + d_3 t^3}\right) & \text{if } 0.5 < p \leq 1 \end{cases} \tag{2.5}$$

where $c_0 = 2.515517$; $c_1 = 0.802583$; $c_2 = 0.010328$; $d_1 = 1.432788$; $d_2 = 0.189269$; $d_3 = 0.001308$; and

$$t = \begin{cases} \sqrt{\ln \frac{1}{p^2}} \\ \\ \sqrt{\ln \frac{1}{(1-p)^2}} \end{cases} \tag{2.6}$$

Several studies argue that a single drought index may not be sufficient to describe all aspects of drought onset, persistence and termination [110, 68, 6, 148]. For example, **(author?)** [110] illustrated that precipitation detects the drought onset earlier, while soil moisture describes the drought persistence more reliably (see also, [117, 76]). The suggested nonparametric

approach can be extended to higher dimensions to derive multivariate drought indicators. Having two drought-related variables (e.g., X = precipitation and Y = soil moisture), the bivariate distribution is defined by **(author?)** [111] as: $p_j = Pr(X \leq x, Y \leq y)$, where p_j is the joint probability of X and Y (e.g., precipitation and soil moisture).

Having the joint probability of two (or more) drought-related variables, the empirical probability can be derived using the multivariate model of the Gringorten plotting position introduced by [340] $p_j(x_k, y_k) = \frac{m_k - 0.44}{n + 0.12}$, where m_k is the number of occurrences of the pair (x_i, y_i) for $x_i \leq x_k$ and $y_i \leq y_k$, and n is the sample size [111]. Similar to univariate drought indices, the joint probability of X and Y can be standardized using Equation 2.4 or Equation 3.3 to derive a Multivariate Standardized Drought Index ($MSDI = \phi^{-1}(p_j)$). This concept has been tested and validated for precipitation and soil moisture for monitoring the 2012 United States Drought [111].

The above univariate and multivariate nonparametric standardized approach can be used with different variables, such as precipitation, soil moisture, and relative humidity. It should be noted that there are other univariate and multivariate nonparametric methods that can be used to derive nonparametric indicators (e.g., Weibull). For long-term data sets, necessary for drought assessment, typically different empirical methods lead to similar results [300]. There are also alternative methods for deriving joint empirical probabilities such as the Kendall τ [155, 90, 300] that can be used for deriving nonparametric multivariate indicators based on multiple variables (e.g., MSDI).

2.3 Results

Since the probability distribution of precipitation is different at various climate conditions, a parametric approach to SPI may lead to inconsistent results, particularly at large scales

(continental to global). The reason is that in certain areas, a distribution function (e.g., gamma) may fit the data, while in another region, the choice of the distribution function may not fit. As an example, Figure 2.1 displays the fit of the Gamma (left) and lognormal (right) distributions to the Global Precipitation Climatology Project (GPCP; [4]) data from 1979-2012. The dark pixels refer to locations where the Kolmogorov-Smirnov test rejects the null-hypothesis that the Gamma (left) or lognormal (right) distribution fits the precipitation data.

An alternative option would be using multiple distributions and selecting one that passes a goodness of fit test such as the Kolmogorov-Smirnov (KS). However, even in a multi-distribution approach, the distribution tails [8] of SPI values would change across space, as the best fitted distribution might be different from grid to grid. Sensitivity of the SPI tails to distribution parameters [210], and hence differences at the tails of SPI across space, may lead to inconsistent or biased interpretation of extreme droughts in different regions. In a multi-distribution approach where the best choice of distribution changes across space, the characteristics of extremes change as well. For example, in two locations with different precipitation distribution functions, a SPI value may correspond to different occurrence probabilities.

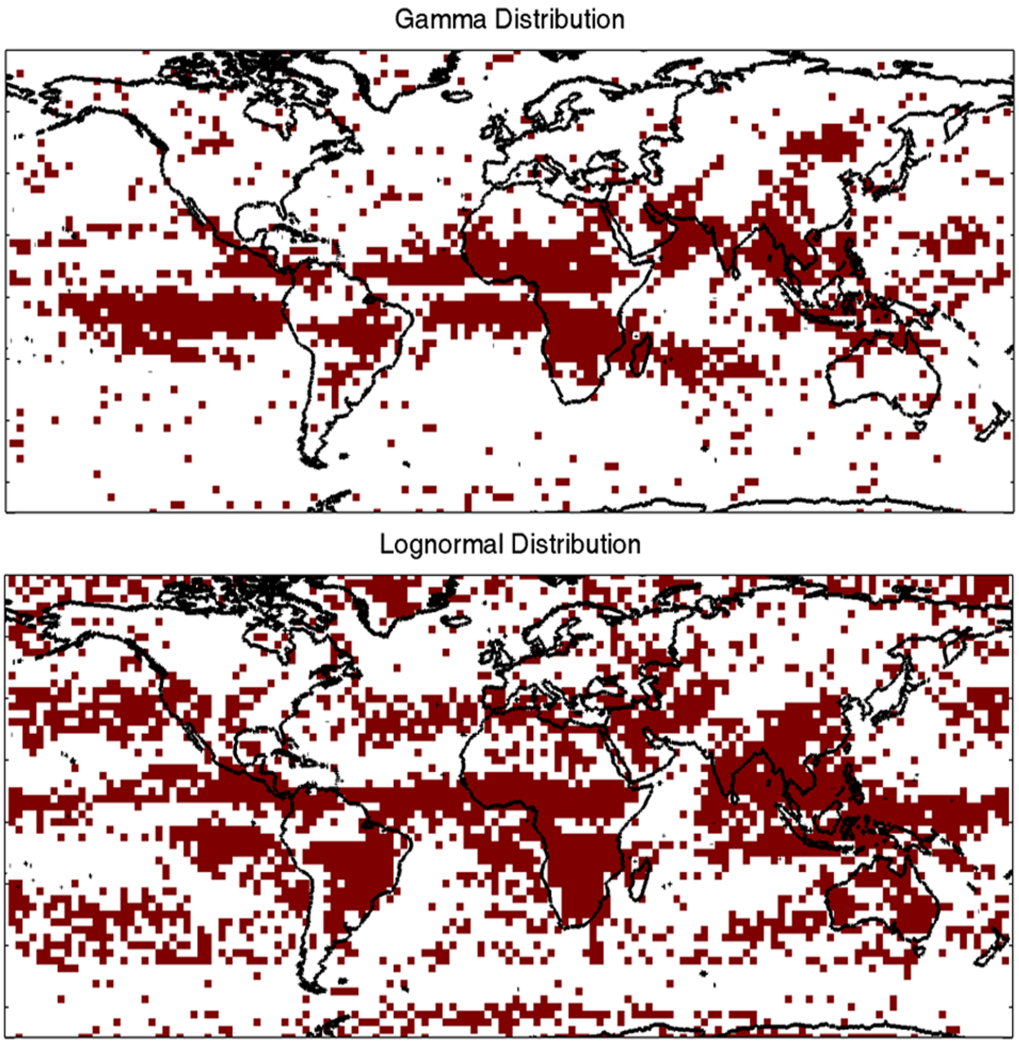

Figure 2.1: Representativeness of the Gamma (left) and lognormal (right) distributions for describing monthly precipitation accumulations. The dark pixels refer to locations where the Kolmogorov-Smirnov test rejects the null-hypothesis that the Gamma (left) or lognormal (right) distribution fits the precipitation data.

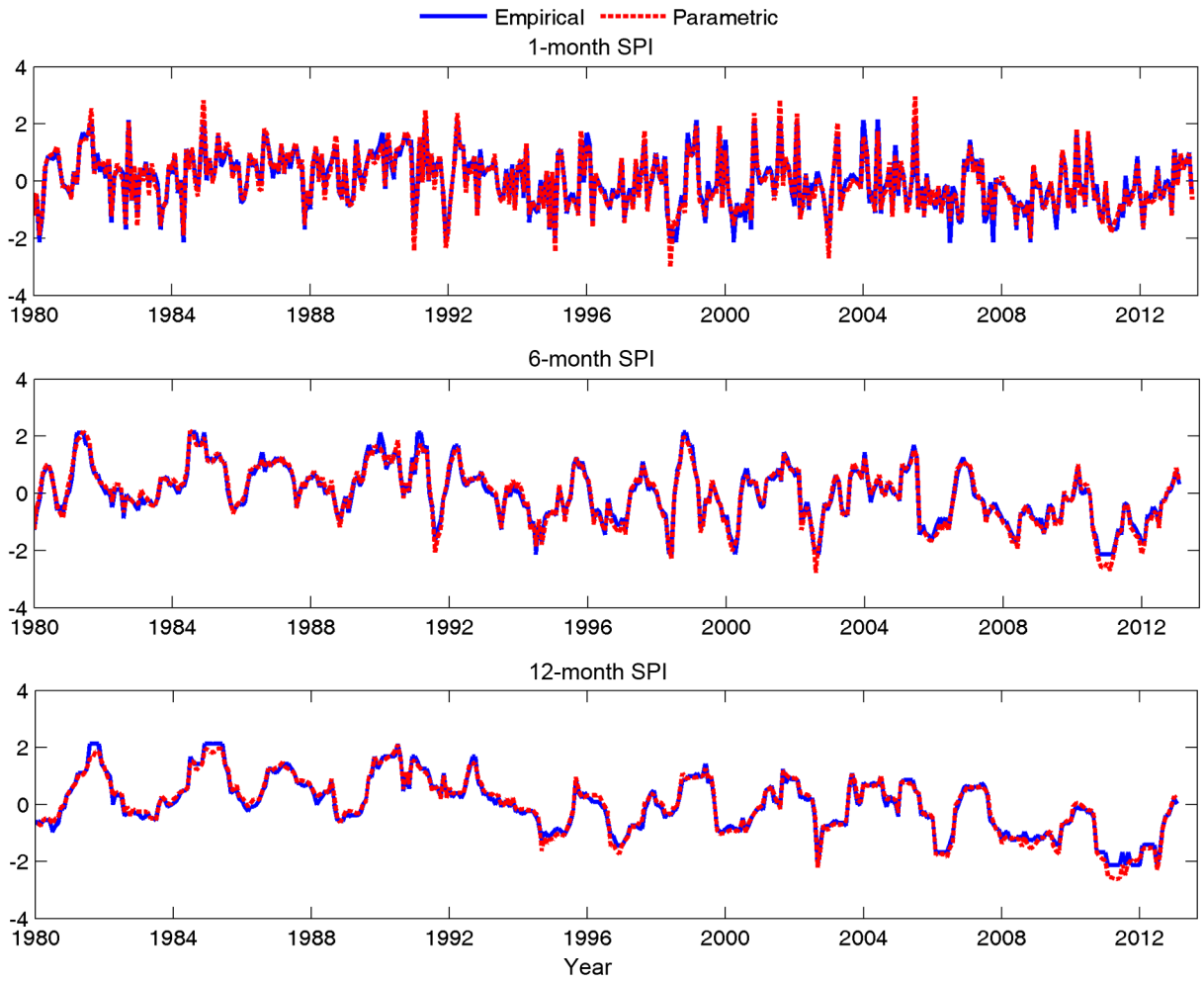

Figure 2.2: Example Empirical (solid blue line) and parametric (dashed red line) 1-month (top panel), 6-month (middle panel), and 12-month (bottom panel) Standardized Precipitation Index (SPI).

To address the above limitation, and to provide statistically consistent and comparable drought indices, the Standardized Drought Analysis Toolbox (SDAT) provides tools for computing generalized univariate and multivariate standardized drought indices. Figure 2.2 shows example Empirical (solid blue line) and parametric (dashed red line) 1-month (top panel), 6-month (middle panel), and 12-month (bottom panel) Standardized Precipitation Index (SPI) based on the GPCP [4] data (location Lat 17.5N, Lon 110W). The time series are primarily consistent, meaning the nonparametric approach can describe wet and dry conditions reliably. However, there are differences in the tails (high and low values) where a

parametric distribution may not be a good fit. It should be noted that similar to parametric indices, the nonparametric standardized drought indicators can also be converted to the D-scale drought categories [286]. The D-scale offers 5 drought categories ranging from D0 (abnormally dry) to D4 (exceptional drought). Each category corresponds to a certain probability in the standard normal distribution and hence, the transformation is straightforward (e.g., D4 corresponds to an event with approximately 2% occurrence probability).

We argue that the suggested nonparametric approach can be used to generate spatially and temporally consistent drought maps based on multiple drought-related variables. For example, in addition to the commonly used SPI and SSI, one can obtain Standardized Relative Humidity Index (SRHI) to provide additional information on wet and dry conditions. For September 2011, Figures 2.3(a) to 2.3(f) display nonparametric 3-month and 6-month SPI, SSI, and SRHI. In Figure 2.3, the SPI and SSI are generated using the precipitation and soil moisture from the Modern Era Retrospective-Analysis for Research and Applications-Land (MERRA-Land; [245]), whereas the SRHI is derived based on the NASA Atmospheric Infrared Sounder (AIRS; [36]) Version 6 relative humidity observations.

In 2011, the Texas-Mexico Drought ([123]) was a major event that let to significant economic losses. As shown, the SPI, SSI and SRHI capture the event at both 3-month and 6-month scales. The SPI and SRHI provide a meteorological perspective, while SSI offers an agricultural perspective. Depending on the application in hand, drought is described using different indicator variables such as soil moisture or precipitation [68]. The nonparametric nature of the suggested framework allows it to derive drought information from different variables (precipitation, soil moisture, relative humidity, etc.) in a consistent and comparable scale. It is worth pointing out that different drought indicators communicate different information about droughts. For instance, a meteorological drought resulting from precipitation deficit may develop rapidly, while a deficit in soil moisture (agricultural drought) in response to precipitation deficit may occur with some time lag. For this reason, the SPI often detects the

drought onset earlier, while SSI describes the drought persistence more reliably [110]. The SDAT allows standardizing various climatic and land-surface variables to assess droughts based on different perspectives.

In Figure 2.3, SPI and SSI are obtained using 33 years (1980-2012) of climatology, while SRHI is generated using only 10 years (2002-2012) of data. Ideally, drought assessment should be based on long-term data (30 years or more). The purpose of showing SRHI is to demonstrate that while relative humidity is not often used for drought analysis, the SDAT can be used to generate SRHI which provides valuable drought information. Also, this example shows that SDAT allows comparing multiple drought indicators based on different variables that may have different distributions.

As mentioned earlier, this framework allows combining multiple data sets for joint (multivariate) analysis of drought based on multiple input variables. The SDAT includes the Multivariate Standardized Drought Index (MSDI) concept that can be used with different drought related variables. The concept of MSDI has been quantitatively validated against other drought indicators and reference data for the 2007 and 2012 United States Droughts in **(author?)** [111]. For this reason, in this paper, only example outputs of the SDAT are presented. Figures 2.3(g) and 2.3(h) show nonparametric 3-month and 6-month MSDI for September 2011, derived from MERRA-Land precipitation and soil moisture data. The MSDI basically combines information from the first two rows in Figure 2.3, and provides composite maps of overall drought conditions based on precipitation and soil moisture (composite information on meteorological and agricultural drought).

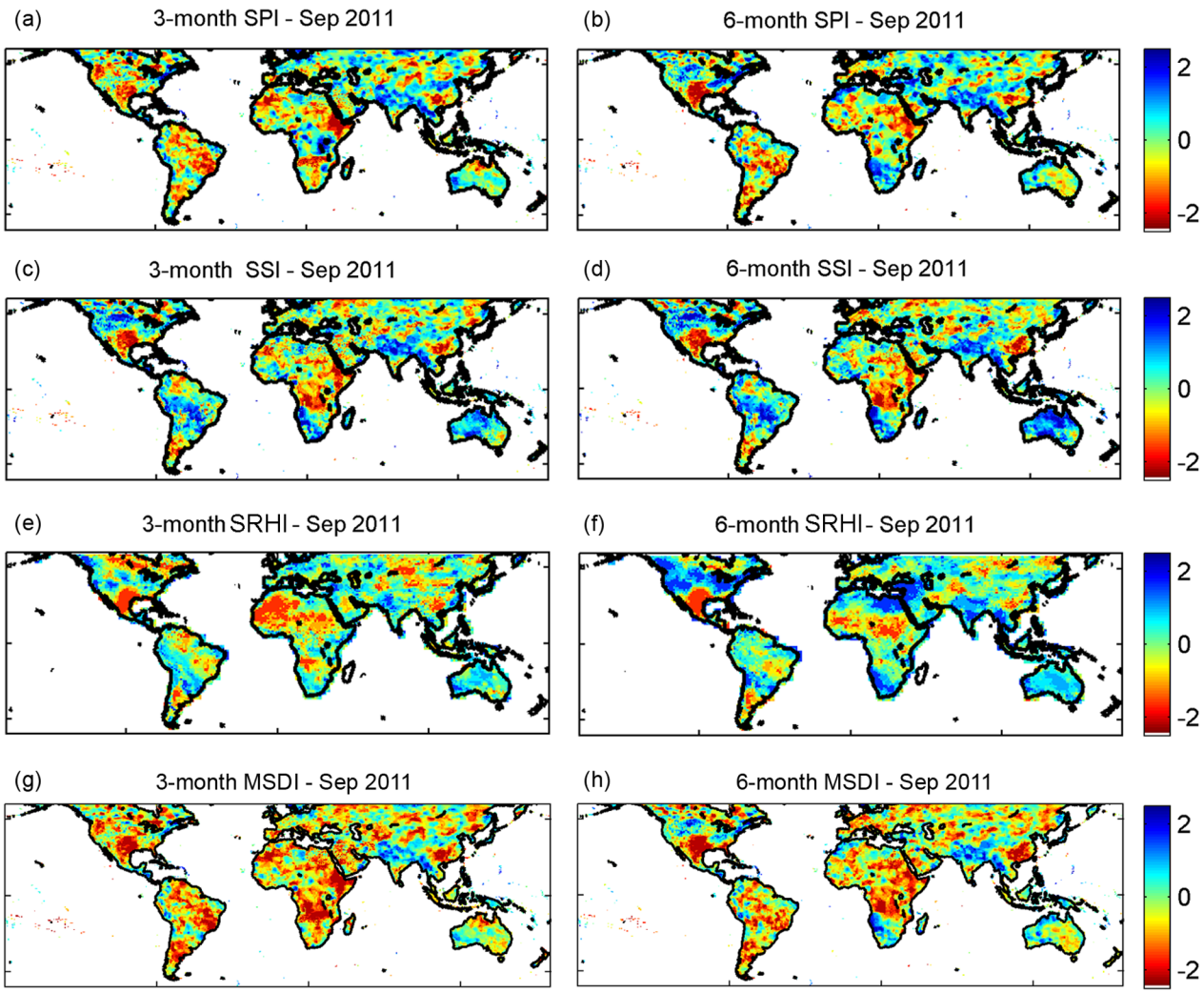

Figure 2.3: Nonparametric 3-month and 6-month Standardized Precipitation Index (SPI), Standardized Soil Moisture Index (SSI), and Standardized Relative Humidity Index (SRHI) for September 2011.

The most attractive feature of the SDAT is providing standardized indices that are statistically, spatially and temporally consistent. It is worth noting that standardized indices can be computed for different time scales (1-, 3-, 6-, 12-month). Empirical distributions are built based on the ranks of data points instead of their actual values. Given that drought analysis is typically based on relative departures from the climatology, empirical distributions are appropriate. However, the sample size should be relatively large, to avoid misleading probabilities. As shown in Figure 2.2, for a 33-year monthly record (33 $\times$ 12 values), the

empirical and parametric estimates are consistent for different variables. For very short data records (e.g., less than 10 variables), which is not common in drought assessment, using an empirical distribution can lead to misleading probabilities.

2.4 Conclusion

In this chapter, Standardized Drought Analysis Toolbox (SDAT) was introduced. Drought mitigation and response plans often rely on information based on different indicator variables and drought triggers. However, many drought indicators are not directly statistically comparable [282]. The presented nonparametric framework of the Standardized Drought Analysis Toolbox (SDAT) offers a generalized approach to develop standardized and statistically consistent drought indicators. The results show that a single distribution function may not fit the global precipitation data and hence, the original parametric SPI may not be applicable. On the other hand, using different distribution functions lead to different tail behavior and thus inconsistencies in characteristics of extremes across space. The SDAT methodology standardizes the marginal probability of drought-related variables (e.g., precipitation, soil moisture, relative humidity) using the empirical distribution function of the data. The approach does not require an assumption on representativeness of a parametric distribution function for describing drought-related variables. It is also worth pointing out that unlike parametric indices, the suggested nonparametric framework does not require parameter estimation and goodness-of-fit evaluation. This means that the SDAT framework is computationally much more efficient than parametric indicator (e.g., original SPI), especially in large scale (continental/global) studies where parameter estimation and goodness-of-fit evaluation needs to be performed at pixel scale. Defining drought is fundamental to both drought monitoring and prediction. Drought is a complex phenomenon that can be defined based on different climatic or land-surface variables. The suggested framework can be applied

to different drought-related variables to study droughts from multiple viewpoints. We show, for example, that by standardizing relative humidity, which is not a common drought indicator, one can obtain drought information consistent with common drought indicators (e.g., SPI). Multiple viewpoints on droughts are essential for planning and management, as some indicators (e.g., SPI) detect droughts earlier while others describe drought persistence (e.g., SSI) more reliably [110]. The SDAT allows standardizing different drought-related variables for a more comprehensive assessment of droughts. There are several drought monitoring systems (e.g., [112, 86, 269, 235, 308, 216]) that provides data based on one or more climatic variables. In such systems, SDAT can offer drought information based on multiple data sets in a consistent way. The SDAT provides tools for not only univariate drought analysis, but also multivariate drought assessment. Multivariate indicators can be used to provide composite drought maps (e.g., composite meteorological-agricultural-hydrological drought conditions). Similar to the commonly used SPI, univariate and multivariate standardized indices can be obtained for different temporal scales (e.g., 1-, 3-, 6-, 12-month). This would allow assessing trends and patterns of droughts at different temporal and spatial scales.

In addition to the nonparametric indices, the SDAT includes the traditional parametric ones for evaluation and cross-comparison. The source code of this MATLAB toolbox is freely available to the public, and interested readers can request a copy of the software from the authors.

Chapter 3

Improving Drought Onset Detection Using Satellite Relative Humidity Information

This Chapter has been published in Advances in Water Resources, Citation: Farahmand A., AghaKouchak A., Teixeira J., (2015), A Vantage from Space Can Detect Earlier Drought Onset: An Approach Using Relative Humidity, *Scientific Reports* , *5*, 8553; doi: 10.1038/srep08553.

3.1 Introduction

Droughts can be described and assessed using different climatic variables such as precipitation, runoff and soil moisture [68]. For example, a meteorological drought is often described as a deficit in precipitation, an agricultural drought is expressed as a deficit in soil moisture, whereas a hydrological drought typically refers to below average surface or sub-surface water [327]. Given that droughts can be described relative to different variables, numerous drought indices have been developed based on one or more climatic variables [208, 329]. For example, the Standardized Precipitation Index (SPI [187, 115]) is widely used as an indicator of meteorological drought, while the Standardized Soil Moisture Index (SSI [111]) and soil moisture percentiles have been used for agricultural drought monitoring. A number of multivariate or multi-index indicators have also been developed such as the Joint Deficit Index [148] and the Multivariate Standardized Drought Index [110].

Drought monitoring indices show substantial variation in their ability to detect drought onset and termination [151, 240]. Generally, precipitation measures detect drought onset earlier than other variables such as soil moisture and runoff [200, 110] because those variables have a delayed response to precipitation deficits. Consequently, the SPI detects the drought onset earlier than the SSI and soil moisture percentiles, and is thus more suitable for drought onset detection [200]. This chapter explores whether even earlier drought onset detection can be accomplished by factoring in the meteorological variables that influence precipitation. It is hypothesized that near surface air relative humidity (hereafter, relative humidity) can detect drought onset earlier than indications provided by precipitation signals. Relative humidity is an important climate variable defined as the ratio of air vapor pressure to the saturated vapor pressure. Precipitation and relative humidity are related to each other in the sense that precipitation is not expected at low relative humidity [184].

Limitations in ground-based observations [69] make satellite observations important for mon-

itoring drought-related variables [27, 13, 73, 214]. These limitations include uneven distribution of ground-based observations, temporal inconsistencies and spatial inhomogeneity in the records, and lack of observations in remote regions [69]. The Evaporative Stress Index [27], the Global Terrestrial Drought Severity Index [208], and the Global Integrated Drought Monitoring and Prediction System (GIDMaPS [112]) all highlight the value of remote sensing observations for monitoring drought.

Drought onset can be detected by standardizing relative humidity data via the relative humidity from the Atmospheric Infrared Sounder (AIRS [36]) satellite mission. Importantly, this detection can be earlier than that indicated by measures of precipitation and soil moisture. The mission's Version 6 data sets are obtained from two instruments: The Atmospheric Infrared Sounder (AIRS) and the Advanced Microwave Sounding Unit (AMSU). AIRS is an infrared spectrometer and radiometer with 2378 spectral channels ranging 3.7-15 μm. AMSU is a 15-channel microwave radiometer covering 23 to 89 GHz [36, 96]. AIRS's monthly surface relative humidity (over equilibrium phase) is utilized for drought onset detection (Version 6, Level 3 data). The relative humidity data are available globally at a 1 $^\circ$ spatial resolution (2002-present). AIRS products are available from ascending and descending tracks, which refer to the direction of movement of the sub-satellite point in the satellite track. We used the descending AIRS data, in which the direction of the movement is from Northern Hemisphere to Southern Hemisphere, with an equatorial crossing time of 1:30 AM local time [292]. To evaluate drought detection using relative humidity, the SPI and SSI data from GIDMaPS [112] are used as additional indicators.

3.2 methods

Standardized drought indices are often derived by normalization after fitting a parametric distribution function to the data [187]. However, a single parametric distribution may not fit

data from different climatic regions [239]. In this study, the Standardized Relative Humidity Index (SRHI) is proposed using a non-parametric standardization approach.

First, the empirical probabilities of the AIRS relative humidity data are computed for each grid, using the empirical Gringorten plotting position [101]:

$$p(RH_i) = \frac{i - 0.44}{n + 0.12} \tag{3.1}$$

Where i is the rank of relative humidity (RH) data from the smallest, and n is the sample size. In this study, an empirical approach is used to avoid any assumption on the underlying distribution function of relative humidity data across space [111]. The empirical probabilities of relative humidity ($p(RH_i)$) is then standardized as:

$$SRHI = \Phi^{-1}(p(RH_i)) \tag{3.2}$$

Where Φ^{-1} is the inverse standard normal distribution function with the mean of zero and standard deviation of one. Here, the standardization is based on the following approximation [72, 210]:

$$SRHI = \begin{cases} -\left(t - \frac{C_0 + C_1 t + C_2 t^2}{1 + d_1 t + d_2 t^2 + d_3 t^3}\right) & \text{if } 0 < p(RH_i) \leq 0.5 \\ \\ +\left(t - \frac{C_0 + C_1 t + C_2 t^2}{1 + d_1 t + d_2 t^2 + d_3 t^3}\right) & \text{if } 0.5 < p(RH_i) \leq 1 \end{cases} \tag{3.3}$$

where $c_0 = 2.515517$; $c_1 = 0.802583$; $c_2 = 0.010328$; $d_1 = 1.432788$; $d_2 = 0.189269$; $d_3 = 0.001308$; and

$$t = \begin{cases} \sqrt{\ln \frac{1}{p(RH_i)^2}} & \text{if } 0 < p(RH_i) \leq 0.5 \\ \\ \sqrt{\ln \frac{1}{(1-p(RH_i))^2}} & \text{if } 0.5 < p(RH_i) \leq 1 \end{cases} \tag{3.4}$$

A negative SRHI is an indication of below average (climatology) relative humidity, and is proposed as a measure of dryness. One attractive feature of SRHI is that, similar to SPI, it can be derived for different time-scales (e.g., 1-, 3-, 6-month SRHI). For consistency and cross-comparison, the three indicators (SRHI, SPI and SSI) are computed using the same non-parametric approach and for a 3-month time scale.

Typically, drought onset assessment is based on a certain drought threshold. In this study, the D0-Drought (Abnormally Dry[286]) condition is used as the drought onset threshold, which corresponds to a drought event with an approximately 30% probability of occurrence. As an example, the global SPI, SSI and SRHI maps for August 2010 are presented in Figure 3.1a, Figure 3.1b, and Figure 3.1c respectively. As shown, all three indices captured the Russian drought. This event and its accompanying heat waves resulted in thousands of casualties and significant economic losses in Russia and eastern Europe [186]. The Amazon drought was another major event in 2010, which led to substantial water level decreases in major Amazon tributaries [185]. At the other extreme, August 2010 was abnormally wet in eastern Australia. These patterns of wet and dry conditions are reflected on all three indices. Overall, Figure 3.1 illustrates that SRHI is consistent with SPI at wet and dry conditions, though there are discrepancies primarily around neutral condition (SPI and SRHI around 0).

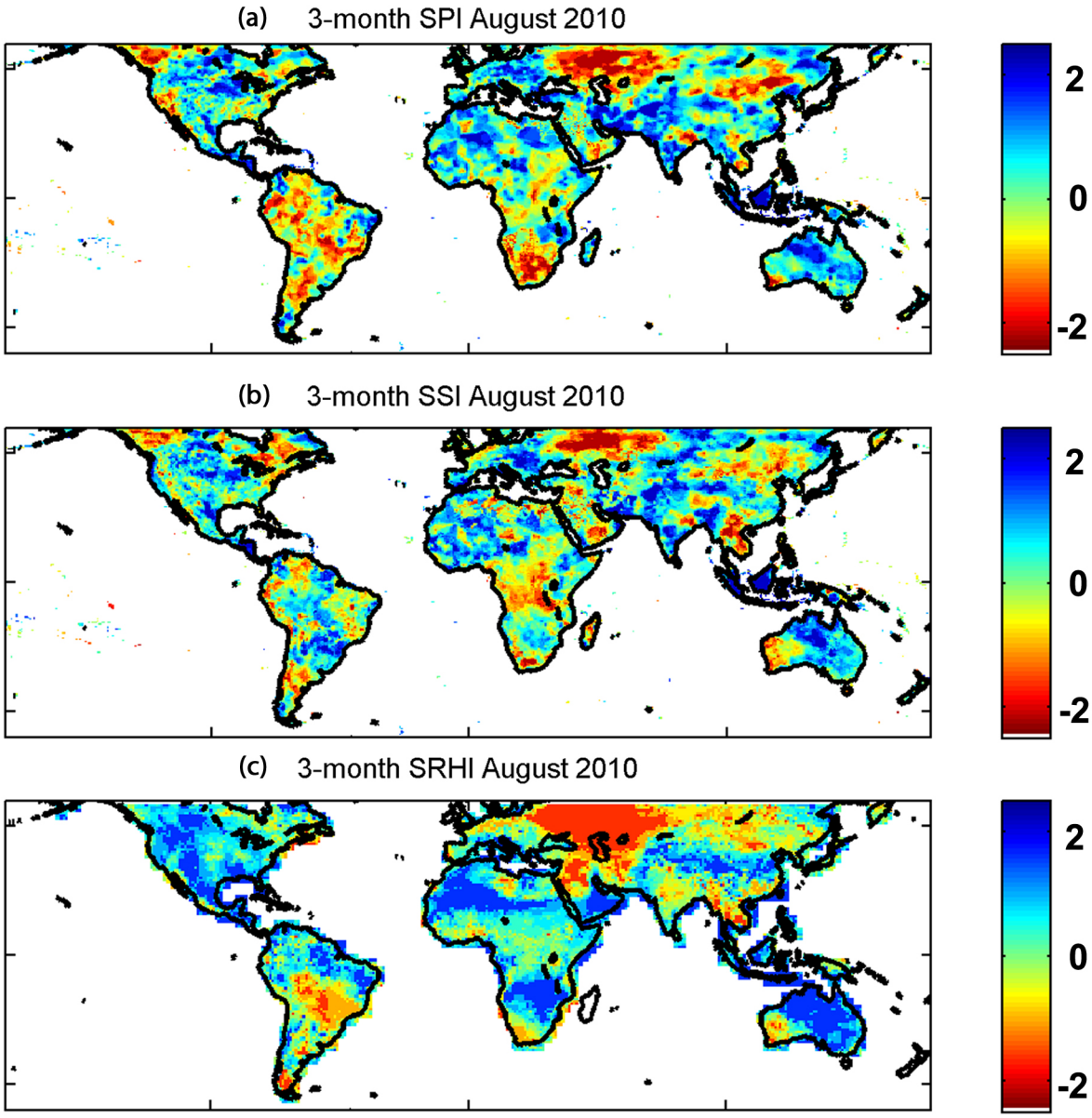

Figure 3.1: Global Standardized Precipitation Index (SPI), Standardized Soil Moisture Index (SSI), and Standardized Relative Humidity Index (SRHI) for August 2010. This map was generated using MATLAB.

To analyze drought early detection, we investigated time series of the SPI, SSI and SRHI over three major drought events: the 2010 Russian drought (Figure 3.2a), the 2010-2011 Texas-Mexico drought (Figure 3.2b), and the 2012 United States drought (Figure 3.2c). As we show, in the 2010 Russian drought, the SRHI indicates the onset nearly two months before both the SPI (Figure 3.2a - compare indices relative to the D0 threshold identified by the green horizontal line). Note that for a more severe drought condition (e.g., a lower threshold of -1), the SRHI detects the drought's onset even earlier.

The same drought indicators over one location in the Texas-Mexico Drought are displayed in Figure 3.2b. This series confirms that the SRHI identifies drought onset earlier than the other indicators. Finally, Figure 3.2c shows the SRHI, SPI and SSI over a specific location in an area affected by the 2012 United States drought. The 2012 drought was one of the most devastating events in the modern times and led to billions of U.S. dollars in economic damage. This event in particular affected crop development and early detection could have reduced agricultural losses [55]. As shown in Figure 3.2c, the SRHI detects the drought onset 3 to 4 months earlier than SPI. Such early detection in the growing season could potentially reduce the effects of droughts on agriculture and society [55].

In the top three panels in Figure 3.2, the SRHI is the earliest drought detector, followed by SPI and SSI. The results are consistent with previous studies indicating that SPI detects the drought onset earlier than SSI. However, the results also show that remotely sensed relative humidity can be used for even earlier drought detection. While the SRHI does show the potential to advance drought early detection, in some cases it may not detect the drought onset earlier than the SPI (e.g., see Figure 3.2d where the SRHI detects the drought onset later than the SPI). Nonetheless, in all cases, the SRHI is consistent with the SPI and SSI on showing the drought signal.

To assess the potential capability of AIRS relative humidity data in drought detection, we statistically evaluated the global SRHI values against SPI during 2002 - 2013 period. Figure

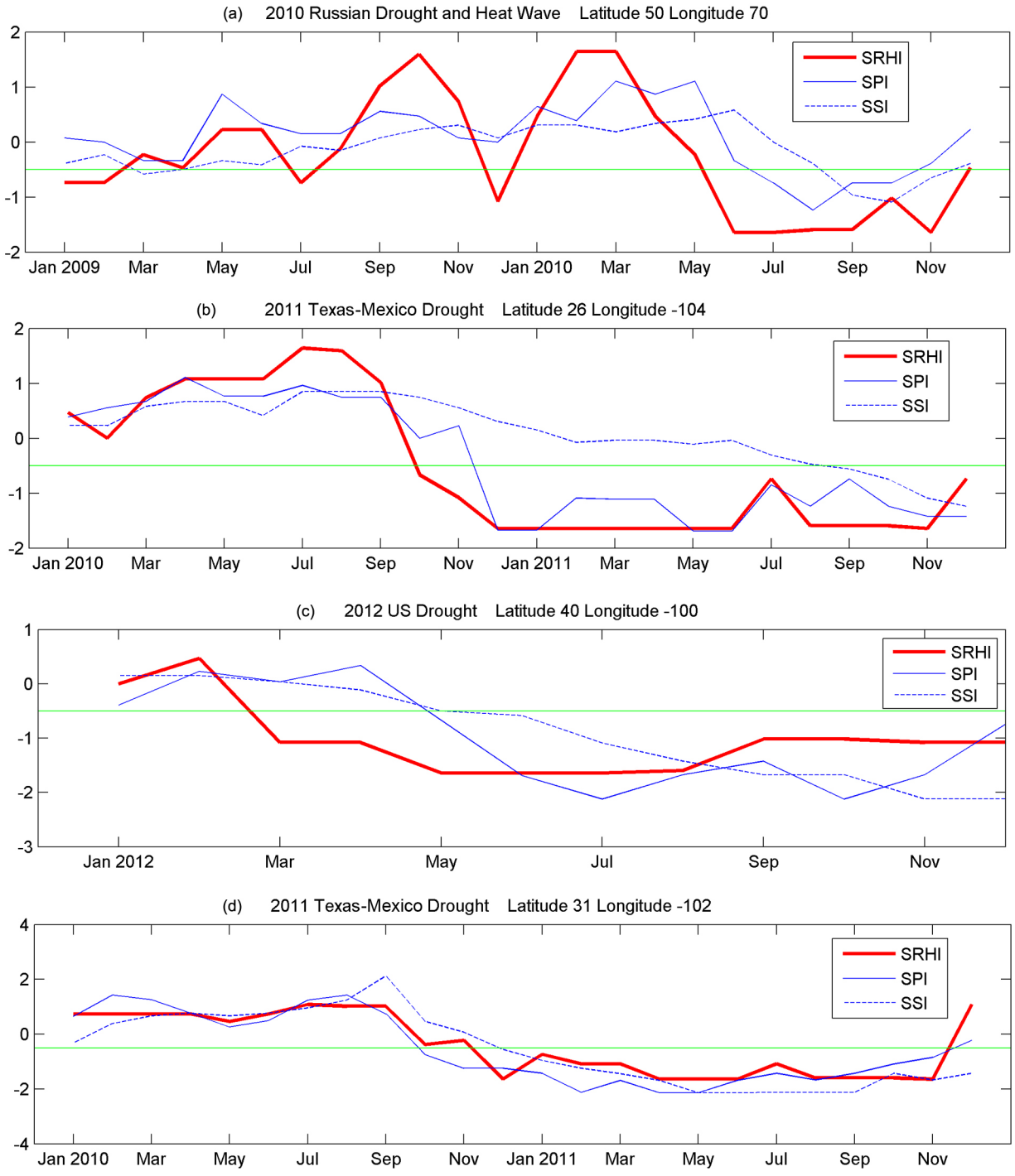

Figure 3.2: Time series of 3-month SPI, SSI and SRHI for several locations in areas affected by the 2010 Russian drought, 2010-2011 Texas-Mexico drought, and 2012 United States drought. This map was generated using MATLAB.

3.3a presents the probability of drought detection. Figure 3.3b and Figure 3.3c shows the false drought ratio and missed drought ratio respectively. Figure 3.3a shows the fraction of the reference data (i.e., negative SPI) identified correctly by the SRHI (perfect score =1), whereas figure 3.3b describes the fraction of drought events identified by SRHI, but not confirmed with the SPI (perfect score =0) [11]. Figure 3.3c displays the fraction of drought events identified by SPI, but missed in SRHI (perfect score =0). Given that there are limited number of droughts in each pixel during 2002-2013, the global statistics is derived for each 10×10 pixels to ensure the statistics is reliable.

An important question is in cases where a drought was detected by both SRHI and SPI, what fraction of events is detected earlier by SRHI. To answer this question, the drought onset based on SRHI (DO_{SRHI}) is evaluated against that of SPI (DO_{SPI}). To avoid unreliable statistics, only drought events longer than three months have been considered. Figure 3.4a shows the probability of drought detection (i.e., fraction of detected drought) when $DO_{SRHI} \leq DO_{SPI}$. As shown, in most parts of the globe this fraction ranges between 0.5 to 0.8, with the global average being approximately 0.6 (i.e., 60% of all events). Figure 3.4b displays the mean lead time for each pixel based on SRHI relative to SPI. The figure indicates that the mean lead time ranges between 1 to 3 months with the global average being approximately 1.9 months. The results presented in Figures 3.3 and 3.4 do not show a strong regional/geographical pattern. This indicates that in most parts of the world the SRHI, combined with other indicators, can potentially improve early drought detection.

3.3 Conclusion

This chapter introduced a new drought monitoring index , Standardized Relative Humidity Index (SRHI) was introduced. SRHI detects drought onset with the average of around 2 months earlier than SPI. SRHI's main limitation is the relatively short length of record

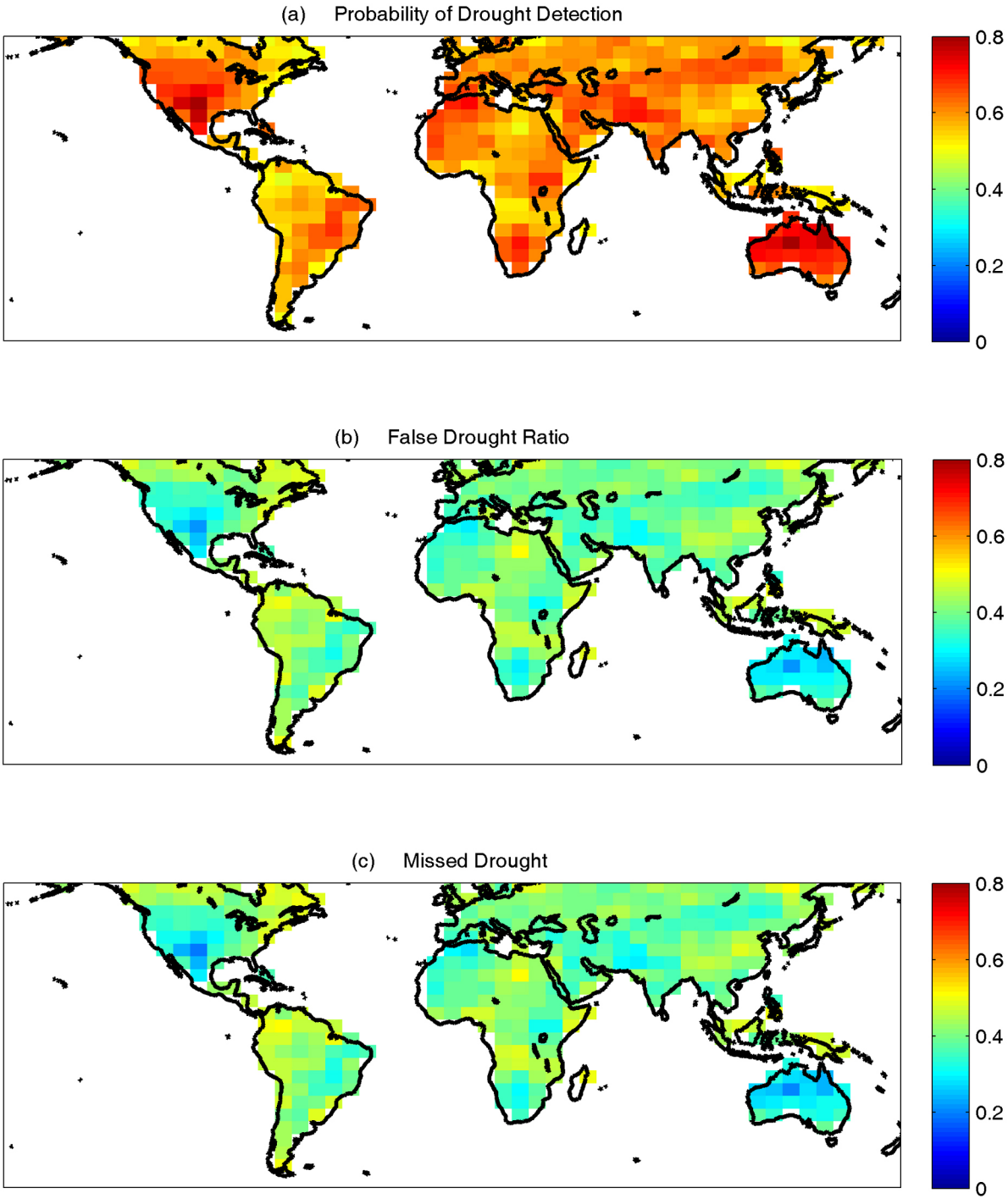

Figure 3.3: Probability of drought detection (a), false drought ratio (b), and missed drought ratio (v) for the SRHI relative to SPI. This map was generated using MATLAB.

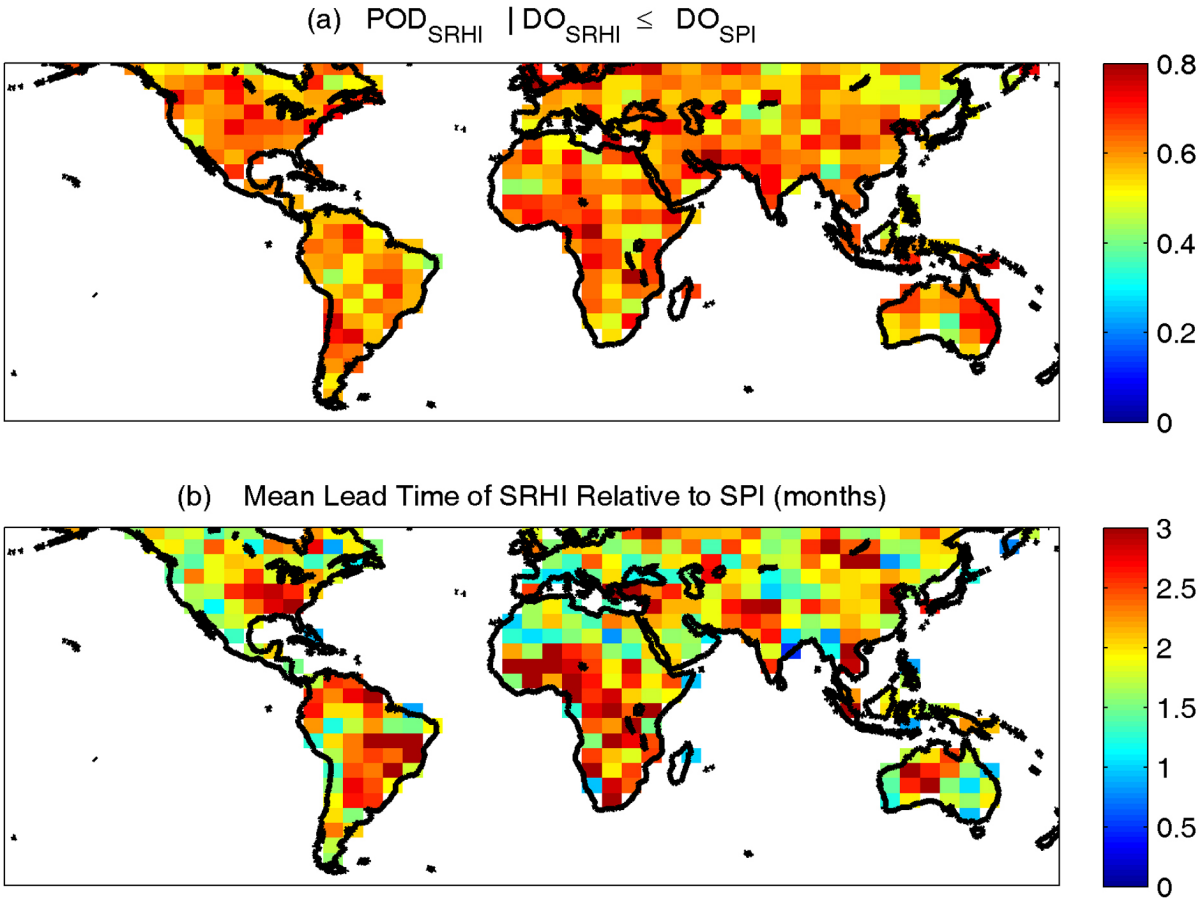

Figure 3.4: Probability of drought detection (i.e., fraction of detected drought) when Drought Onset (DO) based on SRHI is less or equal to that of SPI ($DO_{SRHI} \leq DO_{SPI}$) (a), mean lead time based on SRHI relative to SPI (months) (b). This map was generated using MATLAB.

(2002-present). However, there are other data sets with similar length of record that provide valuable drought information (e.g., GRACE observations, and Evaporative Stress Index data). SRHI can provide valuable information on current conditions but it cannot be used to put an extreme event in historical perspective. In a recent study, a Bayesian algorithm is proposed for combining multiple precipitation data to create a long-term climate data record [13]. Similar algorithms could be used to extend AIRS relative humidity data by combining it with reanalysis data sets (e.g., Modern-Era Retrospective Analysis for Research and Applications [249]). Efforts are underway to create a long-term and real-time relative humidity data set for drought monitoring and assessment. On the other hand, the current resolution (1^o) of the relative humidity data only allows regional to continental scale drought assessment.

Drought monitoring should be based on multiple sources of information. The proposed SRHI is not meant to replace the currently available indicators. Rather, it should be used alongside other drought indicators. This paper does not claim that SRHI alone is always sufficient for early drought detection. In fact, previous studies highlight the limitations of individual drought indicators [240, 282]. Having an additional source of information based on relative humidity can improve our understanding of the drought onset and development. Furthermore, several studies argue that statistical seasonal drought prediction is very sensitive to the initial meteorological and land-surface conditions [5, 6, 183]. Early drought detection can potentially lead to improvements in statistical seasonal drought prediction by providing additional information on the initial meteorological conditions. This issue, however, requires more in-depth research in the future.

Drought early onset detection is fundamental to local and regional mitigation plans, especially in the agriculture and water resources sectors. A water manager may need drought information months in advance for water resource planning, while for a farmer even few weeks of lead time is very important. Early detection, even by few weeks/months, allows

farmers and local agencies to take adaptive measures that include purchasing less fertilizer and increasing insurance coverage, especially before or early in the growing season. The results highlight that the AIRS near surface air relative humidity data can potentially be used for drought early warning if integrated into currently available systems such as the U.S. Drought Monitor [286] or GIDMaPS [112].

Chapter 4

Improving Multi-Index Drought Monitoring Using Satellite Observations

4.1 Introduction

Droughts are considered as one of the main environmental catastrophes worldwide, which have economical, societal, agricultural impacts [320] [329] [197] [228] . Droughts are generally categorized into meteorological, agricultural and hydrologic [68]. A metrological drought is defined as a deficit in precipitation, and agricultural drought is defined as deficit in soil moisture and hydrological drought is defined as below average surface or sub-surface flow [327]. Indices have been designed to investigate various kinds of drought. For example, Standardized Precipitation Index (SPI) is one of the mostly common used indices for monitoring meteorological drought [188]. SPI is derived using a parametric [188] or a non-parametric approach [111]. Standardized Relative Humidity Index (SRHI) monitors meteorological drought using

relative humidity values [79]. Precipitation is often used to detect early signals of drought as precipitation can detect drought signals earlier than other indicators such as soil moisture [200]. [79], however, argues that relative humidity can detect drought signals earlier than precipitation as precipitation is not expected in low relative humidity while high precipitation values do not necessarily lead to precipitation. Standardized Soil Moisture index [111], is used to measure agricultural drought while Multivariate Standardized Drought Index (MSDI) [110], measures agro-meteorological drought using precipitation and soil moisture.

Various global and regional drought monitoring systems have been developed. For example, Global Integrated Drought Monitoring and Prediction System (GIDMaPS) [112] provides drought information based multiple data sets and indicators (i.e., meteorological drought, agricultural drought, and composite agro-meteorological information). University of Washington (UW) Experimental Surface Water Monitor for the Continental US uses updates of soil moisture, runoff, and snow water equivalent to show drought severity maps [334]. UW Drought Monitoring System for Washington State uses near real time hydrologic conditions on Washington State to monitor current drought conditions [274]. US Drought Monitor (USDM) incorporates climate and water expert inputs for drought monitoring [285]. Princeton University produces a drought monitoring and forecasting system that integrates atmospheric and hydrologic processor (VIC) to monitor and forecast droughts [335]. Also Princeton University has developed a flood and drought monitoring system for Africa.

Drought, especially combined with high temperatures, increases the atmospheric evaporative demand, typically resulting in higher Evapotranspiration (ET) rates. ET can be derived using a satellite-based image processing techniques called Mapping evapotranspiration at high resolution with internalized calibration (METRIC) [18]. Several drought indicators have been developed taking into account evapotranspiration (ET). Standardized Precipitation Evapotranspiration Index (SPEI) provides drought information using both precipitation and potential evapotranspiration (PET) [309]. The methodology is similar to SPI, but it relies

on the difference between precipitation and potential evapotranspiration. Crop Water Stress Index (CWSI) is the ratio of actual ET (AET) to potential ET (PET) [135]. Water Deficit Index (WDI) is the ratio of AET rate to PET rate. Evaporative Stress index (ESI) uses the Atmosphere-Land Exchange Inverse (ALEXI) model to quantify anomalies in actual to potential evapotranspiration [27].

Droughts and high evapotranspiration rates (e.g., caused by high temperatures) can be devastating for forest health and also agricultural [15] [180] [59]. High ET values increase tree mortality rates. For example, recent droughts and heat-induced tree mortality posed increasing risk for forest health [15]. Hot droughts (droughts and high temperatures) have increased vulnerability of forests to tree mortality [14] [2]. End of the dry season, land surface temperature has been identified as an indicator of forest cover change in tropical regions [305]. Tree productivity and tree survival have declined under increases in frequency, duration and severity of drought and heatwaves associated with climate change and variability [15].

As shown in Chapter 3, relative humidity can be a good indicator for early drought detection along with precipitation. In this Chapter, we will explore integrating both temperature and relative humidity for forest stress analysis since both are closely related to evapotranspiration. Vapor Pressure Deficit (VPD) combines temperature and humidity and can potentially be use for drought monitoring [41]. Evapotranspiration has a direct relationship with VPD in the sense that large VPD values are associated with large evapotranspiration rates. High VPD is identified as an important driver of the rapid development and evolution of the 2011 Texas and the 2012 Great Plains [41]. Historical forest drought-stress index (FDSI) indicates that tree mortality is closely associated with summer VPD and winter precipitation [330]. If VPD continues to increase, the mean FDSI values will exceed the most severe droughts in the past 1000 years [330].

High ET (and atmospheric evaporative demand) rates have also significant impacts on wildfires. Western United States wildfire has increased over the past decades [324]. Report show

that fires in savannas and evergreen forests increased during drought events in 2005, 2007 and 2010 [52]. Most wildfire increases have been occurred in mid-elevation where fire risks are affected by spring and summer high temperatures. High VPD values and wildfire data show strong correlation in boreal forest ecosystems [261]. Both wildfire and forest health are related to temperature and evaporative demand. For this reason, VPD appears to be a good composite indicator to link meteorological conditions (e.g., temperature and humidity, evaporation) to ecosystem response (i.e., forest health).

Various studies have developed indicators to monitor vegetation health under drought conditions [297]. The first Advanced Very High Resolution Radiometer (AVHRR) instrument was launched in 1979 which revolutionized vegetation and land cover assessment by observing spectral reflectance. Various vegetation indices have been developed to assess vegetation health. The normalized difference vegetation index is the first and most commonly used one developed by [256]. NDVI measures the level of vegetation greenness using red (R) and near-infrared (NIR) portions of electromagnetic spectrum [256]. Other vegetation indices have been developed: Vegetation Condition Index (VCI) [159] which takes into account minimum and maximum amounts of NDVI for scaling NDVI. This enables identifying short term, localized droughts from widespread long term droughts [156]. Temperature Condition Index (TCI) represents drought as an indicator of temperature. It is derived from measurements of remotely sensed surface brightness temperature [157]. The combination of VCI and TCI provides valuable results for detecting agricultural droughts. One of the mostly used indices is Vegetation Health Index (VHI) which combines VCI and TCI [157]. Global Agricultural Drought Monitoring and Forecasting System provides drought information (GADMFS) (http://gis.csiss.gmu.edu/GADMFS/) , along with NDVI and VCI shows drought conditions. It is a prototype of the Global Earth Observation System of Systems (GEOSS) with agricultural drought monitoring skills. Vegetation Drought Response Index (VegDRI) integrates vegetation and climatic data to produce vegetation drought response maps [45].

Western United States has been hit by consecutive droughts since 2010 [9]. Linking climate condition to ecosystem response is important. To address this challenge we need more advance multi-sensor multi-index methods to link climate information to vegetation/forest response. One of our goals is to develop a framework for combining multiple different indicators to advance the field in this area. We have explored three different approaches to link climate anomalies with NDVI response (i.e., investigating the impacts of droughts on forest health):

- Conditional probability of NDVI on high VPD percentiles;
- Conditional probability of NDVI on high temperature and low relative humidity percentiles;
- Conditional probability of NDVI on low precipitation percentiles.

4.2 Data

NDVI data were derived from National Oceanic and Atmospheric Administration Center for Satellite and Research (NOAA-STAR). NOAA STAR provides three AVHRR derived vegetation health indices: raw NDVI, noise reduced NDVI and VHI (vegetation health index). In this study, noise reduced (smoothed) NDVI were used. This data is available globally and with the spatial resolution of 16 km and temporal resolution of 7 days since 1981. Forest map of the United States was derived from Forest Inventory and Analysis National Program. Monthly Temperature and relative humidity were derived from Atmospheric Infrared Sounder (AIRS [36]) Version 6 Level 3 satellite mission. The data are available at 1 ° spatial resolution and are available since the launch of the AIRS satellite in September 2002. AIRS data sets are derived from two instruments: The Atmospheric Infrared Sounder (AIRS) and the Advanced Microwave Sounding Unit (AMSU). AIRS is an infrared spectrometer and ra-

diometer with 2378 spectral channels ranging 3.7-15 μm. AMSU is a 15 channel microwave radiometer covering 23 to 89 GHz. AIRS products are available from ascending and descending tracks, which refer to the direction of movement of the sub-satellite point in the satellite track. In this study, the descending AIRS data, in which the direction of the movement is from Northern Hemisphere to Southern Hemisphere, with an equatorial crossing time of 1:30 AM local time [97] was used. Precipitation data were derived from Modern-Era Retrospective analysis for Research and Applications (MERRA-Land) [113] [244] . Monthly MERRA-Land data are available in 2/3 ° longitude, 1/2 ° latitude and are available since 1980.

4.3 Methodology

As data sets were in different spatial and temporal scales, all datasets had to be converted to a consistent spatial and temporal resolution. The spatial resolution of MERRA-Land (2/3 ° longitude, 1/2 ° latitude) was used as reference. NDVI 7-day data were converted to monthly in order to be consistent with other datasets. AIRS temperature and relative humidity have relatively short length of record (only from late 2002). For this reason, we have focused on 2003 to 2014. As the aim of this study was to investigate the effects of droughts in western United States forests, all datasets were masked into forest areas (-115 to -120 longitudes and 30 to 50 latitudes). Temperature and relative humidity were combined into VPD using the following formula:

$$VPD = c1 \times \exp\left(\frac{c2 \times T_{mean}}{c3 + T_{mean}}\right) + c1 \times \exp(\frac{c2 \times Td_{mean}}{c3 + Td_{mean}}) \tag{4.1}$$

where c1=0.611 kPa, c2=17.5, c3=240.978 ° C, Tmean surface air tempreture ° C, Tdmean

dew point tempreture ° C, and VPD in kPa. Low VPD values indicate favorable conditions while high VPD indicate stressful conditions for plants.

After creating consistent datasets, a nonparametric method was used to determine the empirical ranks of the NDVI time series for each grid:

$$pr(x_i) = \frac{i}{n} \tag{4.2}$$

Where i is the rank of NDVI from the smallest and n is the length of the sample. In this study, an empirical approach was used to avoid any assumption on the underlying distribution function of NDVI data across space [244]. Lower values of probability indicate stressful conditions and higher values indicate non stressful conditions for vegetation health respectively. The distribution of Pr(NDVI) for all forest locations were calculated in three scenarios:

1. (Top 15 percentile VPD) and (Top 15 percentile T and bottom 15 percentile RH) for summer months (June, July and August)
2. (Top 15 percentile VPD) and (Top 15 percentile T and bottom 15 percentile RH) for growing season (April to September)
3. Bottom 15 percentile Precipitation for winter (January, February, March)

For the purpose of investigating the effects of recent droughts on vegetation health, two time periods were selected. First time period was from 2003 till 2010 and the second one was from 2003 till 2014 which includes 2011-2014 recent drought period. For all three scenarios, Pr(NDVI) distribution of first and second time period were compared with each other. The methodology is illustrated in Figure 4.1

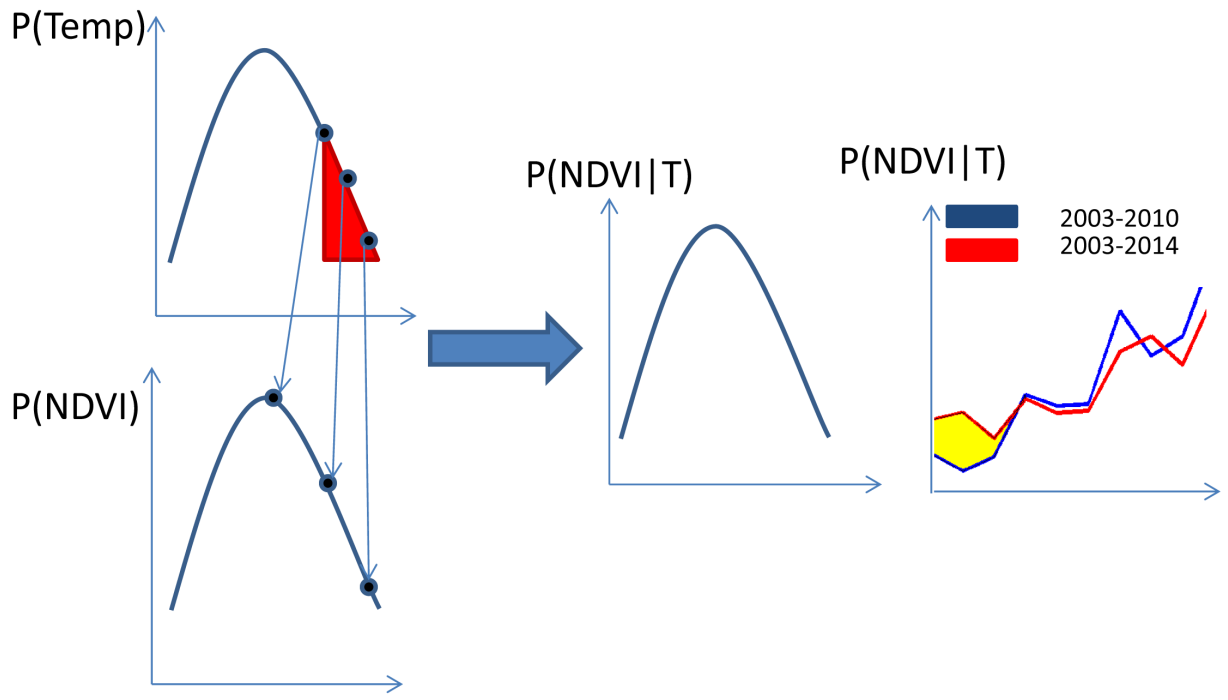

Figure 4.1: A schematic view of the methodology for assessing the effects of droughts on forest health

4.4 Results

Figure 4.2 shows the Pr(NDVI) , Pr(VPD), Pr(T) and Pr(RH) for a wet summer (August 2006) and a warm summer (August 2013) month. High Pr(VPD) and Pr(T) indicate unfavorable conditions, while low Pr(RH) and Pr(NDVI) are indicators of unfavorable conditions. For each cell, all probabilities have been derived using Equation 4.2. As indicated, in August 2006, Pr(VPD), Pr(T) and Pr(NDVI) are in non-stressed zone (blue zone) in most of the locations. On the other hand, in August 2013, Pr(VPD), P(T) and Pr(NDVI) are in red zone (drought zone) in most locations and in agreement with each other. In addition, Figure 4.2 indicates that VPD is largely influenced by temperature. 4.3 shows Pr(P) and Pr(NDVI) for a wet winter (March 2006) and a warm winter (March 2013) month. In this case, empirical precipitation ranking is in agreement with empirical NDVI ranking for most of places. Pr(P) and Pr(NDVI) are high (wet) in March 2013 while Pr(P) and Pr(NDVI) are low (dry) in March 2006.

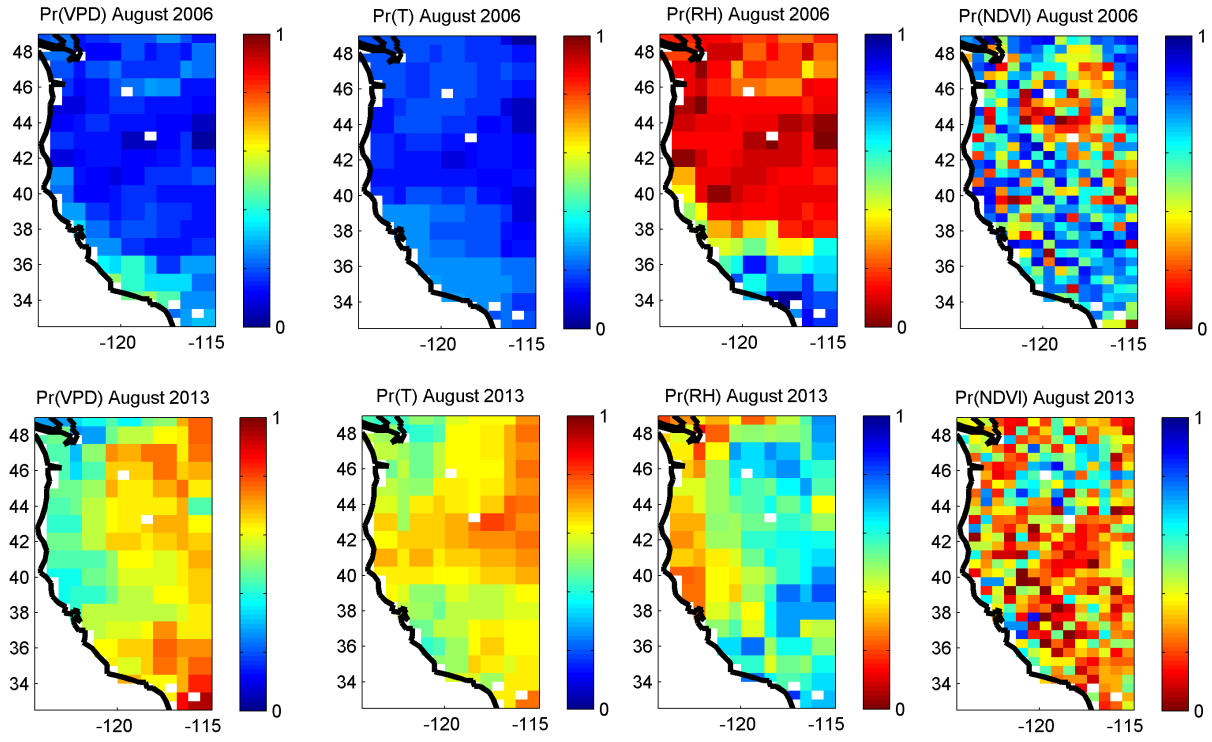

Figure 4.2: Pr(VPD), Pr(T), Pr(RH) and Pr(NDVI) for a wet (August 2006) and a warm month (August 2013)

Figure 4.4 shows the results of the first approach. In the top panel, the blue and the red time series show the distribution of all summer NDVI probabilities in top 15 percentile VPD for period 1 (2003-2010) and period 2 (2003-2014) respectively. The horizontal axis indicates the probability of NDVI and the vertical axis indicates percentage of data in corresponding NDVI probability. The hatched yellow area show the change in the area under the graph from period 1 to period 2 between 0.2 and 0.4 NDVI probability. As shown in Figure 4.4 , the area under the red graph has increased substantially compared to the blue graph in the stressed forest conditions. The bottom panel shows the distribution of summer NDVI probabilities in top 15 percentile temperature and bottom 15 percentile relative humidity. As shown, the bottom panel looks similar to the top panel. Similar to the top panel, the area under the curve has increased from period 1 to period 2 between 0.2 and 0.4 NDVI probabilities. Overall, this figure indicates that the effects of recent droughts on forest health

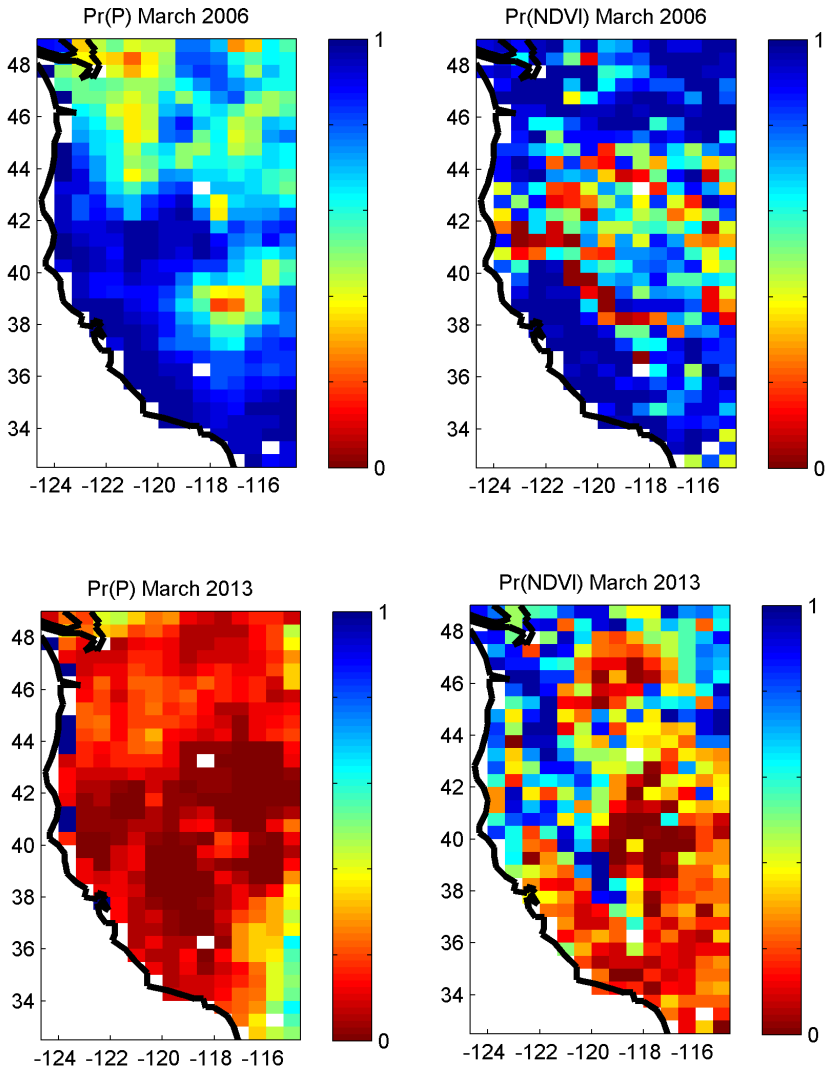

Figure 4.3: Pr(P) and Pr(NDVI) for a wet (March 2006) and a warm (March 2013) month

can be detected through the changes in VPD, temperature and relative humidity during the summer period. Also, evaluating the NDVI probabilities conditioned on VPD alone or the combination of temperature and relative humidity lead to almost similar results.

Figure 4.5 shows the results of the second scenario. The top panel shows the distribution of all growing season NDVI probabilities in top 15 percentile VPD for period 1 (2003-2010) and period 2 (2003-2014) respectively. The bottom panel indicates the distribution of all growing season NDVI probabilities in top 15 percentile temperature and bottom 15 percentile

relative humidity for period 1 and period 2 respectively. As shown, both top and bottom panels show similar time series to each other. The hatched yellow area show the change in the area under the graph from period 1 to period 2 between 0.1 and 0.4 NDVI probability. As shown in Figure 4.5 , the area under the red graph has increased substantially compared to the blue graph in the stressed forest conditions for both top and bottom panels . This shows that temperature, humidity and VPD can be used as an indicator for assessing the effects of droughts on forests during the growing season in addition to summer period. Also, similar to Figure 4.4, assessing the NDVI probabilities conditioned on VPD alone or the combination of temperature and relative humidity lead to similar outputs.

Figure 4.6 shows the results of the third scenario. The blue and the red time series show the distribution of all winter NDVI probabilities in bottom 15 percentile precipitation for period 1 (2003-2010) and period 2 (2003-2014) respectively. Similar to Figure 4.4 ,the hatched yellow area show the change in the area under the graph from period 1 to period 2 between 0.1 and 0.4 NDVI probability. As shown in Figure 4.6, the area under the red graph has increased substantially compared to the blue graph in the stressed forest conditions . Unlike the first scenario that VPD was a good indicator for assessing the effects of droughts on forests in summer, empirical precipitation ranking can be used to detect the effects of droughts on forest health during the winter period.

4.5 Conclusion

This chapter proposes multi-index frameworks for assessing drought impacts on forest health by linking climate information to vegetation response. Studies show that droughts have increased the tree mortality and productivity rates as well as wildfire. Normalized Difference Vegetation Index (NDVI), which is a a measure of greenness or photosynthesis activity of plant, has been widely used for ecosystem response assessment. However, by the time NDVI

shows drought, the system has been under stress for some time. NDVI depends on different climate variables over different periods of time. Here, we use a multi-index approach to link temperature and relative humidity that play a key role in warm seasons, by affecting vegetation health as they influence the evapotranspiration (ET) rate. The combined effect of temperature and relative humidity can be considered by using the vapor pressure deficit (VDP). During summer months and growing season, specifically, high temperatures and low relative humidity values can have devastating impacts on vegetation. High temperatures pose high levels of stress on photosynthetic activities of plants. Low levels of relative humidity increase plant transpiration rate causing water deficits in the plant. During the winter period, on the other hand, low precipitation impacts the vegetation greenness.

For this analysis, a nonparametric method was developed to determine the empirical ranks of the NDVI time series for different climatic conditions. The distribution of NDVI probability values in high summer (and growing season) VPD and low winter precipitation percentiles were calculated. The results show that probabilities of NDVI conditioned on top 15 percentile VPD in summer (and growing season) and bottom 15 percentile precipitation in winter have increased in stressful vegetation health conditions. However, they have not changed significantly in non-stressful vegetation conditions. For the summer and growing season, same analysis was performed conditioned on top 15 percentile temperature and bottom 15 percentile relative humidity instead of VPD. The results show almost identical outputs with the VPD condition. This indicates that during summer period and growing season in which precipitation is low, temperature and relative humidity conditions play a significant role in vegetation greenness and health. However, in winter that temperature and VPD values are low, precipitation plays the key role in vegetation greenness. One of the main limitations of this work is the short length of AIRS temperature and relative humidity record. AIRS provides real-time relative humidity data but with short length of record. Other temperature and humidity datasets such as MERRA provide longer datasets but with a couple of months of delay. Future work includes assessing the effects of droughts on various vegetation covers

including various types of forest trees. As shown in Chapter 3, relative humidity can detect drought onset earlier than other climatic variables. With the advantage of AIRS in providing real time humidity data, earlier signals of drought could be helpful in providing earlier signals of vegetation stress.

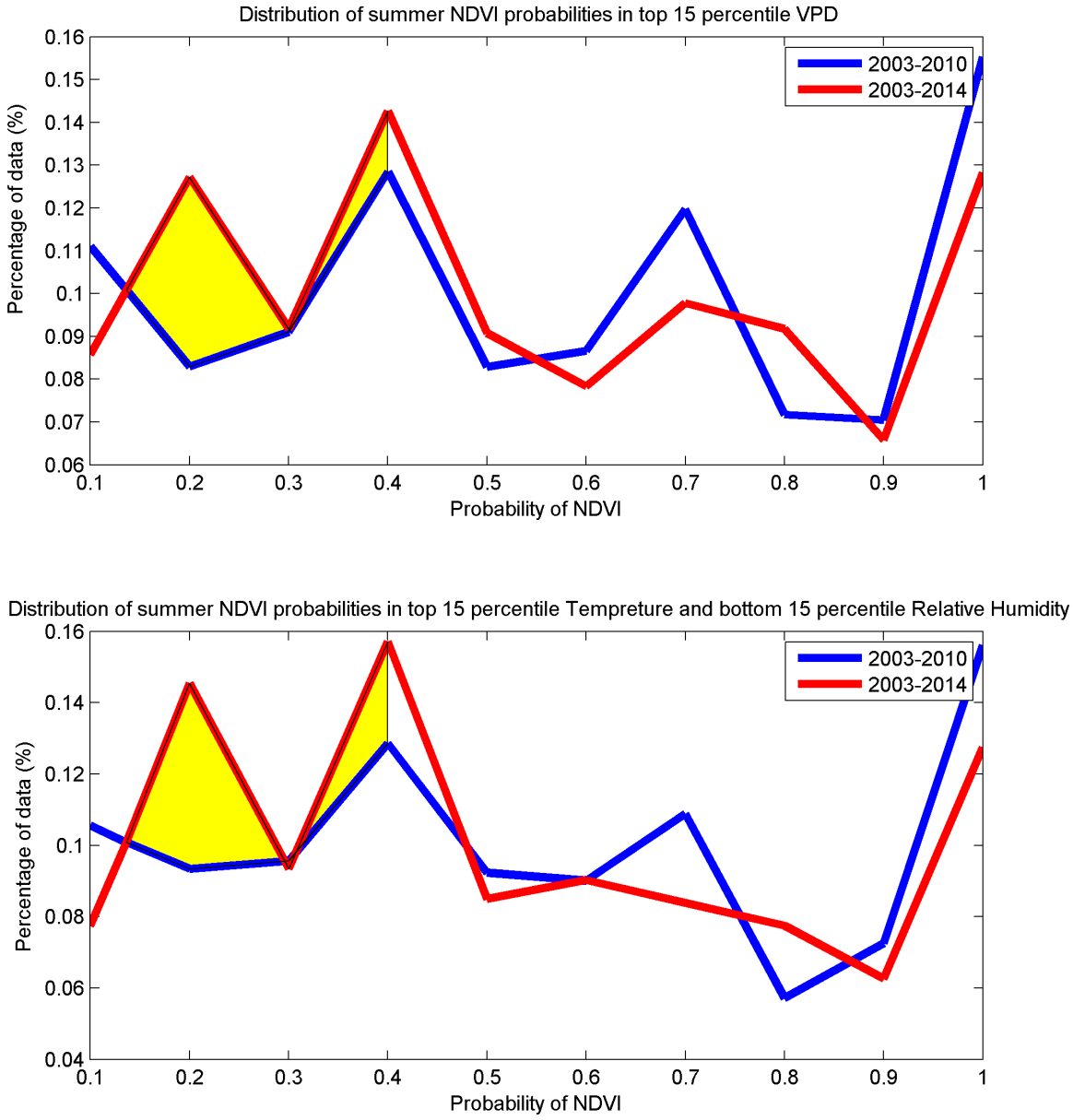

Figure 4.4: Top: Distribution of summer NDVI probabilities in top 15 percentile VPD. Bottom: Distribution of summer NDVI probabilities in top 15 percentile Temperature and bottom 15 percentile Relative Humidity

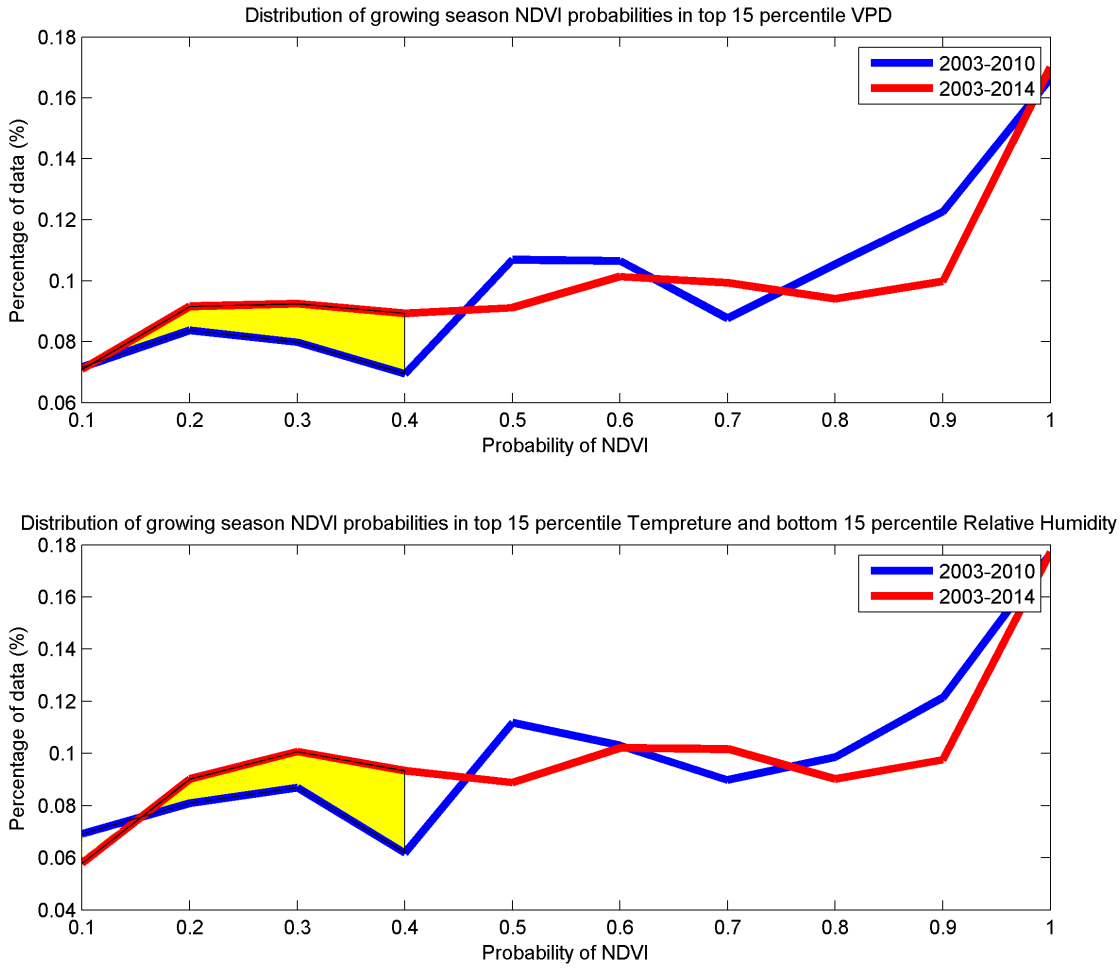

Figure 4.5: Top: Distribution of growing season NDVI probabilities in top 15 percentile VPD. Bottom: Distribution of growing season NDVI probabilities in top 15 percentile Temperature and bottom 15 percentile Relative Humidity

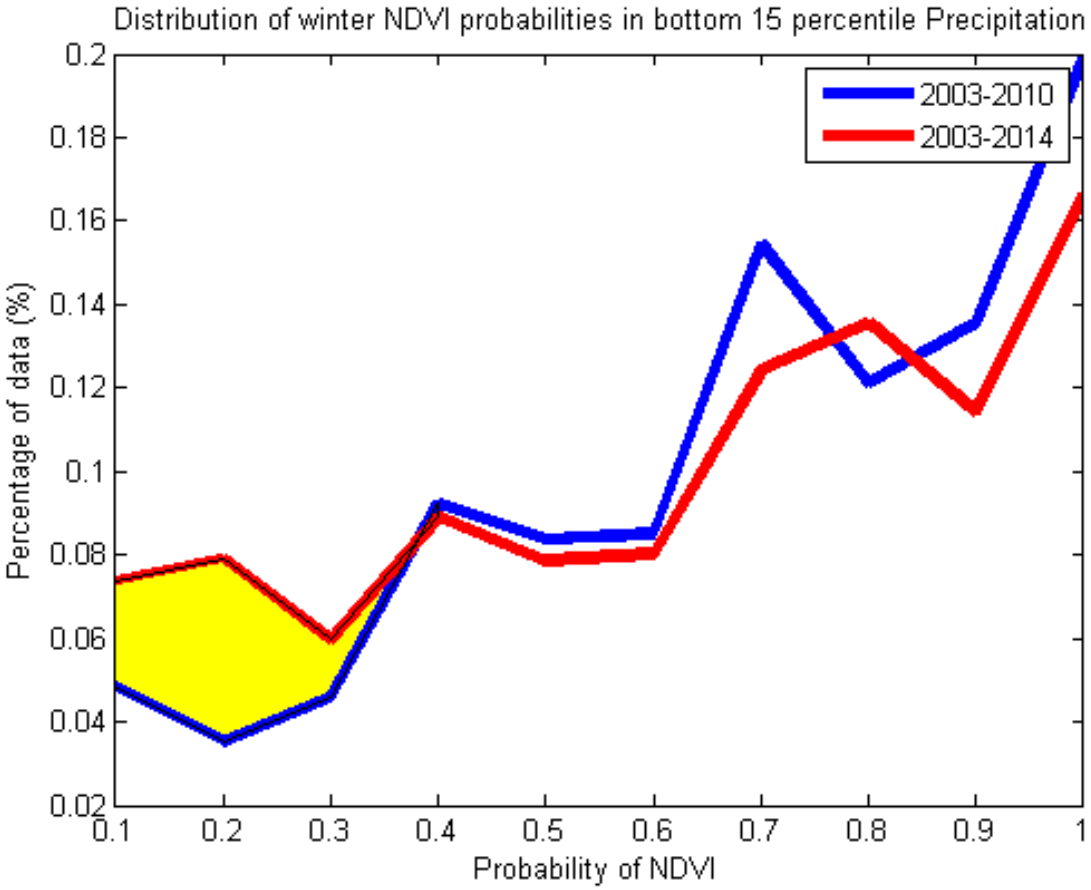

Figure 4.6: Top: Distribution of winter NDVI probabilities in lower 15 percentile precipitation

Chapter 5

Summary and Conclusions

The overarching goal of this dissertation was to improve remote sensing of drought through (a) developing a generalized framework for creating drought information from satellite observations; (b) integrating satellite remote sensing products that are not currently being used for drought monitoring; and (c) developing multi-sensor, multi-index approaches based on multiple satellite observations. These research gaps were identified after a detailed survey of the literature presented in Chapter 1. To address these research gaps, Chapter 2 introduces Standardized Drought Analysis Toolbox (SDAT), which includes a generalized framework for deriving nonparametric univariate and multivariate standardized drought indices. Chapter 3 presents a framework for integrating near-surface air relative humidity data (not currently used for drought monitoring) from the Atmospheric Infrared Sounder (AIRS) mission for early drought onset detection. Finally, Chapter 4 outlines a framework for assessing impacts of droughts on forest health using multi-sensor approach. In the following, the conclusions for each chapter are summarized:

5.1 Chapters 2: A Generalized Framework for Deriving Nonparametric Standardized Drought Indicators

Droughts are complex phenomena and require multiple sources of information for input. SDAT introduces a non-parametric framework for deriving drought indicators based on various inputs. A single parametric distribution function may not fit the global data properly and multiple distribution functions may lead to inconsistencies in the behavior of the extremes. SDAT, therefore, provides a statistically consistent method for drought monitoring. Non-parametric methodology uses empirical distribution function to standardize the marginal probability of a climate variable. Thus, this method does not require parameter estimation and goodness of fit testing. The methodology can be applied to precipitation, soil moisture and relative humidity. SDAT also provides multivariate framework for drought analysis. Combining climate variables can potentially improve drought monitoring skills. For example, precipitation shows better performance for drought onset detection and soil moisture in drought consistency. The multivariate approach can be applied to the joint distribution of precipitation and soil moisture to derive a drought indicator based on precipitation and soil moisture.

5.2 Chapters 3: Improving Drought Onset Detection Using Satellite Relative Humidity Information

Precipitation is often used as an indicator for drought onset detection. Relative humidity is an important climate variables affecting precipitation. Relative humidity and precipitation are related to each other in the sense that precipitation is not expected at low relative

humidity values. Thus, relative humidity could detect drought signals earlier than precipitation. SRHI is a standardized drought monitoring index based on AIRS relative humidity data. SRHI uses the same non-parametric methodology used for deriving SPI. SRHI shows consistent patterns with other drought indicators such as SPI and SSI and it detects drought onset earlier than SPI with the average of 2 months. SRHI has not been developed to replace SPI. However, it provides valuable information about drought monitoring. Drought early detection is fundamental for agriculture, forest and water resources sectors. The main limitation of SRHI is its relatively short length of record (2002-present). Statistical algorithms, such as Bayesian, could be used to extend AIRS relative humidity data by combining it with reanalysis data sets.

5.3 Chapters 4: Improving Multi-Index Drought Monitoring Using Satellite Observations

A Multi-index method was used to derive a framework for assessing the impacts of recent western United States droughts on forest health. Droughts increase tree mortality rates and wildfire activities. One of the most commonly used indices for assessing vegetation health is Normalized Difference Vegetation Index (NDVI). NDVI indicates the level of plant greenness. During the summer and growing season period, evapotranspiration rates are generally high. Temperature and relative humidity affect the vegetation greenness. High temperatures pose high levels of stress on photosynthetic activities of plants. Low levels of relative humidity increase plant transpiration rate causing water deficits in the plant. Temperature and humidity could combine into Vapor Pressure Deficit (VPD). During the winter period, precipitation affects the forest greenness. The distribution of NDVI in top 15 percentile VPD over summer and growing season shows an increase in the tail of the distribution (stressed NDVI zone) from period 2003-2014 to 2003-2010. The distribution

of NDVI conditioned on top 15 percentile temperature and bottom 15 percentile humidity during summer and growing season lead to similar results to VPD. Similarly, the distribution of NDVI in bottom 15 percentile precipitation over winter season shows an increase in stressed NDVI zone from period 2003-2014 to 2003-2010.

Bibliography

[1] M. Abramowitz and I. Stegun. *Handbook of Mathematical Formulas, Graphs, and Mathematical Tables*. Dover Publications, New York, 1965.

[2] H. D. Adams, M. Guardiola-Claramonte, G. A. Barron-Gafford, J. C. Villegas, D. D. Breshears, C. B. Zou, P. A. Troch, and T. E. Huxman. Temperature sensitivity of drought-induced tree mortality portends increased regional die-off under global-change-type drought. *Proceedings of the national academy of sciences*, 106(17):7063–7066, 2009.

[3] J. O. Adegoke and A. M. Carleton. Relations between soil moisture and satellite vegetation indices in the us corn belt. *Journal of hydrometeorology*, 3(4):395–405, 2002.

[4] R. Adler, G. Huffman, A. Chang, R. Ferraro, P. Xie, J. Janowiak, B. Rudolf, U. Schneider, S. Curtis, D. Bolvin, A. Gruber, J. Susskind, and P. Arkin. The version-2 Global Precipitation Climatology Project (GPCP) monthly precipitation analysis (1979–present). *Journal of Hydrometeorology*, 4(6):1147–1167, 2003.

[5] A. AghaKouchak. A baseline probabilistic drought forecasting framework using standardized soil moisture index: application to the 2012 united states drought. *Hydrology and Earth System Sciences*, 18:2485–2492, 2014.

[6] A. AghaKouchak. A multivariate approach for persistence-based drought prediction: Application to the 2010-2011 east africa drought. *Journal of Hydrology*, 526:127–135, 2015. doi: 10.1016/j.jhydrol.2014.09.063.

[7] A. Aghakouchak, L. Cheng, O. Mazdiyasni, and A. Farahmand. Global warming and changes in risk of concurrent climate extremes: Insights from the 2014 california drought. *Geophysical Research Letters*, 41, 2014. doi: 10.1002/2014GL062308.

[8] A. AghaKouchak, G. Ciach, and E. Habib. Estimation of tail dependence coefficient in rainfall accumulation fields. *Advances in Water Resources*, 33(9):1142–1149, 2010.

[9] A. AghaKouchak, D. Feldman, M. Hoerling, T. Huxman, and J. Lund. Recognize anthropogenic drought. *Nature*, 524(7566):409–4011, 2015.

[10] A. Aghakouchak, D. Feldman, M. J. Stewardson, J.-D. Saphores, S. Grant, and B. Sanders. Australias drought: Lessons for california. *Science*, 343(6178):1430–1431, 2014.

[11] A. AghaKouchak and Mehran. Extended Contingency Table: Performance Metrics for Satellite Observations and Climate Model Simulations. *Water Resources Research*, 49:7144–7149, 2013. doi:10.1002/wrcr.20498.

[12] A. AghaKouchak, A. Mehran, H. Norouzi, and A. Behrangi. Systematic and random error components in satellite precipitation data sets. *Geophysical Research Letters*, 39(9):L09406, 2012.

[13] A. AghaKouchak and N. Nakhjiri. A near real-time satellite-based global drought climate data record. *Environmental Research Letters*, 7(4):044037, 2012. doi:10.1088/1748-9326/7/4/044037.

[14] C. D. Allen, D. D. Breshears, and N. G. McDowell. On underestimation of global vulnerability to tree mortality and forest die-off from hotter drought in the anthropocene. *Ecosphere*, 6(8):1–55, 2015.

[15] C. D. Allen, A. K. Macalady, H. Chenchouni, D. Bachelet, N. McDowell, M. Vennetier, T. Kitzberger, A. Rigling, D. D. Breshears, E. T. Hogg, et al. A global overview of drought and heat-induced tree mortality reveals emerging climate change risks for forests. *Forest ecology and management*, 259(4):660–684, 2010.

[16] R. Allen, L. Pereira, D. Raes, and M. Smith. Crop evapotranspiration, guidelines for computing crop water requirements. Technical report, FAO Irrig. and Drain. Paper 56, Food and Agric. Orgn. of the United Nations, Rome, Italy, 300 pp., 1998.

[17] R. G. Allen, M. Tasumi, and R. Trezza. Satellite-based energy balance for mapping evapotranspiration with internalized calibration (metric)model. *Journal of irrigation and drainage engineering*, 133(4):380–394, 2007.

[18] R. G. Allen, M. Tasumi, and R. Trezza. Satellite-based energy balance for mapping evapotranspiration with internalized calibration (metric)model. *Journal of irrigation and drainage engineering*, 133(4):380–394, 2007.

[19] G. M. Ambaw. *Satellite based remote sensing of soil moisture for drought detection and monitoring in the Horn of Africa*. PhD thesis, Politecnico di Torino, 2013.

[20] N. Andela, Y. Y. Liu, A. I. J. M. van Dijk, R. A. M. de Jeu, and T. R. McVicar. Global changes in dryland vegetation dynamics (1988 - 2008) assessed by satellite remote sensing: comparing a new passive microwave vegetation density record with reflective greenness data. *Biogeosciences*, 10(10):6657–6676, 2013.

[21] L. Anderson, Y. Malhi, L. Aragao, and S. Saatchi. Spatial patterns of the canopy stress during 2005 drought in amazonia. In *2007 IEEE International Geoscience and Remote Sensing Symposium, IGARSS 2007*, pages 2294–7, 2008.

[22] M. Anderson, C. Hain, B. Wardlow, A. Pimstein, J. Mecikalski, and W. Kustas. A thermal-based evaporative stress index for monitoring surface moisture depletion. *Remote Sensing of Drought: Innovative Monitoring Approaches*, pages 145–167, 2012.

[23] M. Anderson and W. Kustas. Thermal remote sensing of drought and evapotranspiration. *Eos, Transactions American Geophysical Union*, 89(26):233, 2008.

[24] M. Anderson, W. Kustas, J. Norman, C. Hain, J. Mecikalski, L. Schultz, M. Gonzalez-Dugo, C. Cammalleri, G. d'Urso, A. Pimstein, et al. Mapping daily evapotranspiration at field to continental scales using geostationary and polar orbiting satellite imagery. *Hydrology and Earth System Sciences*, 15(1):223–239, 2011.

[25] M. Anderson, J. Norman, G. Diak, W. Kustas, and J. Mecikalski. A two-source time-integrated model for estimating surface fluxes using thermal infrared remote sensing. *Remote Sensing of Environment*, 60(2):195–216, 1997.

[26] M. C. Anderson, C. Hain, J. Otkin, X. Zhan, K. Mo, M. Svoboda, B. Wardlow, and A. Pimstein. An intercomparison of drought indicators based on thermal remote sensing and NLDAS-2 simulations with us drought monitor classifications. *Journal of Hydrometeorology*, 14(4):1035–1056, 2013.

[27] M. C. Anderson, C. Hain, B. Wardlow, A. Pimstein, J. R. Mecikalski, and W. P. Kustas. Evaluation of Drought Indices Based on Thermal Remote Sensing of Evapotranspiration over the Continental United States. *Journal of Climate*, 24(8):2025–2044, 2011.

[28] M. C. Anderson, J. M. Norman, J. R. Mecikalski, J. A. Otkin, and W. P. Kustas. A climatological study of evapotranspiration and moisture stress across the continental United States based on thermal remote sensing: 1. Model formulation. *Journal of Geophysical Research: Atmospheres (1984–2012)*, 112(D10), 2007.

[29] W. Anderson, B. Zaitchik, C. Hain, M. Anderson, M. Yilmaz, J. Mecikalski, and L. Schultz. Towards an integrated soil moisture drought monitor for east africa. *Hydrology and Earth System Sciences*, 16(8):2893–2913, 2012.

[30] K. M. Andreadis, E. A. Clark, A. W. Wood, A. F. Hamlet, and D. P. Lettenmaier. Twentieth-century drought in the conterminous united states. *Journal of Hydrometeorology*, 6(6):985–1001, 2005.

[31] K. M. Andreadis and D. Lettenmaier. Assimilating passive microwave brightness temperature for snow water equivalent estimation. In *AMS Annual Meeting, 19th Conference on Hydrology*, 2005.

[32] P. Angelidis, F. Maris, N. Kotsovinos, and V. Hrissanthou. Computation of drought index SPI with alternative distribution functions. *Water resources management*, 26(9):2453–2473, 2012.

[33] P. A. Arkin, R. Joyce, and J. E. Janowiak. The estimation of global monthly mean rainfall using infrared satellite data: The GOES Precipitation Index (GPI). *Remote Sensing Reviews*, 11(1-4):107–124, 1994.

[34] G. Asrar, M. Fuchs, E. Kanemasu, and J. Hatfield. Estimating absorbed photosynthetic radiation and leaf area index from spectral reflectance in wheat. *Agronomy journal*, 76(2):300–306, 1984.

[35] G. Asrar, R. B. Myneni, and E. T. Kanemasu. Estimation of plant-canopy attributes from spectral reflectance measurements, 1989.

[36] H. H. Aumann, M. T. Chahine, C. Gautier, M. D. Goldberg, E. Kalnay, L. M. McMillin, H. Revercomb, P. W. Rosenkranz, W. L. Smith, D. H. Staelin, et al. AIRS/AMSU/HSB on the aqua mission: Design, science objectives, data products, and processing systems. *Geoscience and Remote Sensing, IEEE Transactions on*, 41(2):253–264, 2003.

[37] F. Baret and G. Guyot. Potentials and limits of vegetation indices for LAI and APAR assessment. *Remote Sensing of Environment*, 35(2):161–173, 1991.

[38] E. Barrett, M. Beaumont, and R. Herschy. Satellite remote sensing for operational hydrology: present needs and future opportunities. *Remote Sensing Reviews*, 4(2):451–466, 1990.

[39] E. Barrett and R. Herschy. Opportunities for satellite remote sensing in hydrology and water management. *Geocarto International*, 4(2):11–18, 1989.

[40] Y. Bayarjargal, A. Karnieli, M. Bayasgalan, S. Khudulmur, C. Gandush, and C. Tucker. A comparative study of NOAA–AVHRR derived drought indices using change vector analysis. *Remote Sensing of Environment*, 105(1):9–22, 2006.

[41] A. Behrangi, P. Loikith, H. Nguyen, E. Fetzer, S. Granger, and B. Lambrigtsen. On the importance of near surface temperature and humidity information to advance monitoring and prediction of meteorological drought. *Journal of Climate*, 2015.

[42] V. K. Boken, A. P. Cracknell, R. L. Heathcote, et al. *Monitoring and predicting agricultural drought: a global study*. Oxford University Press Caryˆ eNC NC, 2005.

[43] J. D. Bolten, W. T. Crow, X. Zhan, T. J. Jackson, and C. A. Reynolds. Evaluating the utility of remotely sensed soil moisture retrievals for operational agricultural drought monitoring. *Selected Topics in Applied Earth Observations and Remote Sensing, IEEE Journal of*, 3(1):57–66, 2010.

[44] D. H. Bromwich, J. P. Nicolas, K. M. Hines, J. E. Kay, E. L. Key, M. A. Lazzara, D. Lubin, G. M. McFarquhar, I. V. Gorodetskaya, D. P. Grosvenor, et al. Tropospheric clouds in antarctica. *Reviews of Geophysics*, 50(1), 2012.

[45] J. F. Brown, B. D. Wardlow, T. Tadesse, M. J. Hayes, and B. C. Reed. The Vegetation Drought Response Index (VegDRI): A new integrated approach for monitoring drought stress in vegetation. *Geoscience & Remote Sensing*, 45(1):16–46, 2008.

[46] G. Caccamo, L. Chisholm, R. A. Bradstock, and M. Puotinen. Assessing the sensitivity of modis to monitor drought in high biomass ecosystems. *Remote Sensing of Environment*, 115(10):2626–2639, 2011.

[47] T. Carlson. An overview of the" Triangle Method" for estimating surface evapotranspiration and soil moisture from satellite imagery. *Sensors*, 7(8):1612–1629, 2007.

[48] J. Cashion, V. Lakshmi, D. Bosch, and T. J. Jackson. Microwave remote sensing of soil moisture: evaluation of the TRMM microwave imager (TMI) satellite for the Little River Watershed Tifton, Georgia. *Journal of hydrology*, 307(1):242–253, 2005.

[49] A. Chappell, L. J. Renzullo, T. H. Raupach, and M. Haylock. Evaluating geostatistical methods of blending satellite and gauge data to estimate near real-time daily rainfall for australia. *Journal of Hydrology*, 493:105–114, 2013.

[50] D. Chen, J. Huang, and T. J. Jackson. Vegetation water content estimation for corn and soybeans using spectral indices derived from modis near-and short-wave infrared bands. *Remote Sensing of Environment*, 98(2):225–236, 2005.

[51] J. Chen, C. Wilson, B. Tapley, Z. Yang, and G. Niu. 2005 drought event in the amazon river basin as measured by grace and estimated by climate models. *Journal of Geophysical Research*, 114(B5):B05404, 2009.

[52] Y. Chen, D. C. Morton, Y. Jin, G. J. Collatz, P. S. Kasibhatla, G. R. Van Der Werf, R. S. DeFries, and J. T. Randerson. Long-term trends and interannual variability of forest, savanna and agricultural fires in south america. *Carbon Management*, 4(6):617–638, 2013.

[53] M. Choi, J. Jacobs, M. Anderson, and D. Bosch. Evaluation of drought indices via remotely sensed data with hydrological variables. *Journal of Hydrology*, 476(7), 2013.

[54] B. Choudhury, C. Tucker, R. Golus, and W. Newcomb. Monitoring vegetation using Nimbus-7 scanning multichannel microwave radiometer's data. *International Journal of Remote Sensing*, 8(3):533–538, 1987.

[55] S. Crutchfield. Us drought 2012: Farm and food impacts. Technical report, United States Department of Agriculture (USDA), Economic Research Service, 2012.

[56] A. Dai, K. E. Trenberth, and T. Qian. A global dataset of palmer drought severity index for 1870-2002: Relationship with soil moisture and effects of surface warming. *Journal of Hydrometeorology*, 5(6):1117–1130, 2004.

[57] N. Dalezios, A. Blanta, and N. Spyropoulos. Assessment of remotely sensed drought features in vulnerable agriculture. *Natural Hazards and Earth System Science*, 12(10):3139–3150, 2012.

[58] L. Damberg and A. AghaKouchak. Global trends and patterns of drought from space. *Theoretical and Applied Climatology*, 117(3):441–448, 2014. doi:10.1007/s00704-013-1019-5.

[59] S. J. Davis, J. A. Burney, J. Pongratz, and K. Caldeira. Methods for attributing land-use emissions to products. *Carbon Management*, 5(2):233–245, 2014.

[60] D. Deering and J. Rouse. Measuring'forage production' of grazing units from landsat mss data. In *International Symposium on Remote Sensing of Environment, 10 th, Ann Arbor, Mich*, pages 1169–1178, 1975.

[61] L. Di, D. C. Rundquist, and L. Han. Modelling relationships between NDVI and precipitation during vegetative growth cycles. *International Journal of Remote Sensing*, 15(10):2121–2136, 1994.

[62] P. D'Odorico, K. Caylor, G. S. Okin, and T. M. Scanlon. On soil moisture–vegetation feedbacks and their possible effects on the dynamics of dryland ecosystems. *Journal of Geophysical Research: Biogeosciences (2005–2012)*, 112(G4), 2007.

[63] J. Dong, J. P. Walker, P. R. Houser, and C. Sun. Scanning multichannel microwave radiometer snow water equivalent assimilation. *Journal of Geophysical Research: Atmospheres (1984–2012)*, 112(D7), 2007.

[64] R. J. Donohue, T. McVICAR, and M. L. Roderick. Climate-related trends in australian vegetation cover as inferred from satellite observations, 1981–2006. *Global Change Biology*, 15(4):1025–1039, 2009.

[65] R. J. Donohue, T. R. McVicar, and M. L. Roderick. Assessing the ability of potential evaporation formulations to capture the dynamics in evaporative demand within a changing climate. *Journal of Hydrology*, 386(1):186–197, 2010.

[66] W. Dorigo, K. Scipal, R. Parinussa, Y. Liu, W. Wagner, R. De Jeu, and V. Naeimi. Error characterisation of global active and passive microwave soil moisture datasets. *Hydrology and Earth System Sciences*, 14(12):2605–2616, 2010.

[67] J. Dozier, R. O. Green, A. W. Nolin, and T. H. Painter. Interpretation of snow properties from imaging spectrometry. *Remote Sensing of Environment*, 113:S25–S37, 2009.

[68] J. A. Dracup, K. S. Lee, and E. G. Paulson Jr. On the definition of droughts. *Water Resources Research*, 16(2):297–302, 1980.

[69] D. Easterling. Global data sets for analysis of climate extremes. In *Extremes in a Changing Climate*. Springer, 2013. doi: 10.1007/978-94-007-4479-0 12.

[70] E. Ebert, J. Janowiak, and C. Kidd. Comparison of near real time precipitation estimates from satellite observations and numerical models. *Bulletin of the American Meteorological Society*, 88:47–64, 2007.

[71] D. Edwards. Characteristics of 20th Century drought in the United States at multiple time scales. Technical report, Colorado State University, Fort Collins, Colorado, 1997.

[72] D. C. Edwards. Characteristics of 20th century drought in the united states at multiple time scales. Technical report, Department of Atmospheric Science, Colorado State University, Fort Collins, 1997.

[73] D. Entekhabi, E. G. Njoku, P. Houser, M. Spencer, T. Doiron, Y. Kim, J. Smith, R. Girard, S. Belair, W. Crow, et al. The hydrosphere state (hydros) satellite mission: An earth system pathfinder for global mapping of soil moisture and land freeze/thaw. *Geoscience and Remote Sensing, IEEE Transactions on*, 42(10):2184–2195, 2004.

[74] D. Entekhabi, E. G. Njoku, P. E. O'Neill, K. H. Kellogg, W. T. Crow, W. N. Edelstein, J. K. Entin, S. D. Goodman, T. J. Jackson, J. Johnson, et al. The soil moisture active passive (smap) mission. *Proceedings of the IEEE*, 98(5):704–716, 2010.

[75] D. Entekhabi, R. H. Reichle, R. D. Koster, and W. T. Crow. Performance metrics for soil moisture retrievals and application requirements. *Journal of Hydrometeorology*, 11(3):832–840, 2010.

[76] D. Entekhabi, I. Rodriguez-Iturbe, and F. Castelli. Mutual interaction of soil moisture state and atmospheric processes. *Journal of Hydrology*, 184(1):3–17, 1996.

[77] J. S. Famiglietti and M. Rodell. Water in the balance. *Science*, 340(6138):1300–1301, 2013.

[78] A. Farahmand and A. AghaKouchak. A generalized framework for deriving nonparametric standardized drought indicators. *Advances in Water Resources*, 76:140–145, 2015.

[79] A. Farahmand, J. Teixeira, and A. AghaKouchak. A vantage from space can detect earlier drought onset: An approach using relative humidity. *Scientific Reports*, 5:8553, 2015. doi: 10.1038/srep07093.

[80] T. Farrar, S. Nicholson, and A. Lare. The influence of soil type on the relationships between NDVI, rainfall, and soil moisture in semiarid botswana. ii. NDVI response to soil oisture. *Remote Sensing of Environment*, 50(2):121–133, 1994.

[81] R. Fensholt, I. Sandholt, S. Stisen, and C. Tucker. Analysing NDVI for the african continent using the geostationary meteosat second generation seviri sensor. *Remote sensing of environment*, 101(2):212–229, 2006.

[82] J. L. Foster, D. K. Hall, J. B. Eylander, G. A. Riggs, S. V. Nghiem, M. Tedesco, E. Kim, P. M. Montesano, R. E. Kelly, K. A. Casey, et al. A blended global snow product using visible, passive microwave and scatterometer satellite data. *International Journal of Remote Sensing*, 32(5):1371–1395, 2011.

[83] J. L. Foster, C. Sun, J. P. Walker, R. Kelly, A. Chang, J. Dong, and H. Powell. Quantifying the uncertainty in passive microwave snow water equivalent observations. *Remote Sensing of Environment*, 94(2):187–203, 2005.

[84] C. Funk. We thought trouble was coming. *Nature*, 476(7358):7, 2011.

[85] C. Funk and M. E. Budde. Phenologically-tuned modis ndvi-based production anomaly estimates for zimbabwe. *Remote Sensing of Environment*, 113(1):115–125, 2009.

[86] C. Funk and J. P. Verdin. Real-time decision support systems: the famine early warning system network. In *Satellite rainfall applications for surface hydrology*, pages 295–320. Springer, 2010.

[87] J. Gallagher, P. Biscoe, and B. Hunter. Effects of drought on grain growth. *Nature*, 264:541–542, 1976.

[88] B.-C. Gao. Ndwia normalized difference water index for remote sensing of vegetation liquid water from space. *Remote sensing of environment*, 58(3):257–266, 1996.

[89] M. Gebremichael. Framework for satellite rainfall product evaluation. *Geophysical Monograph Series*, 191:265–275, 2010.

[90] K. Ghoudi and B. Rémillard. Empirical processes based on pseudo-observations. ii. the multivariate case. *Asymptotic methods in stochastics*, 44:381–406, 2004.

[91] A. Ghulam, Q. Qin, T. Teyip, and Z.-L. Li. Modified perpendicular drought index (MPDI): a real-time drought monitoring method. *ISPRS journal of photogrammetry and remote sensing*, 62(2):150–164, 2007.

[92] A. Ghulam, Q. Qin, and Z. Zhan. Designing of the perpendicular drought index. *Environmental Geology*, 52(6):1045–1052, 2007.

[93] E. P. Glenn, A. R. Huete, P. L. Nagler, K. K. Hirschboeck, and P. Brown. Integrating remote sensing and ground methods to estimate evapotranspiration. *Critical Reviews in Plant Sciences*, 26(3):139–168, 2007.

[94] E. P. Glenn, C. M. Neale, D. J. Hunsaker, and P. L. Nagler. Vegetation index-based crop coefficients to estimate evapotranspiration by remote sensing in agricultural and natural ecosystems. *Hydrological Processes*, 25(26):4050–4062, 2011.

[95] H. C. J. Godfray, J. R. Beddington, I. R. Crute, L. Haddad, D. Lawrence, J. F. Muir, J. Pretty, S. Robinson, S. M. Thomas, and C. Toulmin. Food security: the challenge of feeding 9 billion people. *science*, 327(5967):812–818, 2010.

[96] M. D. Goldberg, Y. Qu, L. M. McMillin, W. Wolf, L. Zhou, and M. Divakarla. AIRS near-real-time products and algorithms in support of operational numerical weather prediction. *Geoscience and Remote Sensing, IEEE Transactions on*, 41(2):379–389, 2003.

[97] M. D. Goldberg, Y. Qu, L. M. McMillin, W. Wolf, L. Zhou, and M. Divakarla. AIRS near-real-time products and algorithms in support of operational numerical weather prediction. *Geoscience and Remote Sensing, IEEE Transactions on*, 41(2):379–389, 2003.

[98] S. Golian, O. Mazdiyasni, and A. AghaKouchak. Trends in meteorological and agricultural droughts in Iran. *Theoretical and Applied Climatology*, 119:679–688, 2015. doi: 10.1007/s00704-014-1139-6.

[99] B. E. Goodison. Determination of areal snow water equivalent on the canadian prairies using passive microwave satellite data. In *Geoscience and Remote Sensing Symposium, 1989. IGARSS'89. 12th Canadian Symposium on Remote Sensing., 1989 International*, volume 3, pages 1243–1246. IEEE, 1989.

[100] V. F. Grasso and A. Singh. Early warning systems: State-of-art analysis and future directions. *United Nations Environment Programme (UNEP)*, 2011.

[101] I. I. Gringorten. A plotting rule for extreme probability paper. *Journal of Geophysical Research*, 68(3):813–814, 1963.

[102] N. C. Grody and A. N. Basist. Global identification of snowcover using SSM/I measurements. *Geoscience and Remote Sensing, IEEE Transactions on*, 34(1):237–249, 1996.

[103] C. Gruhier, P. De Rosnay, S. Hasenauer, T. R. Holmes, R. A. De Jeu, Y. H. Kerr, E. Mougin, E. Njoku, F. Timouk, W. Wagner, et al. Soil moisture active and passive microwave products: intercomparison and evaluation over a sahelian site. *HAL*, 00463919, 2010.

[104] Y. Gu, J. F. Brown, J. P. Verdin, and B. Wardlow. A five-year analysis of MODIS NDVI and NDWI for grassland drought assessment over the central great plains of the united states. *Geophysical Research Letters*, 34(6), 2007.

[105] Y. Gu, E. Hunt, B. Wardlow, J. B. Basara, J. F. Brown, and J. P. Verdin. Evaluation of modis NDVI and NDWI for vegetation drought monitoring using oklahoma mesonet soil moisture data. *Geophysical Research Letters*, 35(22), 2008.

[106] B. Guan, N. P. Molotch, D. E. Waliser, S. M. Jepsen, T. H. Painter, and J. Dozier. Snow water equivalent in the Sierra Nevada: Blending snow sensor observations with snowmelt model simulations. *Water Resources Research*, 49(8):5029–5046, 2013.

[107] G. G. Gutman. Towards monitoring droughts from space. *Journal of Climate*, 3(2):282–295, 1990.

[108] N. B. Guttman. Accepting the standardized precipitation index: a calculation algorithm. *JAWRA Journal of the American Water Resources Association*, 35(2):311–322, 1999.

[109] D. K. Hall, G. A. Riggs, V. V. Salomonson, N. E. DiGirolamo, and K. J. Bayr. MODIS snow-cover products. *Remote sensing of Environment*, 83(1):181–194, 2002.

[110] Z. Hao and A. AghaKouchak. Multivariate standardized drought index: A parametric multi-index model. *Advances in Water Resources*, 57:12–18, 2013.

[111] Z. Hao and A. AghaKouchak. A nonparametric multivariate multi-index drought monitoring framework. *Journal of Hydrometeorology*, 15:89–101, 2014.

[112] Z. Hao, A. AghaKouchak, N. Nakhjiri, and A. Farahmand. Global integrated drought monitoring and prediction system. *Scientific Data*, 1:140001, 2014. doi: 10.1038/sdata.2014.1.

[113] Z. Hao, A. AghaKouchak, N. Nakhjiri, and A. Farahmand. Global integrated drought monitoring and prediction system. *Scientific data*, 1, 2014.

[114] J. Hatfield, G. Asrar, and E. Kanemasu. Intercepted photosynthetically active radiation estimated by spectral reflectance. *Remote Sensing of Environment*, 14(1):65–75, 1984.

[115] M. Hayes, M. Svoboda, N. Wall, and M. Widhalm. The lincoln declaration on drought indices: Universal meteorological drought index recommended. *Bulletin of the American Meteorological Society*, 92(4):485–488, 2011.

[116] M. Hayes, M. Svoboda, D. Wilhite, and O. Vanyarkho. Monitoring the 1996 drought using the standardized precipitation index. *Bull. Amer. Meteor.Soc.*, 80:429–438, 1999.

[117] R. Heim. A review of twentieth-century drought indices used in the United States. *Bulletin Of The American Meteorological Society*, 83(8):1149–1165, 2002.

[118] B. W. Heumann. Satellite remote sensing of mangrove forests: Recent advances and future opportunities. *Progress in Physical Geography*, 35(1):87–108, 2011.

[119] H. G. Hidalgo. Climate precursors of multidecadal drought variability in the western united states. *Water Resources Research*, 40(12):W12504, 2004.

[120] J. Hielkema, S. Prince, and W. Astle. Rainfall and vegetation monitoring in the savanna zone of the democratic republic of sudan using the NOAA Advanced Very High Resolution Radiometer. *International Journal of Remote Sensing*, 7(11):1499–1513, 1986.

[121] M. T. Hobbins, A. Dai, M. L. Roderick, and G. D. Farquhar. Revisiting the parameterization of potential evaporation as a driver of long-term water balance trends. *Geophysical Research Letters*, 35(12), 2008.

[122] M. Hoerling and A. Kumar. The perfect ocean for drought. *Science*, 299(5607):691–694, 2003.

[123] M. Hoerling, A. Kumar, R. Dole, J. W. Nielsen-Gammon, J. Eischeid, J. Perlwitz, X.-W. Quan, T. Zhang, P. Pegion, and M. Chen. Anatomy of an extreme event. *Journal of Climate*, 26(9):2811–2832, 2013.

[124] M. e. a. Hoerling. An interpretation of the origins of the 2012 central great plains drought. Technical report, Assessment Report, National Oceanic and Atmospheric Administration, Drought Task Force, 2013.

[125] Y. Hong, K. Hsu, X. Gao, and S. Sorooshian. Precipitation estimation from remotely sensed imagery using artificial neural network-cloud classification system. *Journal of Applied Meteorology and Climatology*, 43:18341853, 2004.

[126] F. Hossain and G. Huffman. Investigating error metrics for satellite rainfall data at hydrologically relevant scales. *Journal of Hydrometeorology*, 9(3):563–575, 2008.

[127] R. Houborg, M. Rodell, B. Li, R. Reichle, and B. F. Zaitchik. Drought indicators based on model-assimilated gravity recovery and climate experiment (grace) terrestrial water storage observations. *Water Resources Research*, 48(7), 2012.

[128] K. Hsu, X. Gao, S. Sorooshian, and H. Gupta. Precipitation estimation from remotely sensed information using artificial neural networks. *Journal of Applied Meteorology*, 36:11761190, 1997.

[129] A. Huete, K. Didan, T. Miura, E. P. Rodriguez, X. Gao, and L. G. Ferreira. Overview of the radiometric and biophysical performance of the MODIS vegetation indices. *Remote sensing of environment*, 83(1):195–213, 2002.

[130] A. Huete, C. Justice, and W. Van Leeuwen. MODIS vegetation index (MOD13). *Algorithm theoretical basis document*, 1999.

[131] A. R. Huete. A soil-adjusted vegetation index (SAVI). *Remote sensing of environment*, 25(3):295–309, 1988.

[132] G. Huffman, R. Adler, D. Bolvin, G. Gu, E. Nelkin, K. Bowman, E. Stocker, and D. Wolff. The trmm multi-satellite precipitation analysis: Quasi-global, multiyear, combined-sensor precipitation estimates at fine scale. *J. Hydrometeorol.*, 8:3855, 2007.

[133] E. R. Hunt Jr and B. N. Rock. Detection of changes in leaf water content using near-and middle-infrared reflectances. *Remote sensing of environment*, 30(1):43–54, 1989.

[134] S. Idso, R. Jackson, P. Pinter, R. Reginato, and J. Hatfield. Normalizing the stress-degree-day parameter for environmental variability. *Agricultural Meteorology*, 24(1):45–55, 1981.

[135] S. Idso, R. Jackson, P. Pinter, R. Reginato, and J. Hatfield. Normalizing the stress-degree-day parameter for environmental variability. *Agricultural Meteorology*, 24:45–55, 1981.

[136] R. D. Jackson, S. Idso, R. Reginato, and P. Pinter Jr. Canopy temperature as a crop water stress indicator. *Water Resources Research*, 17(4):1133–1138, 1981.

[137] T. J. Jackson. Iii. measuring surface soil moisture using passive microwave remote sensing. *Hydrological processes*, 7(2):139–152, 1993.

[138] T. J. Jackson. Soil moisture estimation using special satellite microwave/imager satellite data over a grassland region. *Water Resources Research*, 33(6):1475–1484, 1997.

[139] T. J. Jackson, D. Chen, M. Cosh, F. Li, M. Anderson, C. Walthall, P. Doriaswamy, and E. Hunt. Vegetation water content mapping using landsat data derived normalized difference water index for corn and soybeans. *Remote Sensing of Environment*, 92(4):475–482, 2004.

[140] S. K. Jain, R. Keshri, A. Goswami, A. Sarkar, and A. Chaudhry. Identification of drought-vulnerable areas using NOAA AVHRR data. *International Journal of Remote Sensing*, 30(10):2653–2668, 2009.

[141] L. Ji and A. J. Peters. Assessing vegetation response to drought in the northern great plains using vegetation and drought indices. *Remote Sensing of Environment*, 87(1):85–98, 2003.

[142] M. O. Jones, L. A. Jones, J. S. Kimball, and K. C. McDonald. Satellite passive microwave remote sensing for monitoring global land surface phenology. *Remote Sensing of Environment*, 115(4):1102–1114, 2011.

[143] R. Joyce and P. A. Arkin. Improved estimates of tropical and subtropical precipitation using the GOES precipitation index. *Journal of Atmospheric and Oceanic Technology*, 14(5):997–1011, 1997.

[144] R. Joyce, J. Janowiak, P. Arkin, and P. Xie. Cmorph: A method that produces global precipitation estimates from passive microwave and infrared data at high spatial and temporal resolution. *J. Hydrometeorol.*, 5:487 503, 2004.

[145] C. Justice, J. Townshend, E. Vermote, E. Masuoka, R. Wolfe, N. Saleous, D. Roy, and J. Morisette. An overview of modis land data processing and product status. *Remote Sensing of Environment*, 83(1):3–15, 2002.

[146] C. O. Justice, M. O. Román, I. Csiszar, E. F. Vermote, R. E. Wolfe, S. J. Hook, M. Friedl, Z. Wang, C. B. Schaaf, T. Miura, et al. Land and cryosphere products from Suomi NPP VIIRS: Overview and status. *Journal of Geophysical Research: Atmospheres*, 118(17):9753–9765, 2013.

[147] J. D. Kalma, T. R. McVicar, and M. F. McCabe. Estimating land surface evaporation: A review of methods using remotely sensed surface temperature data. *Surveys in Geophysics*, 29(4-5):421–469, 2008.

[148] S. Kao and R. Govindaraju. A copula-based joint deficit index for droughts. *Journal of Hydrology*, 380(1-2):121–134, 2010.

[149] A. Karnieli, N. Agam, R. T. Pinker, M. Anderson, M. L. Imhoff, G. G. Gutman, N. Panov, and A. Goldberg. Use of NDVI and land surface temperature for drought assessment: merits and limitations. *Journal of Climate*, 23(3):618–633, 2010.

[150] R. E. Kelly, A. T. Chang, L. Tsang, and J. L. Foster. A prototype AMSR-E global snow area and snow depth algorithm. *Geoscience and Remote Sensing, IEEE Transactions on*, 41(2):230–242, 2003.

[151] J. Keyantash and J. Dracup. The quantification of drought: An evaluation of drought indices. *Bulletin Of The American Meteorological Society*, 83(8):1167–1180, 2002.

[152] J. Keyantash and J. Dracup. An aggregate drought index: Assessing drought severity based on fluctuations in the hydrologic cycle and surface water storage. *Water Resources Research*, 40(9):W09304, SEP 11 2004.

[153] C. Kidd. Satellite rainfall climatology: a review. *International Journal of Climatology*, 21:10411066, 2001.

[154] R. I. Kiladze and A. S. Sochilina. On the new theory of geostationary satellite motion. *Astrononzical and Astrophysical Transactions*, 22(4-5):525–528, 2003.

[155] W. R. Knight. A computer method for calculating kendall's tau with ungrouped data. *Journal of the American Statistical Association*, 61(314):436–439, 1966.

[156] F. Kogan. Application of vegetation index and brightness temperature for drought detection. *Advances in Space Research*, 15(11):91–100, 1995.

[157] F. Kogan. Application of vegetation index and brightness temperature for drought detection. *Advances in Space Research*, 15(11):91–100, 1995.

[158] F. Kogan and J. Sullivan. Development of global drought-watch system using noaa/avhrr data. *Advances in Space Research*, 13(5):219–222, 1993.

[159] F. Kogan and J. Sullivan. Development of global drought-watch system using noaa/avhrr data. *Advances in Space Research*, 13(5):219–222, 1993.

[160] F. N. Kogan. Global drought watch from space. *Bulletin of the American Meteorological Society*, 78(4):621–636, 1997.

[161] F. N. Kogan. Operational space technology for global vegetation assessment. *Bulletin of the American Meteorological Society*, 82(9):1949–1964, 2001.

[162] C. Kongoli, C. A. Dean, S. R. Helfrich, and R. R. Ferraro. Evaluating the potential of a blended passive microwave-interactive multi-sensor product for improved mapping of snow cover and estimations of snow water equivalent. *Hydrological processes*, 21(12):1597–1607, 2007.

[163] C. Kongoli, P. Romanov, and R. Ferraro. Snow cover monitoring from remote sensing satellites. *Remote Sensing of Drought: Innovative Monitoring Approaches*, pages 359–386, 2012.

[164] R. D. Koster, M. J. Suarez, A. Ducharne, M. Stieglitz, and P. Kumar. A catchment-based approach to modeling land surface processes in a general circulation model: 1. model structure. *Journal of Geophysical Research: Atmospheres (1984–2012)*, 105(D20):24809–24822, 2000.

[165] C. Kummerow, Y. Hong, W. Olson, S. Yang, R. Adler, J. McCollum, R. Ferraro, G. Petty, D.-B. Shin, and T. Wilheit. The evolution of the Goddard Profiling Algorithm (GPROF) for rainfall estimation from passive microwave sensors. *Journal of Applied Meteorology*, 40(11):1801–1820, 2001.

[166] C. Kummerow, W. S. Olson, and L. Giglio. A simplified scheme for obtaining precipitation and vertical hydrometeor profiles from passive microwave sensors. *Geoscience and Remote Sensing, IEEE Transactions on*, 34(5):1213–1232, 1996.

[167] K. F. Kunzi, S. Patil, and H. Rott. Snow-cover parameters retrieved from Nimbus-7 scanning multichannel microwave radiometer (SMMR) data. *Geoscience and Remote Sensing, IEEE Transactions on*, GE-20(4):452–467, 1982.

[168] E. Lambin and D. Ehrlich. The surface temperature-vegetation index space for land cover and land-cover change analysis. *International journal of remote sensing*, 17(3):463–487, 1996.

[169] M. J. Leblanc, P. Tregoning, G. Ramillien, S. O. Tweed, and A. Fakes. Basin-scale, integrated observations of the early 21st century multiyear drought in southeast australia. *Water Resources Research*, 45(4), 2009.

[170] V. Levizzani, P. Bauer, and F. Turk. *Measurement of Precipitation from Space: EURAINSAT and Future*. Springer, Dordrecht, The Netherlands, 2007.

[171] S. L. Lewis, P. M. Brando, O. L. Phillips, G. M. F. van der Heijden, and D. Nepstad. The 2010 Amazon Drought. *Science*, 331(6017):554, FEB 4 2011.

[172] B. Li, M. Rodell, B. F. Zaitchik, R. H. Reichle, R. D. Koster, and T. M. van Dam. Assimilation of grace terrestrial water storage into a land surface model: Evaluation and potential value for drought monitoring in western and central europe. *Journal of Hydrology*, 446:103–115, 2012.

[173] T. Liang, X. Zhang, H. Xie, C. Wu, Q. Feng, X. Huang, and Q. Chen. Toward improved daily snow cover mapping with advanced combination of MODIS and AMSR-E measurements. *Remote Sensing of Environment*, 112(10):3750–3761, 2008.

[174] W. Liu and F. Kogan. Monitoring regional drought using the vegetation condition index. *International Journal of Remote Sensing*, 17(14):2761–2782, 1996.

[175] Y. Liu, R. Parinussa, W. Dorigo, R. D. Jeu, W. Wagner, A. v. Dijk, M. McCabe, and J. Evans. Developing an improved soil moisture dataset by blending passive and active microwave satellite-based retrievals. *Hydrology and Earth System Sciences*, 15(2):425–436, 2011.

[176] Y. Y. Liu, R. A. de Jeu, M. F. McCabe, J. P. Evans, and A. I. van Dijk. Global long-term passive microwave satellite-based retrievals of vegetation optical depth. *Geophysical Research Letters*, 38(18), 2011.

[177] Y. Y. Liu, A. I. Dijk, M. F. McCabe, J. P. Evans, and R. A. Jeu. Global vegetation biomass change (1988–2008) and attribution to environmental and human drivers. *Global Ecology and Biogeography*, 22(6):692–705, 2013.

[178] Y. Y. Liu, J. P. Evans, M. F. McCabe, R. A. de Jeu, A. I. van Dijk, A. J. Dolman, and I. Saizen. Changing climate and overgrazing are decimating mongolian steppes. *PloS one*, 8(2):e57599, 2013.

[179] Y. Y. Liu, R. M. Parinussa, W. A. Dorigo, R. A. M. De Jeu, W. Wagner, A. I. J. M. van Dijk, M. F. McCabe, and J. P. Evans. Developing an improved soil moisture dataset by blending passive and active microwave satellite-based retrievals. *Hydrology And Earth System Sciences*, 15(2):425–436, 2011.

[180] D. B. Lobell, W. Schlenker, and J. Costa-Roberts. Climate trends and global crop production since 1980. *Science*, 333(6042):616–620, 2011.

[181] D. Long, B. R. Scanlon, L. Longuevergne, A.-Y. Sun, D. N. Fernando, and S. Himanshu. GRACE satellites monitor large depletion in water storage in response to the 2011 drought in texas. *Geophysical Research Letters*, 2013.

[182] H. Lu, M. R. Raupach, T. R. McVicar, and D. J. Barrett. Decomposition of vegetation cover into woody and herbaceous components using avhrr ndvi time series. *Remote Sensing of Environment*, 86(1):1–18, 2003.

[183] B. Lyon, M. A. Bell, M. K. Tippett, A. Kumar, M. P. Hoerling, X.-W. Quan, and H. Wang. Baseline probabilities for the seasonal prediction of meteorological drought. *Journal of Applied Meteorology and Climatology*, 51(7):1222–1237, 2012.

[184] S. Manabe and R. T. Wetiierald. Thermal equilibrium of the atmosphere with a given distribution of relative humidity. *Journal of the Atmospheric Sciences*, 24(3):241–259, 1967.

[185] J. A. Marengo, J. Tomasella, L. M. Alves, W. R. Soares, and D. A. Rodriguez. The drought of 2010 in the context of historical droughts in the Amazon region. *Geophysical Research Letters*, 38:L12703, JUN 22 2011.

[186] M. Matsueda. Predictability of Euro-Russian blocking in summer of 2010. *Geophysical Research Letters*, 38(6), 2011.

[187] T. McKee, N. Doesken, and J. Kleist. The relationship of drought frequency and duration to time scales. In *In Proceedings of the 8th Conference of Applied Climatology, 17-22 January 1993. Anaheim, CA, American Meteorological Society*, pages 179–184, 1993.

[188] T. B. McKee, N. J. Doesken, J. Kleist, et al. The relationship of drought frequency and duration to time scales. In *Proceedings of the 8th Conference on Applied Climatology*, volume 17, pages 179–183. American Meteorological Society Boston, MA, USA, 1993.

[189] T. McVicar and P. Bierwirth. Rapidly assessing the 1997 drought in Papua New Guinea using composite AVHRR imagery. *International Journal of Remote Sensing*, 22(11):2109–2128, 2001.

[190] T. R. McVicar and D. L. Jupp. The current and potential operational uses of remote sensing to aid decisions on drought exceptional circumstances in australia: a review. *Agricultural systems*, 57(3):399–468, 1998.

[191] T. R. McVicar and D. L. Jupp. Estimating one-time-of-day meteorological data from standard daily data as inputs to thermal remote sensing based energy balance models. *Agricultural and forest meteorology*, 96(4):219–238, 1999.

[192] T. R. McVicar and D. L. Jupp. Using covariates to spatially interpolate moisture availability in the murray–darling basin: A novel use of remotely sensed data. *Remote sensing of environment*, 79(2):199–212, 2002.

[193] T. R. McVicar, M. L. Roderick, R. J. Donohue, L. T. Li, T. G. Van Niel, A. Thomas, J. Grieser, D. Jhajharia, Y. Himri, N. M. Mahowald, et al. Global review and synthesis of trends in observed terrestrial near-surface wind speeds: Implications for evaporation. *Journal of Hydrology*, 416:182–205, 2012.

[194] J. R. Mecikalski, G. R. Diak, M. C. Anderson, and J. M. Norman. Estimating fluxes on continental scales using remotely sensed data in an atmospheric-land exchange model. *Journal of Applied Meteorology*, 38(9):1352–1369, 1999.

[195] A. G. Meesters, R. A. De Jeu, and M. Owe. Analytical derivation of the vegetation optical depth from the microwave polarization difference index. *Geoscience and Remote Sensing Letters, IEEE*, 2(2):121–123, 2005.

[196] A. Mehran and A. AghaKouchak. Capabilities of satellite precipitation datasets to estimate heavy precipitation rates at different temporal accumulations. *Hydrological Processes*, 28:2262–2270, 2014. doi: 10.1002/hyp.9779.

[197] A. Mehran, O. Mazdiyasni, and A. AghaKouchak. A hybrid framework for assessing socioeconomic drought: Linking climate variability, local resilience, and demand. *Journal of Geophysical Research: Atmospheres*, 120(15):7520–7533, 2015.

[198] A. K. Mishra and V. P. Singh. A review of drought concepts. *Journal of Hydrology*, 391(1-2):204–216, 2010.

[199] K. Mo. Model based drought indices over the United States. *Journal of Hydrometeorology*, 9:1212–1230, 2008.

[200] K. C. Mo. Drought onset and recovery over the United States. *Journal of Geophysical Research-Atmospheres*, 116:D20106, OCT 19 2011.

[201] N. P. Molotch and S. A. Margulis. Estimating the distribution of snow water equivalent using remotely sensed snow cover data and a spatially distributed snowmelt model: A multi-resolution, multi-sensor comparison. *Advances in water resources*, 31(11):1503–1514, 2008.

[202] F. Momtaz, N. Nakhjiri, and A. AghaKouchak. Toward a drought cyberinfrastructure system. *Eos, Transactions American Geophysical Union*, 95(22):182–183, 2014.

[203] M. Moran, T. Clarke, Y. Inoue, and A. Vidal. Estimating crop water deficit using the relation between surface-air temperature and spectral vegetation index. *Remote sensing of environment*, 49(3):246–263, 1994.

[204] J. Morgan. Satellite remote sensing in meteorology and climatology- status, perspectives and challenges. In *Deutsche Meteorologen-Tagung ueber Atmosphaere, Ozeane, Kontinente, Kiel, Federal Republic of Germany, May 16-19, 1989 Annalen der Meteorologie*, number 26, pages 39–43, 1989.

[205] L. Morillas, R. Leuning, L. Villagarcía, M. García, P. Serrano-Ortiz, and F. Domingo. Improving evapotranspiration estimates in mediterranean drylands: The role of soil evaporation. *Water Resources Research*, 49(10):6572–6586, 2013.

[206] Q. Mu, F. A. Heinsch, M. Zhao, and S. W. Running. Development of a global evapotranspiration algorithm based on MODIS and global meteorology data. *Remote Sensing of Environment*, 111(4):519–536, 2007.

[207] Q. Mu, L. A. Jones, J. S. Kimball, K. C. McDonald, and S. W. Running. Satellite assessment of land surface evapotranspiration for the pan-arctic domain. *Water Resources Research*, 45(9), 2009.

[208] Q. Mu, M. Zhao, J. S. Kimball, N. G. McDowell, and S. W. Running. A remotely sensed global terrestrial drought severity index. *Bulletin of the American Meteorological Society*, 94:83–98, 2013.

[209] Q. Mu, M. Zhao, and S. W. Running. Improvements to a modis global terrestrial evapotranspiration algorithm. *Remote Sensing of Environment*, 115(8):1781–1800, 2011.

[210] M. Naresh Kumar, C. Murthy, M. Sesha Sai, and P. Roy. On the use of standardized precipitation index (SPI) for drought intensity assessment. *Meteorological applications*, 16(3):381–389, 2009.

[211] NASA. *Space-based remote sensing of the earth: a report to the Congress*. National Aeronautics and Space Administration, 1987.

[212] NASA. Guidelines and assessment procedures for limiting orbital debris. *National Aeronautics and Space Administration*, 1740:14, 1995.

[213] NASA. 2010 science plan for NASA's science mission directorate. Technical report, National Aeronautics and Space Administration, Washington, DC, 2010.

[214] R. Nemani, H. Hashimoto, P. Votava, F. Melton, W. Wang, A. Michaelis, L. Mutch, C. Milesi, S. Hiatt, and M. White. Monitoring and forecasting ecosystem dynamics using the terrestrial observation and prediction system (tops). *Remote Sensing of Environment*, 113(7):1497–1509, 2009.

[215] S. E. Nicholson, C. J. Tucker, and M. Ba. Desertification, drought, and surface vegetation: An example from the west african sahel. *Bulletin of the American Meteorological Society*, 79(5):815–829, 1998.

[216] B. Nijssen, S. Shukla, C. Lin, H. Gao, T. Zhou, J. Sheffield, E. F. Wood, and D. P. Lettenmaier. A prototype global drought information system based on multiple land surface models. *Journal of Hydrometeorology*, (15):1661–1676, 2014.

[217] E. G. Njoku and D. Entekhabi. Passive microwave remote sensing of soil moisture. *Journal of Hydrology*, 184(1):101–129, 1996.

[218] E. G. Njoku, T. J. Jackson, V. Lakshmi, T. K. Chan, and S. V. Nghiem. Soil moisture retrieval from AMSR-E. *Geoscience and Remote Sensing, IEEE Transactions on*, 41(2):215–229, 2003.

[219] J. M. Norman, M. Divakarla, and N. S. Goel. Algorithms for extracting information from remote thermal-IR observations of the earth's surface. *Remote Sensing of Environment*, 51(1):157–168, 1995.

[220] J. A. Otkin, M. C. Anderson, C. Hain, and M. Svoboda. Examining the relationship between drought development and rapid changes in the evaporative stress index. *Journal of Hydrometeorology*, 15(3), 2014.

[221] M. Owe, R. de Jeu, and J. Walker. A methodology for surface soil moisture and vegetation optical depth retrieval using the microwave polarization difference index. *Geoscience and Remote Sensing, IEEE Transactions on*, 39(8):1643–1654, 2001.

[222] T. H. Painter, F. C. Seidel, A. C. Bryant, S. McKenzie Skiles, and K. Rittger. Imaging spectroscopy of albedo and radiative forcing by light-absorbing impurities in mountain snow. *Journal of Geophysical Research: Atmospheres*, 118(17):9511–9523, 2013.

[223] W. Palmer. Meteorological drought. Technical report, Weather Bureau Res. Paper 45, U.S. Dept. of Commerce, 1965. 58 pp.

[224] W. C. Palmer. Keeping track of crop moisture conditions, nationwide: The new crop moisture index. *Weatherwise*, 21(4), 1968.

[225] W. C. Palmer and A. V. Havens. A graphical technique for determining evapotranspiration by the thornthwaite method. *Monthly Weather Review*, 86(4):123–128, 1958.

[226] B. R. Paridal, W. B. Collado, R. Borah, M. K. Hazarika, and L. Sarnarakoon. Detecting drought-prone areas of rice agriculture using a modis-derived soil moisture index. *GIScience & Remote Sensing*, 45(1):109–129, 2008.

[227] J.-S. Park, K.-T. Kim, and Y.-S. Choi. Application of vegetation condition index and standardized vegetation index for assessment of spring drought in south korea. In *Geoscience and Remote Sensing Symposium, 2008. IGARSS 2008. IEEE International*, volume 3, pages III–774. IEEE, 2008.

[228] J. Passioura. The drought environment: physical, biological and agricultural perspectives. *Journal of experimental botany*, 58(2):113–117, 2007.

[229] N. Patel, B. Parida, V. Venus, S. Saha, and V. Dadhwal. Analysis of agricultural drought using vegetation temperature condition index (VTCI) from terra/modis satellite data. *Environmental monitoring and assessment*, 184(12):7153–7163, 2012.

[230] J. Payero, C. Neale, and J. Wright. Comparison of eleven vegetation indices for estimating plant height of alfalfa and grass. *Applied Engineering in Agriculture*, 20:385–393, 2004.

[231] C. R. Perry and L. F. Lautenschlager. Functional equivalence of spectral vegetation indices. *Remote Sensing of Environment*, 14(1):169–182, 1984.

[232] A. J. Peters, E. A. Walter-Shea, L. Ji, A. Vina, M. Hayes, and M. D. Svoboda. Drought monitoring with NDVI-based standardized vegetation index. *Photogrammetric engineering and remote sensing*, 68(1):71–75, 2002.

[233] T. C. Piechota and J. A. Dracup. Drought and regional hydrologic variation in the united states: Associations with the el niño-southern oscillation. *Water Resources Research*, 32(5):1359–1373, 1996.

[234] R. T. Pinker, D. Sun, M.-P. Hung, C. Li, and J. B. Basara. Evaluation of satellite estimates of land surface temperature from GOES over the United States. *Journal of Applied Meteorology and Climatology*, 48(1):167–180, 2009.

[235] W. Pozzi, J. Sheffield, R. Stefanski, D. Cripe, R. Pulwarty, J. V. VOGT, R. R. Heim Jr, M. J. Brewer, M. Svoboda, R. Westerhoff, et al. Toward global drought early warning capability. *Bulletin of the American Meteorological Society*, 94(6), 2013.

[236] J. C. Price. Estimation of regional scale evapotranspiration through analysis of satellite thermal-infrared data. *Geoscience and Remote Sensing, IEEE Transactions on*, GE-20(3):286–292, 1982.

[237] S. D. Prince, D. Colstoun, E. Brown, and L. Kravitz. Evidence from rain-use efficiencies does not indicate extensive sahelian desertification. *Global Change Biology*, 4(4):359–374, 1998.

[238] Q. Qin, C. Jin, N. Zhang, and X. Yang. An two-dimensional spectral space based model for drought monitoring and its re-examination. In *Geoscience and Remote Sensing Symposium (IGARSS), 2010 IEEE International*, pages 3869–3872. IEEE, 2010.

[239] S. Quiring. Monitoring drought: an evaluation of meteorological drought indices. *Geography Compass*, 3(1):64–88, 2009.

[240] S. M. Quiring. Developing objective operational definitions for monitoring drought. *Journal of Applied Meteorology and Climatology*, 48(6):1217–1229, 2009.

[241] S. M. Quiring and S. Ganesh. Evaluating the utility of the Vegetation Condition Index (VCI) for monitoring meteorological drought in texas. *Agricultural and forest meteorology*, 150(3):330–339, 2010.

[242] D. Rajsekhar, V. P. Singh, and A. K. Mishra. Multivariate drought index: An information theory based approach for integrated drought assessment. *Journal of Hydrology*, 2014. doi: 10.1016/j.jhydrol.2014.11.031.

[243] E. M. Rasmusson, J. M. Wallace, et al. Meteorological aspects of the El Nino/southern oscillation. *Science*, 222(4629):1195–1202, 1983.

[244] R. H. Reichle, R. D. Koster, G. J. De Lannoy, B. A. Forman, Q. Liu, S. P. Mahanama, and A. Touré. Assessment and enhancement of merra land surface hydrology estimates. *Journal of Climate*, 24(24):6322–6338, 2011.

[245] R. H. Reichle, R. D. Koster, G. J. M. De Lannoy, B. A. Forman, Q. Liu, S. P. P. Mahanama, and A. Toure. Assessment and Enhancement of MERRA Land Surface Hydrology Estimates. *Journal Of Climate*, 24(24):6322–6338, 2011.

[246] R. H. Reichle, R. D. Koster, J. Dong, and A. A. Berg. Global soil moisture from satellite observations, land surface models, and ground data: Implications for data assimilation. *Journal of Hydrometeorology*, 5(3):430–442, 2004.

[247] J. Rhee, J. Im, and G. J. Carbone. Monitoring agricultural drought for arid and humid regions using multi-sensor remote sensing data. *Remote Sensing of environment*, 114(12):2875–2887, 2010.

[248] Y. Richard and I. Poccard. A statistical study of NDVI sensitivity to seasonal and interannual rainfall variations in southern africa. *International Journal of Remote Sensing*, 19(15):2907–2920, 1998.

[249] M. M. Rienecker, M. J. Suarez, R. Gelaro, R. Todling, J. Bacmeister, E. Liu, M. G. Bosilovich, S. D. Schubert, L. Takacs, G.-K. Kim, S. Bloom, J. Chen, D. Collins, A. Conaty, A. Da Silva, W. Gu, J. Joiner, R. D. Koster, R. Lucchesi, A. Molod, T. Owens, S. Pawson, P. Pegion, C. R. Redder, R. Reichle, F. R. Robertson, A. G. Ruddick, M. Sienkiewicz, and J. Woollen. MERRA: NASA's Modern-Era Retrospective Analysis for Research and Applications. *Journal Of Climate*, 24(14):3624–3648, 2011.

[250] M. Rodell. Satellite gravimetry applied to drought monitoring. *Remote Sensing of Drought: Innovative Monitoring Approaches*, page 261, 2012.

[251] M. Rodell, J. Chen, H. Kato, J. S. Famiglietti, J. Nigro, and C. R. Wilson. Estimating groundwater storage changes in the mississippi river basin (usa) using grace. *Hydrogeology Journal*, 15(1):159–166, 2007.

[252] M. Rodell and J. Famiglietti. The potential for satellite-based monitoring of groundwater storage changes using grace: the high plains aquifer, central us. *Journal of Hydrology*, 263(1):245–256, 2002.

[253] M. L. Roderick, I. R. Noble, and S. W. Cridland. Estimating woody and herbaceous vegetation cover from time series satellite observations. *Global Ecology and Biogeography*, 8(6):501–508, 1999.

[254] P. Romanov, G. Gutman, and I. Csiszar. Automated monitoring of snow cover over north america with multispectral satellite data. *Journal of Applied Meteorology*, 39(11):1866–1880, 2000.

[255] H. Rott, S. H. Yueh, D. W. Cline, C. Duguay, R. Essery, C. Haas, F. Heliere, M. Kern, G. Macelloni, E. Malnes, et al. Cold regions hydrology high-resolution observatory for snow and cold land processes. *Proceedings of the IEEE*, 98(5):752–765, 2010.

[256] J. Rouse, R. Haas, J. Schell, D. Deering, and J. Harlan. *Monitoring the vernal advancement and retrogradation (greenwave effect) of natural vegetation*. Texas A & M University, Remote Sensing Center, 1974.

[257] S. W. Running, R. R. Nemani, F. A. Heinsch, M. Zhao, M. Reeves, and H. Hashimoto. A continuous satellite-derived measure of global terrestrial primary production. *Bioscience*, 54(6):547–560, 2004.

[258] S. W. Running, R. R. Nemani, D. L. Peterson, L. E. Band, D. F. Potts, L. L. Pierce, and M. A. Spanner. Mapping regional forest evapotranspiration and photosynthesis by coupling satellite data with ecosystem simulation. *Ecology*, pages 1090–1101, 1989.

[259] J. F. Santos, I. Pulido-Calvo, and M. M. Portela. Spatial and temporal variability of droughts in Portugal. *Water Resources Research*, 46:W03503, MAR 4 2010.

[260] E. Schanda, C. Matzler, and K. Kunzi. Microwave remote sensing of snow cover. *International Journal of Remote Sensing*, 4(1):149–158, 1983.

[261] F. Sedano and J. Randerson. Multi-scale influence of vapor pressure deficit on fire ignition and spread in boreal forest ecosystems. *Biogeosciences*, 11(14), 2014.

[262] R. Seiler, F. Kogan, and J. Sullivan. AVHRR-based vegetation and temperature condition indices for drought detection in argentina. *Advances in Space Research*, 21(3):481–484, 1998.

[263] S. Sellars, P. Nguyen, W. Chu, X. Gao, K.-l. Hsu, and S. Sorooshian. Computational earth science: Big data transformed into insight. *Eos, Transactions American Geophysical Union*, 94(32):277–278, 2013.

[264] G. B. Senay. Modeling landscape evapotranspiration by integrating land surface phenology and a water balance algorithm. *Algorithms*, 1(2):52–68, 2008.

[265] G. B. Senay, S. Bohms, , and J. P. Verdin. Remote sensing of evapotranspiration for operational drought monitoring using principles of water and energy balance. *Remote Sensing of Drought: Innovative Monitoring Approaches*, pages 123–144, 2012.

[266] G. B. Senay, M. Budde, J. P. Verdin, and A. M. Melesse. A coupled remote sensing and simplified surface energy balance approach to estimate actual evapotranspiration from irrigated fields. *Sensors*, 7(6):979–1000, 2007.

[267] J. Sheffield, G. Goteti, F. Wen, and E. Wood. A simulated soil moisture based drought analysis for the United States. *Journal Of Geophysical Research-Atmospheres*, 109(D24), 2004.

[268] J. Sheffield, G. Goteti, and E. Wood. Development of a 50-yr, high resolution global dataset of meteorological forcings for land surface modeling. *J. Climate*, 13:3088–3111, 2006.

[269] J. Sheffield, E. Wood, D. Lettenmaier, and A. Lipponen. Experimental drought monitoring for africa. *GEWEX News*, 18(3):4–6, 2008.

[270] J. Sheffield, E. Wood, and M. Roderick. Little change in global drought over the past 60 years. *Nature*, 491(7424):435–438, 2012.

[271] J. Sheffield, E. F. Wood, N. Chaney, K. Guan, S. Sadri, X. Yuan, L. Olang, A. Amani, A. Ali, S. Demuth, and L. Ogallo. A Drought Monitoring And Forecasting System For Sub-Sahara African Water Resources And Food Security. *Bulletin of the American Meteorological Society*, 95(6):861–882, 2014.

[272] H. W. Shen and G. Q. Tabios. *Modeling of precipitation-based drought characteristics over California*. Centers for Water and Wildland Resources, 1996.

[273] J. Shi, T. Jackson, J. Tao, J. Du, R. Bindlish, L. Lu, and K. Chen. Microwave vegetation indices for short vegetation covers from satellite passive microwave sensor amsr-e. *Remote sensing of environment*, 112(12):4285–4300, 2008.

[274] S. Shukla, A. C. Steinemann, and D. P. Lettenmaier. Drought monitoring for washington state: Indicators and applications. *Journal of Hydrometeorology*, 12(1):66–83, 2011.

[275] S. Shukla and A. Wood. Use of a standardized runoff index for characterizing hydrologic drought. *Geophysical Research Letters*, 35(2), 2008. L02405.

[276] N. G. Silleos, T. K. Alexandridis, I. Z. Gitas, and K. Perakis. Vegetation indices: advances made in biomass estimation and vegetation monitoring in the last 30 years. *Geocarto International*, 21(4):21–28, 2006.

[277] J. Simpson, J. Stitt, and M. Sienko. Improved estimates of the areal extent of snow cover from avhrr data. *Journal of Hydrology*, 204(1):1–23, 1998.

[278] R. P. Singh, S. Roy, and F. Kogan. Vegetation and temperature condition indices from NOAA AVHRR data for drought monitoring over India. *International Journal of Remote Sensing*, 24(22):4393–4402, 2003.

[279] N. Son, C. Chen, C. Chen, L. Chang, and V. Minh. Monitoring agricultural drought in the lower mekong basin using MODIS ndvi and land surface temperature data. *International Journal of Applied Earth Observation and Geoinformation*, 18:417–427, 2012.

[280] S. Sorooshian, A. AghaKouchak, P. Arkin, J. Eylander, E. Foufoula-Georgiou, R. Harmon, J. M. H. Hendrickx, B. Imam, R. Kuligowski, B. Skahill, and G. Skofronick-Jackson. Advanced concepts on remote sensing of precipitation at multiple scales. *Bulletin of the American Meteorological Society*, 92(10):1353–1357, 2011.

[281] S. Sorooshian, K. Hsu, X. Gao, H. Gupta, B. Imam, and D. Braithwaite. Evolution of the PERSIANN system satellite-based estimates of tropical rainfall. *Bull. Am. Meteorol. Soc.*, 81(9):2035 2046, 2000.

[282] A. C. Steinemann and L. F. Cavalcanti. Developing multiple indicators and triggers for drought plans. *Journal of water resources planning and management*, 132(3):164–174, 2006.

[283] H. Su, M. McCabe, E. Wood, Z. Su, and J. Prueger. Modeling evapotranspiration during smacex: Comparing two approaches for local-and regional-scale prediction. *Journal of hydrometeorology*, 6(6):910–922, 2005.

[284] D. Sun and M. Kafatos. Note on the NDVI-LST relationship and the use of temperature-related drought indices over north america. *Geophysical Research Letters*, 34(24), 2007.

[285] M. Svoboda, D. LeComte, M. Hayes, R. Heim, et al. The drought monitor. *Bulletin of the American Meteorological Society*, 83(8):1181, 2002.

[286] M. Svoboda, D. LeComte, M. Hayes, R. Heim, K. Gleason, J. Angel, B. Rippey, R. Tinker, M. Palecki, D. Stooksbury, D. Miskus, and S. Stephens. The drought monitor. *Bulletin of the American Meteorological Society*, 83(8):1181–1190, AUG 2002.

[287] S. Swain, B. D. Wardlow, S. Narumalani, T. Tadesse, and K. Callahan. Assessment of vegetation response to drought in nebraska using terra-modis land surface temperature and normalized difference vegetation index. *GIScience & Remote Sensing*, 48(3):432–455, 2011.

[288] T. Tadesse, J. Brown, and M. Hayes. A new approach for predicting drought-related vegetation stress: Integrating satellite, climate, and biophysical data over the US central plains. *ISPRS Journal of Photogrammetry and Remote Sensing*, 59(4):244–253, JUN 2005. 30th International Symposium on Remote Sensing of Environment, Honolulu, HI, NOV, 2003.

[289] M. Takada, Y. Mishima, and S. Natsume. Estimation of surface soil properties in peatland using alos/palsar. *Landscape and Ecological Engineering*, 5(1):45–58, 2009.

[290] A. K. Thiam. *Geographic information systems and remote sensing methods for assessing and monitoring land degradation in the Sahel region: the case of southern Mauritania*. Clark University, 1998.

[291] A. C. Thomas, J. T. Reager, J. S. Famiglietti, and M. Rodell. A grace-based water storage deficit approach for hydrological drought characterization. *Geophysical Research Letters*, 41(5):1537–1545, 2014.

[292] B. Tian, E. Manning, E. Fetzer, E. Olsen, and S. Wong. AIRS/AMSU/HSB version 6 level 3 product user guide. *Jet Propulsion Laboratory, California Institute of Technology, Pasadena, CA, USA*, 2013.

[293] Y. Tian, C. Peters-Lidard, J. Eylander, R. Joyce, G. Huffman, R. Adler, K. Hsu, F. Turk, M. Garcia, and J. Zeng. Component analysis of errors in satellite-based precipitation estimates. *Journal of Geophysical Research*, 114(D24101), 2009.

[294] G. Tsakiris, D. Pangalou, and H. Vangelis. Regional drought assessment based on the Reconnaissance Drought Index (RDI). *Water Resources Management*, 21(5):821–833, 2007.

[295] G. Tsakiris and H. Vangelis. Establishing a drought index incorporating evapotranspiration. *European Water*, 9(10):3–11, 2005.

[296] C. J. Tucker. Red and photographic infrared linear combinations for monitoring vegetation. *Remote sensing of Environment*, 8(2):127–150, 1979.

[297] C. J. Tucker and B. J. Choudhury. Satellite remote sensing of drought conditions. *Remote Sensing of Environment*, 23(2):243–251, 1987.

[298] C. J. Tucker, J. E. Pinzon, M. E. Brown, D. A. Slayback, E. W. Pak, R. Mahoney, E. F. Vermote, and N. El Saleous. An extended AVHRR 8-km NDVI dataset compatible with modis and spot vegetation NDVI data. *International Journal of Remote Sensing*, 26(20):4485–4498, 2005.

[299] F. J. Turk, G. D. Rohaly, J. Hawkins, E. A. Smith, F. S. Marzano, A. Mugnai, and V. Levizzani. Meteorological applications of precipitation estimation from combined ssm/i, trmm and infrared geostationary satellite data. *Microwave Radiometry and Remote Sensing of the Earth's Surface and Atmosphere*, pages 353–363, 1999.

[300] B. W. Turnbull. The empirical distribution function with arbitrarily grouped, censored and truncated data. *Journal of the Royal Statistical Society. Series B (Methodological)*, pages 290–295, 1976.

[301] UNESCO. Map of the world distribution of arid regions. Technical report, The United Nations Educational, Scientific and Cultural Organization (UNESCO), Paris, France, 1979.

[302] L. S. Unganai and F. N. Kogan. Drought monitoring and corn yield estimation in southern africa from avhrr data. *Remote Sensing of Environment*, 63(3):219–232, 1998.

[303] A. van Dijk, L. Renzullo, and M. Rodell. Use of gravity recovery and climate experiment terrestrial water storage retrievals to evaluate model estimates by the australian water resources assessment system. *Water Resources Research*, 47(11), 2011.

[304] A. I. van Dijk, H. E. Beck, R. S. Crosbie, R. A. Jeu, Y. Y. Liu, G. M. Podger, B. Timbal, and N. R. Viney. The millennium drought in southeast australia (2001–2009): Natural and human causes and implications for water resources, ecosystems, economy, and society. *Water Resources Research*, 49(2):1040–1057, 2013.

[305] T. T. van Leeuwen, A. J. Frank, Y. Jin, P. Smyth, M. L. Goulden, G. R. van der Werf, and J. T. Randerson. Optimal use of land surface temperature data to detect changes in tropical forest cover. *Journal of Geophysical Research: Biogeosciences*, 116(G2), 2011.

[306] T. Van Niel, T. McVicar, H. Fang, and S. Liang. Calculating environmental moisture for per-field discrimination of rice crops. *International Journal of Remote Sensing*, 24(4):885–890, 2003.

[307] M. Vargas, T. Miura, N. Shabanov, and A. Kato. An initial assessment of Suomi NPP VIIRS vegetation index EDR. *Journal of Geophysical Research: Atmospheres*, 118(22):12–301, 2013.

[308] J. Verdin, C. Funk, G. Senay, and R. Choularton. Climate science and famine early warning. *Philosophical Transactions of the Royal Society B: Biological Sciences*, 360(1463):2155–2168, 2005.

[309] S. M. Vicente-Serrano, S. Begueria, and J. I. Lopez-Moreno. A Multiscalar Drought Index Sensitive to Global Warming: The Standardized Precipitation Evapotranspiration Index. *Journal of Climate*, 23(7):1696–1718, 2010.

[310] W. Wagner, W. Dorigo, R. de Jeu, D. Fernandez, J. Benveniste, E. Haas, and M. Ertl. Fusion of active and passive microwave observations to create an essential climate variable data record on soil moisture. In *XXII ISPRS Congress, Melbourne, Australia*, 2012.

[311] W. Wagner, J. Noll, M. Borgeaud, and H. Rott. Monitoring soil moisture over the canadian prairies with the ers scatterometer. *Geoscience and Remote Sensing, IEEE Transactions on*, 37(1):206–216, 1999.

[312] Z. Wan, P. Wang, and X. Li. Using MODIS land surface temperature and normalized difference vegetation index products for monitoring drought in the southern great plains, usa. *International Journal of Remote Sensing*, 25(1):61–72, 2004.

[313] A. Wang, T. J. Bohn, S. P. Mahanama, R. D. Koster, and D. P. Lettenmaier. Multimodel ensemble reconstruction of drought over the continental United States. *Journal of Climate*, 22(10):2694–2712, 2009.

[314] D. Wang, M. Hejazi, X. Cai, and A. J. Valocchi. Climate change impact on meteorological, agricultural, and hydrological drought in central Illinois. *Water Resources Research*, 47:W09527, SEP 27 2011.

[315] J. Wang, K. Price, and P. Rich. Spatial patterns of NDVI in response to precipitation and temperature in the central great plains. *International Journal of Remote Sensing*, 22(18):3827–3844, 2001.

[316] K. Wang and R. E. Dickinson. A review of global terrestrial evapotranspiration: Observation, modeling, climatology, and climatic variability. *Reviews of Geophysics*, 50(2), 2012.

[317] L. Wang and J. J. Qu. Nmdi: A normalized multi-band drought index for monitoring soil and vegetation moisture with satellite remote sensing. *Geophysical Research Letters*, 34(20), 2007.

[318] L. Wang and J. J. Qu. Satellite remote sensing applications for surface soil moisture monitoring: A review. *Frontiers of Earth Science in China*, 3(2):237–247, 2009.

[319] L. Wang, J. J. Qu, X. Hao, and Q. Zhu. Sensitivity studies of the moisture effects on modis swir reflectance and vegetation water indices. *International Journal of Remote Sensing*, 29(24):7065–7075, 2008.

[320] B. Wardlow, M. Anderson, and J. Verdin. *Remote Sensing of Drought*. CRC Press, 2012.

[321] S. K. Wegren. Food security and russia's 2010 drought. *Eurasian Geography and Economics*, 52(1):140–156, 2011.

[322] C. Welsch, H. Swenson, S. A. Cota, F. DeLuccia, J. M. Haas, C. Schueler, R. M. Durham, J. E. Clement, and P. E. Ardanuy. VIIRS (Visible Infrared Imager Radiometer Suite): a next-generation operational environmental sensor for npoess. In *Geoscience and Remote Sensing Symposium, 2001. IGARSS'01. IEEE 2001 International*, volume 3, pages 1020–1022. IEEE, 2001.

[323] W. Werick, G. Willeke, N. Guttman, J. Hosking, and J. Wallis. National drought atlas developed. *Eos, Trans. Amer. Geophys. Union*, 75:89, 1994.

[324] A. L. Westerling, H. G. Hidalgo, D. R. Cayan, and T. W. Swetnam. Warming and earlier spring increase western us forest wildfire activity. *science*, 313(5789):940–943, 2006.

[325] C. Wiegand, A. Richardson, D. Escobar, and A. Gerbermann. Vegetation indices in crop assessments. *Remote Sensing of Environment*, 35(2):105–119, 1991.

[326] D. Wiesnet. Winter snow drought. *Eos, Transactions American Geophysical Union*, 62(14):137–137, 1981.

[327] D. Wilhite. *Drought: A global assessment*. Routledge, 2000.

[328] D. Wilhite and M. Glantz. Understanding the drought phenomenon: The role of definitions. *Water Int.*, 10:111–120, 1985.

[329] D. A. Wilhite. *Drought and water crises: science, technology, and management issues*, volume 86. CRC Press, 2005.

[330] A. P. Williams, C. D. Allen, A. K. Macalady, D. Griffin, C. A. Woodhouse, D. M. Meko, T. W. Swetnam, S. A. Rauscher, R. Seager, H. D. Grissino-Mayer, et al. Temperature as a potent driver of regional forest drought stress and tree mortality. *Nature Climate Change*, 3(3):292–297, 2013.

[331] W. J. Wilson, S. H. Yueh, S. J. Dinardo, S. L. Chazanoff, A. Kitiyakara, F. K. Li, and Y. Rahmat-Samii. Passive active L-and S-band (PALS) microwave sensor for ocean salinity and soil moisture measurements. *Geoscience and Remote Sensing, IEEE Transactions on*, 39(5):1039–1048, 2001.

[332] W. J. Wiscombe and S. G. Warren. A model for the spectral albedo of snow. i: Pure snow. *Journal of the Atmospheric Sciences*, 37(12):2712–2733, 1980.

[333] WMO. Inter-regional workshop on indices and early warning systems for drought. Lincoln, nebraska, usa, 8-11 december 2009, World Meteorological Organization, 2009.

[334] A. W. Wood. The university of washington surface water monitor: An experimental platform for national hydrologic assessment and prediction. In *American Meteorology Society annual meeting, 22nd conference on hydrology, New Orleans. p*, volume 13, 2008.

[335] A. W. Wood, E. P. Maurer, A. Kumar, and D. P. Lettenmaier. Long-range experimental hydrologic forecasting for the eastern united states. *Journal of Geophysical Research: Atmospheres*, 107(D20), 2002.

[336] Y. Yao, S. Liang, Q. Qin, and K. Wang. Monitoring drought over the conterminous united states using modis and ncep reanalysis-2 data. *Journal of Applied Meteorology and Climatology*, 49(8):1665–1680, 2010.

[337] Y. Yao, S. Liang, Q. Qin, K. Wang, and S. Zhao. Monitoring global land surface drought based on a hybrid evapotranspiration model. *International Journal of Applied Earth Observation and Geoinformation*, 13(3):447–457, 2011.

[338] M. Yebra, A. Van Dijk, R. Leuning, A. Huete, and J. P. Guerschman. Evaluation of optical remote sensing to estimate actual evapotranspiration and canopy conductance. *Remote Sensing of Environment*, 129:250–261, 2013.

[339] S. Z. Yirdaw, K. R. Snelgrove, and C. O. Agboma. Grace satellite observations of terrestrial moisture changes for drought characterization in the canadian prairie. *Journal of Hydrology*, 356(1):84–92, 2008.

[340] S. Yue, T. Ouarda, B. Bobee, P. Legendre, and P. Bruneau. The Gumbel mixed model for flood frequency analysis. *Journal of Hydrology*, 226(1-2):88–100, DEC 20 1999.

[341] B. F. Zaitchik, M. Rodell, and R. H. Reichle. Assimilation of grace terrestrial water storage data into a land surface model: Results for the mississippi river basin. *Journal of Hydrometeorology*, 9(3):535–548, 2008.

[342] A. Zhang and G. Jia. Monitoring meteorological drought in semiarid regions using multi-sensor microwave remote sensing data. *Remote Sensing of Environment*, 134:12–23, 2013.

[343] N. Zhang, Y. Hong, Q. Qin, and L. Liu. Vsdi: a visible and shortwave infrared drought index for monitoring soil and vegetation moisture based on optical remote sensing. *International Journal of Remote Sensing*, 34(13):4585–4609, 2013.